PETROPHYSICAL EVALUATION OF FLOW UNITS OF THE AGBADA-AKATA FORMATIONS IN THE NIGER DELTA

A thesis presented to the Department of Petroleum Engineering

African University of Science and Technology, Abuja

In partial fulfilment of the requirements for the award

MASTER OF SCIENCE

By

ANNAN BOAH EVANS

Supervised by

Prof. Djebbar Tiab

African University of Science and Technology

www.aust.edu.ng

P.M.B 681, Garki, Abuja F.C.T

Nigeria

June 2016

PETROPHYSICAL EVALUATION OF FLOW UNITS OF THE AGBADA-AKATA FORMATIONS IN THE NIGER DELTA

A THESIS APPROVED BY THE PETROLEUM ENGINEERING DEPARTMENT

RECOMMENDED

.....
Supervisor, Prof. Djebbar Tiab

.....
Committee Member, Prof. David Ogbe

.....
Committee Member, Dr. Alpheus Igbokoyi

.....
Head, Department of Petroleum Engineering

APPROVED

.....
Chief Academic Officer

.....
Date

ABSTRACT

Clastic reservoirs may be heterogeneous and exhibit lateral and vertical variations in porosity and permeability. Therefore, the spatial distribution of the petrophysical properties within the reservoirs is important to provide a reliable reservoir description. An improved understanding of clastic reservoirs has led to more detailed reservoir description by flow unit delineation.

In this study, six active wells which cut across zone D3000 in the Tertiary Niger Delta clastic reservoir were used for the petrophysical analysis. The study tests the applicability of the RQI method as a tool for identifying and characterizing reservoir flow units in the Agbada-Akata formations. Gamma ray log, caliper log, density log and core data from the offshore Tertiary Niger Delta field were used in the petrophysical evaluation of the flow units.

Based on the petrophysical data generated, the characteristics, variability and distribution patterns of porosity, permeability and facies within the flow zones were analyzed for the reservoir sands of the formations. The properties (porosity, permeability, and facies) were distributed stochastically within a 3D grid using Sequential Gaussian Simulation, Sequential Gaussian Cosimulation, Sequential Indicator Simulation and Kriging Algorithms to describe the flow characteristics of the study reservoir.

This study has demonstrated the effectiveness of the RQI method coupled with 3D geostatistical modeling technique, as a tool for better understanding the spatial distribution of continuous and discrete reservoir properties, hence it has provided the framework for the future prediction of performance and production behavior of the Agbada-Akata petroleum system.

Keywords: Petrophysical evaluation, flow units, static reservoir models, wireline log, porosity, permeability.

ACKNOWLEDGEMENT

I am greatly indebted to my supervisor, Professor Djebbar Tiab, a visiting Professor of Petroleum Engineering at the African University of Science and Technology and a Senior Professor Emeritus of the University of Oklahoma, United States of America, Who, in diverse ways guided me on the principles of choosing the research topic and expanded the title to the frontiers of knowledge. Thank you very much for your wonderful efforts, cooperation, motivation and direction towards successful completion of this project. My heartfelt gratitude goes to the God Almighty, through whose Grace and Mercy I have reached this level of life. I also appreciate my family for all the wonderful support they have given me. To my mother, Mrs. Monica Bomful and my siblings, Pius, Godfred and Abigail, I say, I am forever grateful for your love and care.

Special thanks to my co-supervisor, Dr. Alpheus Igbokoyi. You were always there for me. My appreciation also goes to all faculties of AUST especially the heads of department: Prof. David Ogbe, Prof. Wumi Iledare, and Dr. Abdulkadir Muktar.

My sincerest gratitude also goes to my mentor, Mr. Onuh Haruna (Boss). I am full of appreciation for all the effort you put to get me data and prepare me for this project. I could not have done it without you. I will never forget how you sacrificed your time to continuously guide me. Thank you and God bless you.

I also acknowledge the support of my classmates and friends. Special thanks go to Abraham Aidoo Borsah the best room-mate ever, Daniel Rainner Lenny Ocran, Belinda Akua Abekah, Obed Kwame Senyo and Catherine Ayimah Kwatia my darling sister, it is great having friends like you.

DEDICATION

I dedicate this work to the love of my life Eva Abena Manteaw, Acquah Michael (a.k.a Carica) and not forgetting the late Kasapreko Kwame Bassanyin III , The Paramount Chief and President of Wassa Amenfi Traditional Area for their remarkable support.

I thank you very much, for your love, care, guidance and financial support during my stay at the African University of Science and Technology, Abuja, Nigeria.

TABLE OF CONTENTS

Contents **Pages**

LIST OF FIGURES

LIST OF TABLES

CHAPTER 1

1.1 Introduction

Reservoir characterization is considered to be one of the most challenging aspects of reservoir engineering, and more specifically, identification and characterization of flow units. The improvement in reservoir description is essential. This will provide extensive knowledge of the petrophysical properties so that questions concerning the amount of fluids, various types of fluids, rates of fluid flow and fluid recovery estimates can easily be answered.

Reservoir characterization relies heavily on a detailed understanding of the reservoir geology that is obtained primarily from analysis of cores and well logs. Accurate determination of pore throat attributes and fluid distribution are key elements in improved reservoir description. Presently, there is no clear-cut methodology/procedure for reservoir description.

An important aspect of the reservoir characterization process is to subdivide the reservoir into zones or reservoir flow units. As core sampling and well testing are costly and only available from limited numbers of wells, a common approach is to predict permeability using well logs by establishing a correlation based on data from the cored wells.

The fundamental key to understanding and accurately predicting the geologic controls on fluid patterns and reservoir performance is to define and correlate the distribution of flow units within the reservoir. Therefore hydraulic flow units and permeability prediction is a crucial aspect of reservoir characterization.

Several techniques have been used to improve reservoir description in the Niger Delta Province. The main focus of this study is to follow a systematic methodology in order to integrate core and well log data for the petrophysical evaluation of flow units of the Agbada-Akata formations in the Niger Delta Province.

This approach is solely based on the concept of hydraulic flow unit, which takes into consideration the mineralogy and geological attributes of the texture of petrophysical data to delineate the reservoir into units of similar fluid flow characteristics. The large volume of core information and well log data available for this study will help us to identify and characterize the significant flow units present in the Niger Delta Province.

1.2 Statement of the Problem

Hydraulic flow unit and permeability are important parameters for quantifying and characterizing reservoir rocks.

Hydraulic flow unit according to Tiab *et al.* (2000) is defined as a continuous body over a specific volume within the reservoir that practically exhibits consistent petrophysical and fluid properties, which uniquely describes its dynamic and static communication with the wellbore.

Hydraulic flow units and permeability prediction in clastic reservoirs, particularly in the Agbada-Akata petroleum system, are quite challenging due to the complex nature of pores, mineralogical composition, and high spatial heterogeneity.

The sedimentary structure of the Tertiary Niger Delta silici-clastic (Agbada-Akata) petroleum system is usually described by its late diagenetic settings. This makes the system possess various inherent geological complexities, and therefore poses major challenges to petroleum engineers, explorationists and geoscientists in modeling these systems. Although the average permeabilities of the various genetic reservoir units is relatively high, the low permeabilities of the component shale strata usually results in low sweep efficiencies and may form effective flow baffles. These clay breaks are expected to have a relatively low correlatability. The variation in clay groups as a function of depth within various depobelts, suggest that the diagenetic overprint affecting the clastic rocks of the Niger Delta are both of environmental and sedimentary origin (Weber, 1971). Therefore, extensive knowledge of the petrophysical properties is essential to better understand the reservoir fluid mechanics.

Several techniques have been used to characterize hydraulic flow units and predict the permeability distribution patterns in clastic reservoirs for improved reservoir description.

The common practice to predict permeability is to establish a relationship between porosity and permeability. One of these correlations that define the relationship between porosity and permeability for a given reservoir rock is, the Carman-Kozeny's. This relationship shows the dependency of permeability on average grain size, tortuosity, and the flow zone index. Tixier developed a simple model to estimate permeability as a function of residual water saturation and porosity of the rock formation. Morris and Biggs had also spotted the permeability as a function of connate water saturation and porosity of the reservoir rock. Timur, Coates, and Denoo also proposed other models to predict permeability.

This study seeks to adopt the Amaefule and Tiab's (1993) techniques which is the RQI and FZI Concept, to characterize hydraulic flow units and predict the permeability distribution patterns in reservoirs of the study area**.**

The technique is based on a modified Carman-Kozeny equation and the mean hydraulic radius concept proposed basically for delineating and characterizing reservoir rock formations having the same hydraulic characteristics and precise flow units. It is largely based on the microscopic measurements of rock core samples.

1.3 Objectives

The primary objective of this study is to provide a petrophysical description and properties that can be used for performance prediction. Specific objectives of the study are:

- To acquire petrophysical data from the Agbada-Akata petroleum formations
- To identify and characterize the hydraulic flow units in the reservoir for a better understanding of the flow characteristics of these formations
- To build static models of the reservoir properties to describe its flow behavior using geostatistical approach

1.4 Methodology

The methods used in this study include:

- Data collection and gathering
- Reviewing of existing literature
- Data quality assessment and quality control
- Data analysis which includes;
  Computations of input parameters
  Correlation and linear regression analysis
- Simulation runs
  Static modeling of the various flow properties
- Statistical analysis of input variables
- Discussion and Conclusions

1.4.1 Flow Chart

Proposed Flow Chart for petrophysical evaluation of flow units of the Tertiary Niger Delta silici-clastic (Agbada-Akata) petroleum system is as follows:

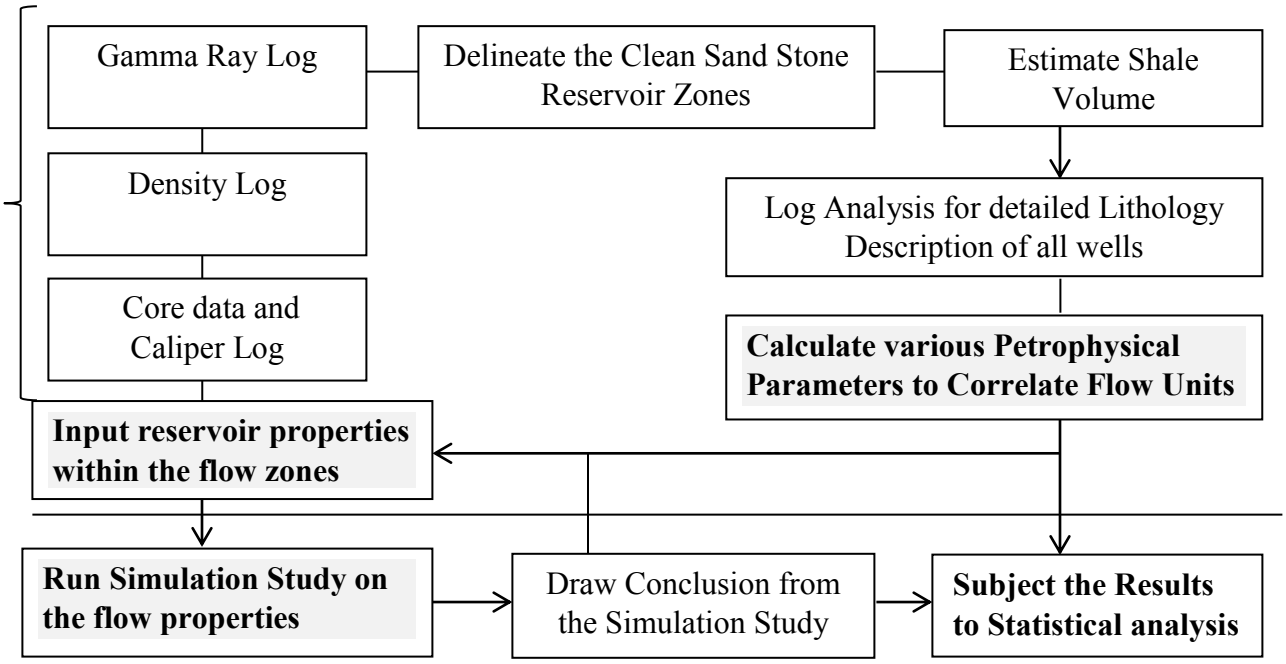

Figure 1.1: Flow chart of methods adopted in conducting the research

1.5 Facilities and Personnel

The facilities used for this project include:

- Internet and library facilities at the African University of Science and Technology, Abuja
- Technical and academic expertise of supervisors
- Computer Software which includes; Schlumberger Techlog Application suite for Petrophysical Analysis and Core Analysis, Microsoft Excel Application suite for Statistical Analysis, and SGEMS/Gaussian Simulator Modeling Tools for Geostatistical Analysis

1.6 Structure of the Report

This report consist of five main (5) chapters:

Chapter one contains the introduction, statement of the problem, objectives, method employed, and the facilities. The special personalities that were consulted during the process of executing this research are all outlined briefly in this chapter. This chapter also gives a summary of the various methods adopted in carrying out and organizing this research, as well as the process of preparing the thesis report.

Chapter two focuses on the detailed information of all necessary literature reviewed concerning this research. The topics of interest treated in this chapter consist of an overview of the study area and all relevant information about the geology and structures within. The recent methods adopted for this research area are also explained. The simulation process and software used is also discussed.

Chapter three reveals the precise method adopted in the study. The methods used to estimate and correlate the relevant petrophysical parameters examined are stated and defined. The significance of the various parameters estimated is also discussed.

Chapter four describes how all the various analyses were eventually carried out and detailed interpretations of the results were done. The equations used in correlating all relevant parameters for the petrophysical study and the result from each is analyzed. The chapter also outlines the computations that were done from the data used to ascertain meaningful parameters.

Chapter five recaps on the discussions and conclusions, as well as the recommendations that were drawn from the various analyses. The detailed interpretation of the results obtained from chapter four are also carried out.

CHAPTER 2

REGIONAL SETTING AND LITERATURE REVIEW

2.1 Geology of the Niger Delta

2.1.1 Geological Overview of the Niger Delta

The Niger Delta is found in the Gulf of Guinea and it extends across the-Niger-Delta Province. The delta was originally formed from the Eocene of the recent and pro-graded southwestward, forming series of depo-belts that significantly represent the most active region of the delta at each stage of its development. Among the largest deltas in the world, the depo-belts within the Niger Delta Province form one of the largest prolific deltas which cover a total area of about 300,000 km^2 (Kulke, 1995). The average thickness of sediments in the center of the depo-belts is about 10 km with an estimated volume of 500,000 km^3 (Kaplan, 1994).

2.1.2 Structural pattern of the Niger Delta Province

The geology of southern Nigeria and southwestern portions of Cameroon specifically describe the onshore regions of the Niger Delta Province. The province is bounded to the north by the Benin Flank, a hinge line that trends east-northeast and south by the West Africa base line. Some outcrops of the cretaceous on the Abakaliki high, define the northeastern boundary. The Precambrian is located at the east-south-east and it is bounded by the Calabar flank hinge line. The province is delineated in the offshore territory by the Cameroon volcanic line trending towards the east. The Dahomey Basin which constitutes the eastern boundary of the popular West African transform-fault passive margin trends to the west, and consists of two-kilometer sediment thickness contour, or the 4000-meter bathymetric contour in portions where sediment thickness is more than two kilometers to the south and southwest. The approximate area covered by the province is 300,000 km² and this incorporates the geologic extent of the Tertiary Niger Delta (Agbada-Akata) Petroleum System.

2.1.3 Stratigraphy

The Niger Delta Basin is generally composed of a massive clastic sequence that reaches a maximum thickness of 9,000 meters to 12,000 meters (29,500 ft. to 39,400 ft.), with an overall area of about 75,000 km². Three basic distinctive formations describe the Niger Delta province. These are the Benin, Agbada and Akata formations. The formations represent pro-grading depositional facies that are highly distinguished by their sand-shale ratios.

The Akata formation forms the base of the delta. The potential source rock is of marine origin which consists mainly of thick shale sequence, turbidite sand in potential reservoirs with deep water and minor quantities of clay and silt. The Akata formation was originally formed during low stands when terrestrial organic contents and clays were deposited into deep water regions characterized by low energy conditions and oxygen deficiency, beginning from the Paleocene through to the Recent era, (Stacher, 1995). The formation is described by its high over pressure zones and underlies the whole delta. The overall thickness of the Akata formation is 6,000 meters. Overlying the Akata formation is the Agbada formation. This formation was deposited beginning from the Eocene and continues into the Recent. It is the major sequence regarded as a petroleum-bearing formation in the Niger Delta. The formation composed of paralic silici-clastics thickness approximately 3,700 meters which represent the actual deltaic portion of the sequence. They form the accumulated clastics in delta-front, delta-topset and fluvio-deltaic environments of the province. A third formation known as the Benin formation overlies the Agbada formation. The Benin formation is a continental up-to-date Eocene to the recent deposit of alluvial with top most coastal plain sands thickness of about 2,000 meters (Avbovbo, 1978).

2.1.4 Tectonics and Structure

The tectonic setting of the continental boundary along the West Coast of Equatorial Africa is largely controlled by cretaceous fracture zones in the form of ridges and trenches, within the deep Atlantic regions. These ridges of the fracture zones subdivide the various margins into individual basins which form the boundary faults of the Cretaceous Benue-Abakaliki Trough in Nigeria and cuts across the West African shield. The Benue-Abakaliki Trough signifies a failed arm of a rift triple junction called aulacogen, which is associated with the opening of the South Atlantic regions. In this area, continental rifting started in the Late Jurassic and extended throughout the Middle Cretaceous regions (Lehner and De Ruiter, 1977).

In the Niger Delta, it is believed that rifting diminished altogether in the Late Cretaceous. Gravity tectonism is considered as the primary deformational process after the process of rifting. Shale mobility incurred internal deformation and transpired in response to two consistent processes (Kulke, 1995). The first process was the formation of shale diapirs due to the packing of poorly compacted, over-pressured, and pro-delta and delta-slope clays (Akata formation) by the relatively higher density delta front sand units (Agbada formation). The second process involves the occurrence of slope instability due to the lack of lateral and basin ward, which provide support for the under-compacted delta-slope clays (Akata formation). Gravity tectonics settings were ascertained for each of the depobelts before deposition of the Benin formation. These are expressed in complex geological structures which include shale diapirs, roll-over anticlines, collapsed growth fault crests, back-to-back features, and dipping steeply with related spaced flank faults (Evamy et al., 1978). These faults flatten into detachment planes near the upper portions of the Akata formation and usually offset certain distinct sections of the Agbada formation.

2.1.5 Lithology

Cretaceous rocks are the main lithologies deposited in what is the now Niger Delta basin and this can only be extended from the visible cretaceous regions in the next basin to the northeast of Anambra. The shoreline was concave into the Anambra Basin originating from the Campanian through to the Paleocene (Hospers, 1965). This resulted in convergent long-shore drift cells that led to the formation of river deposited sedimentation during periods of regressions and tide-dominated deltaic sedimentation for periods of sea transgressions (Reijers, 1997). Clastics of shallow marine were deposited from remote areas offshore. These are represented by the Cenomanian-Santonian Eze-Aku, Albian-Cenomanian Asu River Group, Awgu Shale, and Campanian/Maastrichtian Nkporo Shale, among others in the Anambra Basin (Nwachukwu, 1972 Reijers). Shale distribution of the late cretaceous beneath the Niger Delta is completely unknown. The Sokoto transgression which is a major transgression is considered to have occurred in Paleocene (Reijers, 1997) and originated with the Imo Shale deposited in the Anambra Basin towards the northeast, and the Akata Shale in the Niger Delta Basin area towards the southwest.

The configuration of the coastline became convexly curvilinear in the Eocene, the long-shore drift cells switched to divergent, and sedimentation transformed to being wave-dominated (Reijers, 1997). In the Niger Delta Basin, deposition of paralic sediments completely began at this time and as the sediments prograded south, the coastline became increasingly more convex seaward.

2.1.6 Depo-belts

Sedimentation cycles that make up the Niger Delta consist of deposition of the three formations which occurred in each of the five off lapping silici-clastics**.** The sedimentation cycles of the various depo-belts are 30-60 kilometers wide, prograded south-westward 250 kilometers over oceanic crust into the Gulf of Guinea (Stacher, 1995). These are well defined by syn sedimentary faulting that resulted from the various rates of subsidence and sediment supply (Doust and Omatsola, 1990). Each depo-belt is a distinctive unit that relates to changes in regional dip of the delta. The depo-belts of the delta are bounded by landward growth faults and seaward by large counter-regional faults which are growth faults of the next seaward belts (Evamy, Doust, and Omatsola, 1990). There are five main depo-belts that are commonly recognized within the delta, with each of them demonstrating their own deposition, deformation, and petroleum history (Doust and Omatsola, 1990). The shallow basement is comparatively overlain by the northern delta province and it has the oldest growth faults that are commonly rotational, evenly spaced with better steepness seaward. The dominant delta province has depo-belts with definite structures such as sequentially deeper rollover crests that move seaward for any specified growth fault. The most structurally complex distal delta province is due to the internal gravity tectonics on the modern continental slope.

2.1.7 Hydrocarbon Source

Several discussions have been made about the Niger Delta in terms of the source rock for petroleum. The leading potential zones in the delta include variable contributions from the marine shale inter-bedded with paralic sandstone in the Agbada formation and the marine Akata shale. Based on the amount and type of organic matter (Evamy, 1978) suggested both the marine shale in the Akata formation and the shale inter-bedded with paralic sandstone in the lower Agbada formation , were the potential source rocks for oils in the Delta Niger.

2.1.8 Reservoir Rock

In the Niger Delta province, petroleum is obtained basically from sandstone and unconsolidated sands, particularly in the Agbada formation. The depth of burial and the environment of deposition control the characteristics of the reservoirs present in the Agbada formation. Reservoir rocks are commonly from the Eocene to Pliocene in age, and are frequently stacked (Evamy, 1978). Kulke based on the reservoir quality and geometry describes the most significant reservoir types as a point of bars with coastal barrier intermittently cut by sand-filled channels and bars of distributary channels. The reservoir's sandstone grain size is extremely variable, with fluvial sandstones being coarser than their delta front counterparts with fine upward point bars, and barrier bars that tend to exhibit the best grain sorting. This sandstone is much nearly unconsolidated, some with a minor constituent of argillo-silicic cement (Kulke, 1995). The young age of the sediment, coolness of the delta as well as its complexities make porosity only decrease slowly with depth.

Figure 2.1 shows the schematic map for the Niger Delta Depo-belts.

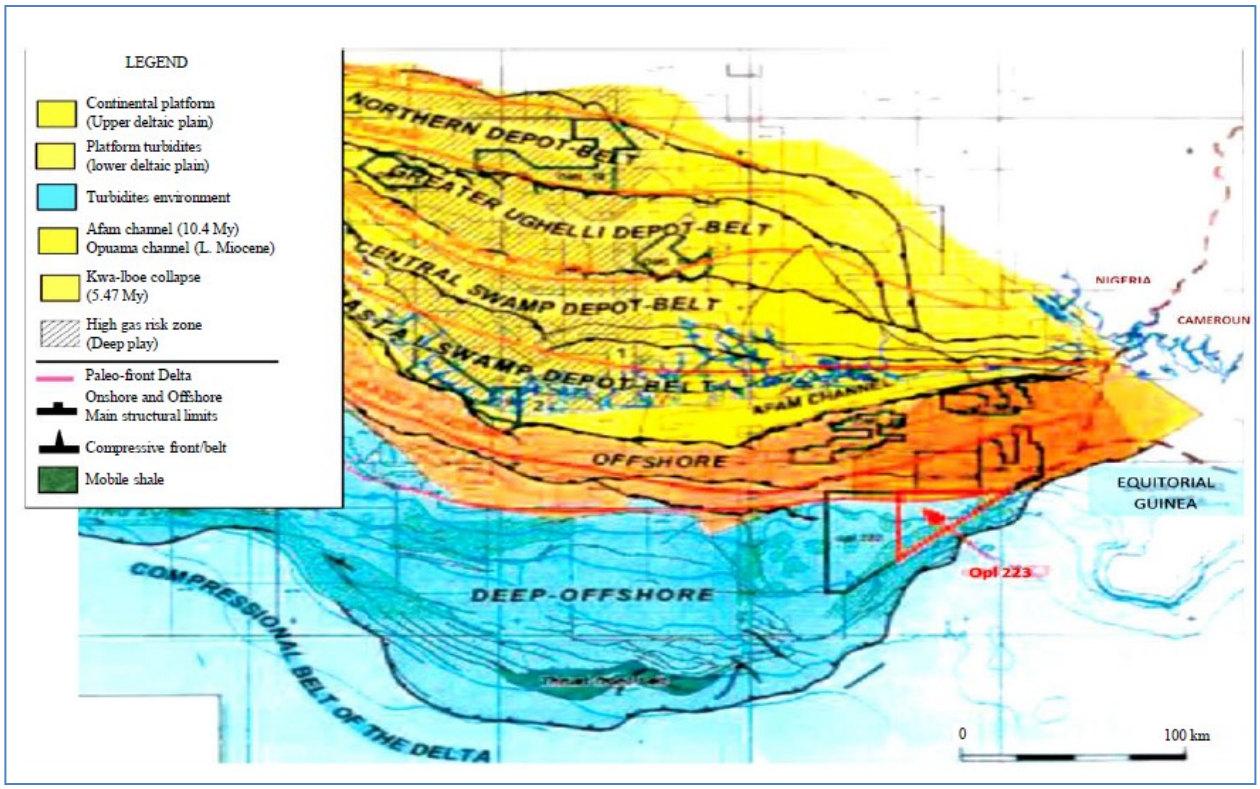

Figure 2.1: Map showing the Niger Delta Depo-belts (Ameloko *et al.,* 2013)

2.2 Types of Petrophysical Logs

2.2.1 Gamma Ray Log

Measuring of naturally occurring gamma radiations to characterize rock or sediment in a borehole or drill hole is the method used by the Gamma ray logging tool. This is a wire-line logging technique used in mining, mineral exploration, water-well drilling and for formation evaluation in oil and gas industry. Different spectra and amounts of natural gamma radiations are usually emitted by various rock types. Gamma rays are typically emitted more frequently by shales than any other sedimentary rocks such as limestone, sandstone, gypsum, salt, coal, dolomite and many more. This is because radioactive potassium is a common constituent in clay minerals and the quantity of clay is directly proportional to the quantity of radiation emitted. In this case, more uranium and thorium is adsorbed by the clay due to its cation exchange capacity nature. The gamma logging tool allows distinguishing between shales and non-shales, by using the difference in radioactivity between shales and sandstones/carbonate rocks. Like other types of well-logging, the gamma ray log process is conducted by lowering the device down the drill hole and the amount of gamma radiations relative to depth along the well bore are recorded. Generally, gamma radiation is recorded in API units, a measurement invented by the petroleum industry. Gamma logs are affected by the diameter of the borehole because of the fluid properties filling the borehole, but because gamma logs are frequently used in a qualitative way, certain corrections are usually not relevant. Radiations that are emitted by rocks are as a result of some elements and their decay chains. These elements include potassium, thorium, and uranium. Potassium is often contained in shales as part of their clay content, and tends to absorb uranium and thorium as well. Gamma-ray log commonly records the total radiation but cannot differentiate between the radioactive elements, while a spectral gamma ray log is able to distinguish between them. Standard Gamma Ray logs value measured is computed from thorium in ppm, Uranium in ppm and potassium in percent. GR API = 8 × Uranium concentration in parts per million + 4 × thorium concentration in parts per million + 15 × potassium concentration in percentage. Anomalous concentrations of uranium can cause clean sand reservoirs to appear shaly due to the weight of uranium concentration in the calculation. Anomalies in concentration can be found and interpreted by providing an individual reading for each element using spectral gamma ray.

Gamma log has advantages over some other types of well-logs because it easily penetrates through steel and cement walls of cased boreholes. Although steel and concrete absorb some of the gamma radiation; enough penetrates the steel and cement to allow qualitative determinations. Non-shales sometimes also have elevated levels of gamma radiation. Sandstones can contain potassium feldspar, uranium mineralization, clay filling or rock fragments that cause it to exhibit higher-than-usual gamma readings. Uranium may be absorbed by Coal and dolomite. Evaporites deposits may have potassium minerals such as carnallite. When this is the case, these anomalies can be identified by spectral gamma ray logging.

2.2.2 Resistivity Log

The method used by the resistivity logging in characterizing the reservoir rock or sediment in a borehole is by measuring its electrical resistivity. Resistivity basically describes the property of material which represents how strongly a material opposes the flow of electric current. Resistivity in these logs is measured using electrical probes to eradicate the resistance of the contact leads. In order to allow these types of logs to be run, the mud or fluid in the well must have electrical conductance. In mineral exploration and water-well drilling, resistivity logging is sometimes used but most commonly for formation evaluation in oil and gas industry. The enclosed fluids in most rocks conduct electric current while the rock materials are essentially insulators. However, hydrocarbon fluids do not conduct electricity due to their infinite resistive nature. Porous formation when it contains salty water has overall resistivity to be lower. The formation when it contains hydrocarbon or very low porosity, it will have higher resistivity. Hydrocarbon bearing formation may be indicated by higher resistivity values. Sometimes fluids used during drilling invade the formation and the resistivity from this invaded zone is measured by the tool, as well as a deeper resistivity where there has not been any fluid invasion. Several resistivity tools with different investigation lengths are used to measure the formation resistivity for this reason. Deeper resistivity logs (or those of the "virgin zone") will show higher resistivity if water-based mud is used and oil is displaced than the invaded zone. Deeper logs will show higher conductivity than the invaded zone if oil-based mud is used and water is displaced. An indication of the fluids present is not only provided, but also, at least qualitatively, whether the formation is permeable or not.

2.2.3 Density Log

Gamma rays with medium energy are radiated into the formation and detected. The number of rays detected depends on amount of Compton Scattering which depends on the electron density of formation and is related to the bulk density. The medium-energy gamma rays radiated into-the formation collides with electrons in the rock formation to determine porosity. Gamma ray loses some energy at each collision, but not all of its energy to the electron and then continues with reduced energy. This type of interaction is referred to as Compton scattering. At a fixed distance, the scattered gamma rays reaching a detector from the point of emission are counted as an indication of the formation density. The number of electrons in the formation is related directly to the number of Compton scattering collisions. The response of the density tool is therefore determined essentially by the electron density which is the number of electrons per cubic cm of the formation. The true bulk density in g/cm^3 is related to the electron density. This, in turn depends on the density of the rock matrix, the density of the pore fluids and the porosity of the formation.

The electron density index for a pure element, which is proportional to the electron density, is defined as: $\rho_e = \rho_b * [\frac{2Z}{A}]$ ..... (2.1)

Where:

ρ_e is the electron density index

ρ_b is the bulk density

Z is the atomic number of the element

A is the atomic weight of the element.

Fresh water filled with limestone formation of high purity to give an apparent density is used to calibrate the density tool and is related to the electron density index by:

$\rho_a = 1.0704\rho e - 0.1883$ ..... (2.2)

For limestones, dolomites and liquid filled sandstones, the apparent density read by the tool is essentially equal to bulk density of the formation. Clean formation bulk density is given by:

$$\rho_b = \Phi\rho_f + \rho_{ma}(1 - \Phi) \quad \text{..... (2.3)}$$

The matrix and fluid densities must either be known or assumed so that this equation can be solved for porosity. The fluid density in most cases is assumed to be 1.0 g/cm^3 whereas the density for sandstone matrix is assumed to be 2.65g/cm^3. Density log has depth of investigation to be relatively shallow. Therefore, the pore fluid in most permeable formations is considered to be the drilling mud filtrate along with any residual hydrocarbons. High residual hydrocarbon saturations can cause the calculated porosity values to be higher than the actual porosity. Hence, corrections must be applied to this effect.

2.2.4 Neutron Log

In this method, neutrons with high energy are emitted into formation. The amount of neutrons that are captured are detected and the stage of their capture from the transmission point recorded by two receivers. This effect is mainly due to the number of hydrogen in formation. This wire-line log method is used in combination with the density log to detect presence of gas in formation, identification of GOC (gas oil contact), as well as identifying the lithology of the formation. The basic idea behind the neutron logging method is as follows; a neutron sonde which comprises a radioactive source emits active neutrons into the formation. Energy is lost by the neutrons as they bombard with the nuclei of the atoms in the formation and this process continues until the energy of the neutrons has fallen to the thermal energy. Thermal neutrons reach their peak in distribution at a shorter or longer distance from the source, depending on the efficiency of the formation to slow the neutrons. The amount of hydrogen present determines the ability of the formation to slow down neutrons. This is due to the fact that, the nucleus of a hydrogen atom, a proton, has approximately the same mass as a neutron, and causes maximum energy to be lost by the neutrons for each bombardment. The position of the peak in the thermal neutron distribution is located by two neutron detectors. The interpretations for the amount of hydrogen present in the formation depend on distance of this peak from the neutron source. This can then be converted into the amount of water or hydrocarbon present.

2.2.5 Sonic Log

Transmitters and receivers are parts of typical sonic logging tool, usually placed in the wellbore. Pressure pulse in the borehole fluid is generated by the transmitter. When this pulse reaches the borehole wall, it generates primary and secondary wave-fronts in the formation. The portions near the wellbore create pressure disturbances in the borehole fluid as the waves travel away from the source in the formation. These fluid waves are referred to as head waves and they travel at the same velocity as the wave-fronts that created them. The sonic logging tools then record the head waves.

2.2.6 Caliper Log

The caliper logging tool measures the shape and size (diameter) of a bore hole along its depth. The tool has two, four or more elongated arms. The in and out movement of the arms of the tool, is converted into an electrical signal by potentiometer as the tool is withdrawn from the bore hole. The caliper logs are plotted in tracks to compare the drilling bit sizes, as discrepancy caliper reading, where the reading indicates the caliper value minus the drill bit size. The scale is usually given in inches, which is standard for measuring bit diameter.
Principal uses of the caliper log include:

- Providing contributory information for assessment of lithology
- Determining good permeability and porosity zones of reservoir rocks, due to the development of mudcake in association with gamma log
- Computation of mudcake thickness
- Borehole volume measurement
- For cement volume measurements

2.3 Importance of Well Logging

The geophysical parameter being recorded continuously along a borehole produces a geophysical well log. Well log is very essential with respect to its interpretation to describe the geophysical parameter along a well bore. Measurement values for well logs are usually plotted continuously against respective depth in the well. Successful development of a hydrocarbon reservoir depends largely on well logging.

Measurements from a well log is essential in the life of a given well because it has absolute influence on the decision for the well location and the formation evaluation.

2.3.1 Uses of Well Logging in the Petroleum Engineering

In the oil and gas industry, well logging plays a central role. The most important application and purpose of well logging is to provide measurements which can be connected to the type of hydrocarbon present and volume fraction in porous formations. Well logging measurement techniques are used from three broad perceptions. These are the nuclear, electrical and acoustic. The measurement is usually sensitive either to the pore-filling fluid or the properties of the rock. The applications of well logging for petroleum engineering are stated below:

- Rock typing and petrophysical studies
- Geological environment identification
- Reservoir fluid contact location
- Detection of fractures
- Estimation of hydrocarbon in place
- Estimation of recoverable hydrocarbons
- Estimation of water salinity
- Determination of average reservoir pressure
- Determination of porosity or pore size distribution
- Feasibility of water flooding studies
- Mapping of reservoir quality
- Probability assessment of inter-zone fluid communication
- Monitoring of reservoir fluid movement

2.4 Methods for Petrophysical Analysis of Flow Units

The recent discovery of significant amounts of hydrocarbons in clastic reservoirs has necessitated the need to re-focus on obtaining a better understanding of the petrophysical properties of these formations. Many methods have been proposed to derive flow unit to improve reservoir description and to increase the confidence in petrophysical analysis of clastic reservoirs. The most common among these techniques include:

1. Amaefule and Tiab‘s (1993) FZI Method
2. Gunter *et al.* (1997) Stratigraphic Flow Profile (SFP)
3. Gunter *et al.* (1997) Winland R35 Porosity-permeability Cross Plot
4. Gunter *et al.* (1997) Stratigraphic Modified Lorenz Plot (SMLP) and
5. Gunter *et al.* (1997) Modified Lorenz Plot (MLP)

These methods begin by establishing rock types within a geologic framework. The geologic framework allows the flow units to be interpreted within a sequence stratigraphic model determining well-to-well correlation strategies.

The key flow unit characteristics to be identified are barriers (seal to flow), speed zones (conduits), and baffles (zones that throttle fluid movement).

2.4.1 Concept of Flow Units

The hydraulic concept of flow units was proposed by Hearn *et al.* (1984) to assist in grouping sedimentary facies into units which imitate a specific environment of deposition and thus signifies peculiarities of fluid flow. These models are characterized by sudden lateral changes in petrophysical properties at flow-unit boundaries (Silseth *et al.,* 1993). Separation of a sedimentary interval into flow units is somewhat critical and is very sensitive to the available core and well data used. It is commonly based on concerns of reservoir stratigraphy and vertical and lateral distribution of parameters of the reservoir. Flow units delineation is more complicated by the fact that these units do not essentially coincide with the reservoir facies. This indicates that they may not be areally contiguous (Canas, 1993). The flow units delineated usually reflect the ability of rocks to conduct fluids and can, therefore, be considered as a grid block in the flow reservoir simulation study. Several techniques have been suggested to derive flow units (see Hearn et al., 1984; Silseth et al., 1993; Ti et al., 1995).

2.4.2 Characteristics of Flow Units

The concept of flow units by Amaefule *et al.* (1993) revealed that flow units have the following characteristics:

i. **Flow units referred to as definite volume of a reservoir; consist of one or more reservoir quality lithologies and non-reservoir quality features within the same specific volume including the fluids they contain.**

Flow units are inherent in nature, but not essentially homogeneous, in terms of either petrophysical characteristics or geological framework. Flow units may contain more than one reservoir quality lithology and may include non-reservoir features such as cemented layers and shales. Petrophysical properties may correspond to certain lithofacies geologically defined.

Petrophysical similarities, however, among lithofacies may specify that those lithofacies should be classified into one flow unit if they are contiguous. Also, petrophysical differences within a geologically defined lithofacies may predict that subdivision of a single lithofacies into several flow units is guaranteed.

Flow unit zonation changes in principle from a lithofacies zonation in that, it incorporates petrophysical, geological and production data with the aim of defining fluid flow paths in the reservoir, not distribution of lithologies in a given depositional environment.

ii. Flow unit is mapable and correlative within given interval scales.

Flow units are deterministic components used for describing reservoirs; they are usually of scales that are correlative and mappable relative to a given well spacing.

Flow units are continuous at interwell scales, but they do not cut across the entire reservoir. This is because certain parts of a reservoir can effectively be drained only on closer well intervals, some definition of flow units may differ with infill drilling and in production mechanism such as water flooding initiation during field life of the reservoir.

iii. Zonation of flow unit is recognizable on wire-line log.

In the subsurface, mapping individual flow paths require that flow units be recognizable on wireline logs. Recognizing flow units only in the core are valuable if only all wells have been cored. Some methods must be adopted to explain a flow unit zonation based on core data to flow zonations using wireline log suite available in a specific reservoir.

iv. Flow unit may be in communication with other flow units for the same reservoir.

Communication with other flow units may occur across the reservoir boundaries with respect to both pressure and ability to conduct fluids vertically and laterally, or they may be absolutely separated from one another by permeability baffles and barriers. The basic requirement for defining flow unit is that reservoir volumes in which properties significantly affect fluid flow differ consistently. However, the intensity of these volumes should be delineated in the subsurface depending predominantly on wireline logs at existing well intervals.

2.4.3 Theory of Flow Units

The theory of hydraulic flow unit was proposed by Amaefule *et al.* (1993) to be used as the basis for subdividing reservoirs in various rock types reflecting distinctive pore-throat attributes. A hydraulic flow unit (HFU) represents specific volume or section within the reservoir rock. Petrophysical and geological properties are different in each hydraulic flow unit. It varies from properties of other sections of the reservoir. A flow unit is thus, a reservoir unit that is vertically and laterally continuous, and exhibits the same flow and bedding characteristics. The pore geometry controls the hydraulic quality of a rock. This is a function of the mineralogical composition such as the type, abundance, morphology, and location comparative to pore-throat and texture in terms of grain size, grain shape, sorting and packing. Permutations of geological attributes frequently show the existence of different rock units with same pore throat attributes. Accurate zoning of reservoirs into units with similar hydraulic properties determines the pore throat attributes. The concept of mean hydraulic unit radius (r_{mh}) is vital to delineate the hydraulic units and links permeability, porosity and capillary pressure.

$$r_{mh} = \frac{\text{Cross Sectional Area}}{\text{Wetted Perimeter}} = \frac{\text{Volume open to flow}}{\text{Wetted surface area}} \quad \ldots\ldots (2.4)$$

For a circular, cylindrical capillary tube

$$r_{mh} = \frac{r}{2} \quad \ldots\ldots (2.5)$$

Carman and Kozeny (1938) invoked the concept of the mean hydraulic radius by considering the reservoir rock to be composed of a bundle of capillary tubes. This was based on the application of Darcy's (1856) and Poiseuille's (1838) Laws to derive a relationship (Eqn. 2.6) between porosity and permeability of the reservoir rock. The basic assumptions used in their derivation are that "the average time of a fluid component in a capillary tube is equal to that in a representative elementary volume (REV) given that porosity is effective.

$$K = \frac{\Phi e r^2}{8\tau^2} = \frac{\Phi e}{2\tau^2}\left(\frac{r}{2}\right)^2 = \frac{\Phi e r^2 mh}{2\tau^2} \quad \ldots\ldots (2.6)$$

The mean hydraulic radius (rmh) is related to the effective porosity (Φ_e) and surface area per unit grain volume (S_{gv}) of the rock by the equation below:

$$S_{gv} = \frac{2}{r}\left(\frac{\Phi e}{1-\Phi e}\right) = \frac{1}{rmh}\left(\frac{\Phi e}{1-\Phi e}\right) \quad \ldots\ldots (2.7)$$

Substituting Eqn. (2.7) for r_{mh} in Eqn. (2.6), Carman and Kozeny (1938) arrived at the following relationship for permeability as follows:

$$K = \frac{\Phi e^3}{(1-\Phi e)^2} \left[\frac{1}{2\tau^2 S^2 gv}\right] \quad \text{..... (2.8)}$$

Where k is in μm² and Φ_e is a fraction.

The Carman–Kozeny (1938) relationship in the generalized form is given by Eqn. (2.9)

$$K = \frac{\Phi e^3}{(1-\Phi e)^2} \left[\frac{1}{Fs\tau^2 S^2 gv}\right] \quad \text{..... (2.9)}$$

Where F_s represents the shape factor; 2 for circular cylinder. The term $Fs\tau^2$ has officially been known as the Kozeny constant. Carman (1937) and Leverett (1941) calculated the value of this term to be about five (5) for ideal cases of uniform and unconsolidated reservoir rocks. However, Rose and Bruce (1944) proved that this term ($Fs\tau^2$) could vary from 5 to 100 in actual reservoir rocks. Many researchers have attempted to compute permeability from porosity by using Eqn. (2.9) These investigations have not generally been successful because of the constant use of the value (typically 5) for ($Fs\tau^2$) and the inability to consider S^2gv in these calculations. Practically, the Kozeny constant is a variable "constant" which remains the same within a given reservoir unit but varies consistently between hydraulic units.

The issue concerning the variability of the Kozeny constant is addressed as follows:

Dividing both sides of Eqn. 6 by porosity (Φ_e) and taking the square root of both sides yields

$$\sqrt{\frac{k}{\Phi e}} = \left[\frac{\Phi e}{1-\Phi e}\right] \left[\frac{1}{\sqrt{Fs}\ \tau Sgv}\right] \quad \text{..... (2.10)}$$

Where k is in μm²

If permeability is however presented in millidarcies, then the following parameters can be defined:

$$RQI\ (\mu m) = \text{Reservoir Quality Index} = 0.0314 \sqrt{\frac{k}{\Phi e}} \quad \text{..... (2.11)}$$

$$\Phi_z = \left(\frac{\Phi e}{1-\Phi e}\right) \quad \text{..... (2.12)}$$

Where Φz represents the pore volume to grain volume ratio of the rock; also called normalized porosity.

FZI (μm), designated as the flow zone indicator, is given by:

$$FZI = \frac{1}{\sqrt{Fs}\ \tau Sgv} = \frac{RQI}{\Phi z} \quad \text{..... (2.13)}$$

Substituting these variables into Eqn. (2.10) and taking the logarithm of both sides gives

$$\text{Log RQI} = \log \Phi z + \log \text{FZI} \quad \ldots\ldots (2.14)$$

According to the flow unit concept, all samples with similar FZI values will lie on a straight line with unit slope on log- log plot of RQI versus Φz. However, samples with different FZI will lie on other parallel lines. The value of the FZI constant can be determined from the intercept at $\Phi z = 1$ of the unit slope line.

Samples that lie on the same straight line possess similar pore throat attributes and hence constitute a hydraulic flow unit (Amaefule *et al*., 1993).

Different relationships that yield FZI values similar to those derived in Eqn. (2.14) have also been developed from Eqn. (6) as follows:

If k (md), FZI (μm) and Φ_e (fraction) then we can obtain permeability as below:

$$K = 1014(FZI)^2\left[\frac{\Phi e^3}{(1-\Phi e)^2}\right] \quad \ldots\ldots (2.15)$$

If Φ_R is defined as

$$\Phi_R = \frac{\Phi e^3}{(1-\Phi e)^2} \quad \ldots\ldots (2.16)$$

Then

$$K = 1014(FZI)^2\,\Phi_R \quad \ldots\ldots (2.17)$$

Taking the logarithm of both sides of Eqn. (2.17) then results in

$$\log K = \log(\Phi_R) + \log[1014(FZI^2)] \quad \ldots\ldots (2.18)$$

A log-log plot of k versus Φ_R results in a straight line with a unit slope and an intercept (at $\Phi_R = 1$) of $1014(FZI)^2$. Some researchers have made attempts to zone reservoirs into various layers by using the parameter (k/Φ). Dividing both sides of Eqn. (2.15) by Φ gives the results below:

$$\frac{k}{\Phi e} = 1014(FZI)^2\left[\frac{\Phi e}{1-\Phi e}\right]^2 = 1014\,(FZI)^2\,(\Phi z) \quad \ldots\ldots (2.19)$$

Taking the logarithm of both sides of Eqn. (2.20) yields

$$\log\left(\frac{k}{\Phi e}\right) = 2\log\Phi_z + \log[1014(FZI)^2] \quad \ldots\ldots (2.20)$$

A log-log plot of (k/Φ) versus Φ_z results in a straight line with a slope of 2 at an intercept of $\Phi_z = 1$ of $1014(FZI)^2$. All samples with similar FZI values as noted earlier belong to the similar hydraulic unit and will, definitely, lie on the same straight line. The FZI designated as, "FIow Zone Indicator" is determined at the intercept of the unit slope line with $\Phi_z = 1$. This is a unique parameter for each hydraulic unit delineated. RQI, Φ_z and FZI are based on permeability data and stressed porosity measured on rock core samples.

2.4.4 Wells Correlation of Flow Units

Flow units delineation in each well permits us to define the original stratigraphic correlations and identify the distribution of interwell flow units. Correlating flow paths between individual wells is a highly crucial process because there are many possible dimensional arrangements of flow units. Not only a number of layers derived from the flow units with similar characteristics can be different, but also the spatial architecture can be different. In this study, flow units in each well were identified, correlated and grouped into a different number of layers for use in a stimulation study to build a static model of the flow properties.

Figure 2.2 shows an example of a cross-section of flow units and their distribution between three wells.

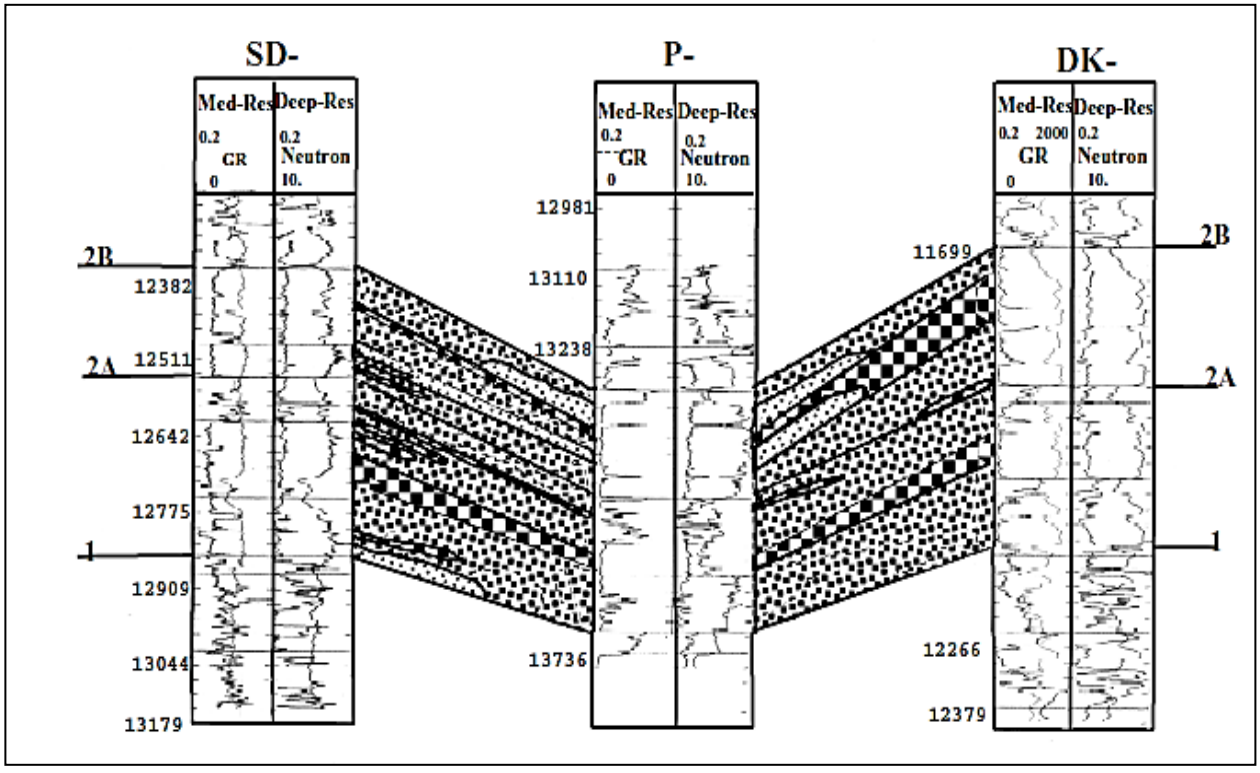

Figure 2.2: Example of interwell distribution of flow units (Artem Ratchkovski *et al.,* 1999)

2.5 Work Flow

1. Sampled depth from matched well logs
2. Delineate the Top and Bottom/Base Sands using well logs
3. Delineate permeable (good porosity and permeability) zones from well logs
4. Volumetric computation of shale content and effective porosity
5. Computation of petrophysical parameters from adjusted geological core and log values
6. Identification and correlation of flow units from adjusted values
7. Static modeling of flow properties using Geostatistical approach

2.5.1 Limitations

1. Delineation of reservoirs into flow zones and facies classification absolutely depends on the interpretation of the individual.
2. Thin shale layers zones within sand units may be overestimated as the net sand thickness.
3. Hard streaks may be included as being clean sand zones.
4. Sand laminae less than an inch was not captured since high resolution operation is required. This may result in under-estimation of resources.

2.5.2 Laminated Shaly Sands

Petrophysical parameters such as shale volume, porosity, and water saturation are important for estimating layers of sand. The most essential of all the parameters is the shale content because it controls the other two parameters. Therefore Vsh values should be well estimated. This is ascertained by using different techniques in the estimation of Vsh. Also, it is necessary to integrate with an external data source such as core data. The values of Vsh and total porosity are used in the Thomas Stieber (1975) method to estimate shale distribution.
There are three basic categories of shale distributions. These are:
1. Laminated- a layer of shale found in the sand.
2. Dispersed shale which is found on sand grains or pore filling.
3. Structural sand-sized shale particles in load bearing position within the rock.

Shale distributions as well as the porosity can be computed directly from Thomas-Stieber cross-plot, where total porosity on the y-axis is plotted against the volume of shale on x-axis respectively.

In this cross plot, depending on the position of data points, laminar (V_L), dispersed (V_D), structural (V_S) shale volumes and porosity of sand laminae can be estimated using the following correlations:

1. Dispersed Shale only ($V_{SH} = V_D$)
   $\phi_T = \phi_{MAX} - V_D (1 - \phi_{Tsh})$

2. Laminated Shale only ($V_{SH} = V_L$)
   $\phi_T = \phi_{MAX} - V_L (\phi_{MAX} - \phi_{Tsh})$

3. Structural Shale only ($V_{SH} = V_S$)
   $\phi_T = \phi_{MAX} + V_S \phi_{Tsh}$

4. Material Balance Equation for Shale
   $V_{SH} = V_L + V_D + V_S$

For special cases where the volumetric content of dispersed shale is minimal, then the hydrocarbon saturation can be estimated directly from the Archie equation. Alternatively, there are other equations that can be used, provided the volume of shale is significant. These include the Waxman-smith, Clavier and Larionov‘s equation.

2.6 Reservoir Modeling

Reservoir modeling is basically the construction, planning and operation of a model whose behavior mimics the behavior of the actual reservoir. In reservoir modeling, computable procedure or mathematical algorithms are normally used to infer and gain insights into the physical behavior of the real reservoir under study. Petrophysical parameters estimated in the field have been a critical aspect in the development of petrophysics due to the desire to quantify the uncertainty associated with them. Several attempts have been made to completely describe and understand the various uncertainties associated with petrophysical parameters. Reservoir modeling and its applications to quantify uncertainties have brought better comprehension in the accuracy of results from uncertain inputs.

2.6.1 3D Static Modeling

Static modeling specifically involves a combination of stratigraphic, structural and property models into one single model to describe the reservoir. It basically involves populating the reservoir architecture such as the stratigraphy and structure with the reservoir rock properties.

The static model helps to capture the behavior of the pores to describe the flow characteristics within the area of interest in the reservoir.

2.6.2 Geostatistical Analysis Software (SGEMS)

SGEMS means Stanford Geostatistical Earth Modeling Software. This is a computer application suite designed fundamentally for solving real life problems involving spatially related parameters. It gives geostatistics analysts a platform with a three-dimensional view, interactive interface, and a broad perspective of algorithms.
More recent development is its application in multiple-point statistics simulation technique, mostly adopted by industries including the oil and gas industry for characterizing reservoirs of various types (Kelsall and Wakefield, 2002).

2.6.2.1 Kriging as a Geostatistical Tool

The principle behind kriging is that it uses sampled points at a known location to populate points at the unsampled locations. However, to obtain the best linear unbiased predictor, kriging takes into account the covariance structure. The covariance structure is a function of distance which is used to predict new locations on the basis of the distance between the pairs. This Geostatistical approach provides selected models such as variogram models which affect the prediction of the unknown properties, especially when the shape of the curve close the origin varies significantly. The neighboring data points have total influence on the prediction of the property if the curve distribution close to the origin is relatively steeper in nature.

2.6.2.2 Gaussian Simulation Module

The Gaussian Simulator allows you to:

- Run simulations in your existing PS pad-based models using DAT extension
- Generate equiprobable realizations and extract simulation predictions
- Perform distributional fitting and finding best-fitting statistical distribution
- Perform geostatistical analyses between different estimated parameters of interest

2.6.3 Permeability Prediction

One of the most critical aspects of geologic model preparation is mapping the permeability distribution in a reservoir for performance-prediction studies. The basis in the geology and the physics of flow at the pores scale depends on the permeability prediction/correlation method used. This is very important although it seems complex, it is best ascertained by establishing connectivity between porosity and permeability to geological variations in the reservoir rock, and expressing permeability as functional relationships that capture the geological attributes of fluid flow characteristics. Predicted permeability values from regression model lack the variability observed in the geological core data because the regression-based methods only assign a single trend to data. Hydraulic flow unit classification offers an improved approach over the traditional regression-based method since ‘‘average relationship’’ is used to estimate permeability. Also, it incorporates fluid flow principles and geology into the process. In this study, the permeability within the identified flow zones in the reservoir is predicted by the Geostatistical approach using kriging tools.

CHAPTER 3

STUDY METHODOLOGY

3.1 Outline of Methodology

The methods adopted for analysis of the corrected petrophysical log data is as follows:
1. The gamma ray log was imported into petrophysical analysis software to delineate the sand zones. This was done after correlating all the wells with common baseline using gamma ray log reading a value of 15 GAPI for clean sand. The gamma ray log is also used for estimating the shale content for each of the gross sand thickness delineated. This is ascertained by first computing the gamma ray index and then using the gamma ray index in the Larionov‘s (1969) equation for tertiary rocks to evaluate the volume of shale within the study reservoir.

2. The total porosities for all the gross sand zones delineated were estimated from the density logs. The relationship established between the core-derived and the log data is then used to correct the estimated porosities. More representative porosities were generated by averaging the porosities over the sand zones that were delineated. The effective porosities are then determined from the corrected porosities by adjusting the calculated porosities for the volume of shale present in the reservoir sands.

3. The caliper, as well as gamma logs are used in techlog-view to obtain permeable zones in the various wells of interest. These logs are used to establish zones of good porosity and permeability for lithological assessment and flow unit correlations. The caliper log provided continuous measurements of the shape, size as well as the rigorosity of the holes along its depth. The Gamma logs are attenuated by the diameter of the hole because of the properties of the fluid filling the bore-hole. The caliper log is used to assess the quality of the hole against bad-hole conditions in each well.

4. Permeabilities within the gross sand zone are computed from established correlations and net pay cutoff for porosity is established from these permeabilities. Also, effective porosities are computed as well.

5. The permeability is used with the porosity to establish and correlate the flow units within the reservoir sands. This is done to define the possible flow path of liquids during production as well as to establish the best possible intervals for perforation to obtain optimum recovery.

6. Geological/Static modeling is built to describe the flow characteristics of the reservoir using simulation tools. Permeability, porosity and facies (sand and shale volume) within the reservoir sands is predicted with the Gaussian Simulator/SGEMS, and results obtained from the simulation study are subjected to statistical analysis.

3.1.1 Flow Chart of Methodology

A flow chart describing the methodology used in this study is represented in figure 3.1.

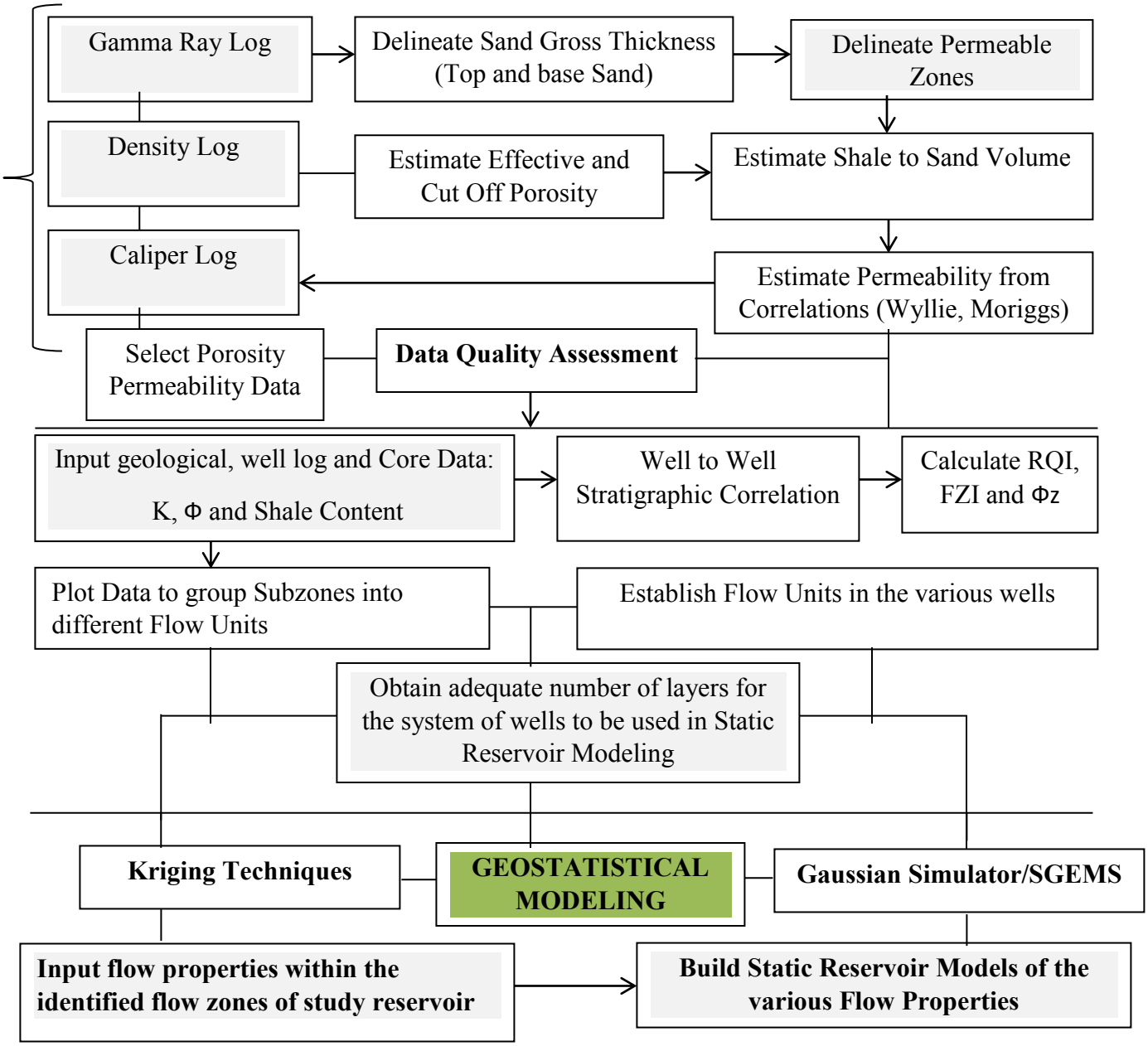

Figure 3.1: Flow chart showing the data analysis processes involved in the study

3.2 Lithology Determination from Wire-Line Logs

The various log data for each of the six active wells of interest acquired in the systematic methodology adopted above were plotted on the techlog-view and interpreted. This was done after core-derived data have been corrected alongside the log data for quality assurance. Since there was core data for only four wells, the correction was first made for these wells before it was extended across the other wells of the study reservoir. Lithological determination and its interpretation were carried out, from which sand and/or shale were basically delineated and compared at a given measured depth laterally to the gamma ray logs on the petrophysical analysis software view. These interpretations were also performed for other logs which included: caliper and density. The lithology was noted and matched to the core for depths for which all the logs gave the same interpretation. There was quality checking in areas where the various logs gave incoherent interpretations. This was done in order to detect possible reasons for the errors incurred as well as to correct the inconsistencies in the interpretations.

3.3 Estimation of Petrophysical Parameters

The various petrophysical parameters used in this study were estimated using well established equations and methods, which conform to the Niger Delta Petroleum Province. The petrophysical parameters of interest namely permeability, porosity, shale volume, net thickness and net pay cut-offs were used in the delineation of the various flow zones, as well as estimation of the reserves within the Agbada-Akata formations.

The procedure for estimating all relevant petrophysical parameters is described briefly as follows:

3.3.1 Net Pay Thickness (Net/Gross)

The net pay thickness is the section within the reservoir from which hydrocarbons, .i.e., oil and or gas can be produced at economic conditions, given a specific recovery method. The fraction of the sum of the thicknesses of the net pay zone to the total thickness or depth of the well under study describes the net-to-gross ratio of that reservoir. The gross thickness is usually obtained by measuring from the top of the well to the base, while the net thickness is composed of the accumulation of delineated net pay zones as established with the various petrophysical logs.

From the above concept, the ratio of the net to gross reservoir thickness is estimated for all the various wells. To assess the impact of all the wells net to gross values, an average net to gross is then calculated.

3.3.2 Shale Volume

Reservoir sand units delineated by gamma ray logs are often not expected to be 100% but a combination of predominantly sand intercalated with some minor and major amount of shale or clay minerals. Shale is usually more radioactive than sand and therefore its volume in porous reservoirs can be estimated. The amount of shale expressed as a decimal fraction or percentage is called Vshale. Calculation of the gamma ray index is the first step required to estimate the amount of shale from gamma ray logs.

The gamma ray index designated I_{GR} is first computed from the gamma ray log as below:

$$I_{GR} = \frac{(GR_{log} - GR_{min})}{(GR_{max} - GR_{min})} \quad \text{..... (3.1)}$$

Where:

I_{GR} is the gamma ray index

GR_{log} is the Gamma Ray Log reading of the formation

GR_{min} is the Gamma Ray for a complete sand matrix zone (Clay free zone)

GR_{max} is the Gamma Ray for a complete shale zone (100% Clay zone)

The Volume of shale is then determined using the gamma ray index obtained above using the Larionov's (1969) equation for calculating the volume of shale for tertiary clastic reservoirs.

$V_{sh} = 0.083*[2^{(3.7*IGR)} - 1]$ ..... (3.2)

3.3.3 Porosity

The porosity of a reservoir rock is the volume of the void spaces expressed as a percentage of the given total or bulk volume of the rock. Besides the presence of pore spaces in a rock volume, the magnitude of these pores is also relevant with respect to the movement of fluids.

According to this definition, porosity of any porous media could have any value, but the porosity of a sedimentary rock is generally much lower than 50%.

During the sedimentation process by which the rock was originally formed, primary porosity is usually developed. The total porosity of the reservoir in this report is estimated by using the density log.

The porosity of the reservoir rock was computed as shown in the following equations:

$$\Phi_{TD} = \frac{(\rho_{ma} - \rho_b)}{(\rho_{ma} - \rho_f)} \quad \text{..... (3.3)}$$

Where:

$\Phi_T = \Phi_{TD}$ = Total Porosity estimated from density log

ρ_{ma} = Matrix (or grain) density

ρ_b = Bulk density (as obtained from the tool and hence includes porosity and grain density)

ρ_f = Density of the fluid.

Following the above calculation, the effective porosity was then determined using the equation given below:

$$\Phi_e = \frac{(\rho_{ma} - \rho_b)}{(\rho_{ma} - \rho_f)} - \left[V_{sh} * \frac{(\rho_{ma} - \rho_{sh})}{(\rho_{ma} - \rho_f)}\right] \quad \text{..... (3.4)}$$

$$V_{sh} * \frac{(\rho_{ma} - \rho_{sh})}{(\rho_{ma} - \rho_f)} \quad \text{..... (3.5)}$$

Where:

Φ_e = Effective porosity

ρ_{sh} = Density of shale

Equation (3.5) = Clay bound water

(ρ_{ma} = 2.65g/cm^3, ρ_f = 1.0g/cm^3, ρ_{sh} = 2.60 g/cm^3)

3.3.4 Net Thickness

The permeability-porosity cross-plot was used in this study to determine porosity cut off for the reservoir. This application is the rule of thumb for establishing base permeability for the estimation of porosity cutoffs.

According to this rule of thumb, the porosity cut off for oil zones principally correspond to permeability equal to 1mD, whereas the permeability of 0.1mD was applied to obtain the cut-off porosity for the gas zones. A 45% cut-off for shale volume was applied and the cut-off applied for water saturation was also 45%, respectively. Porosity, as determined from the permeability-porosity cutoff analysis using a shale volume less than 45% defines the reservoir of interest. In this case, a significant amount of hydrocarbon is considered to be contained by the reservoir when the water saturation is less than 60%.

The following figure shows the porosity net thickness cut-off for oil determined in the reservoir.

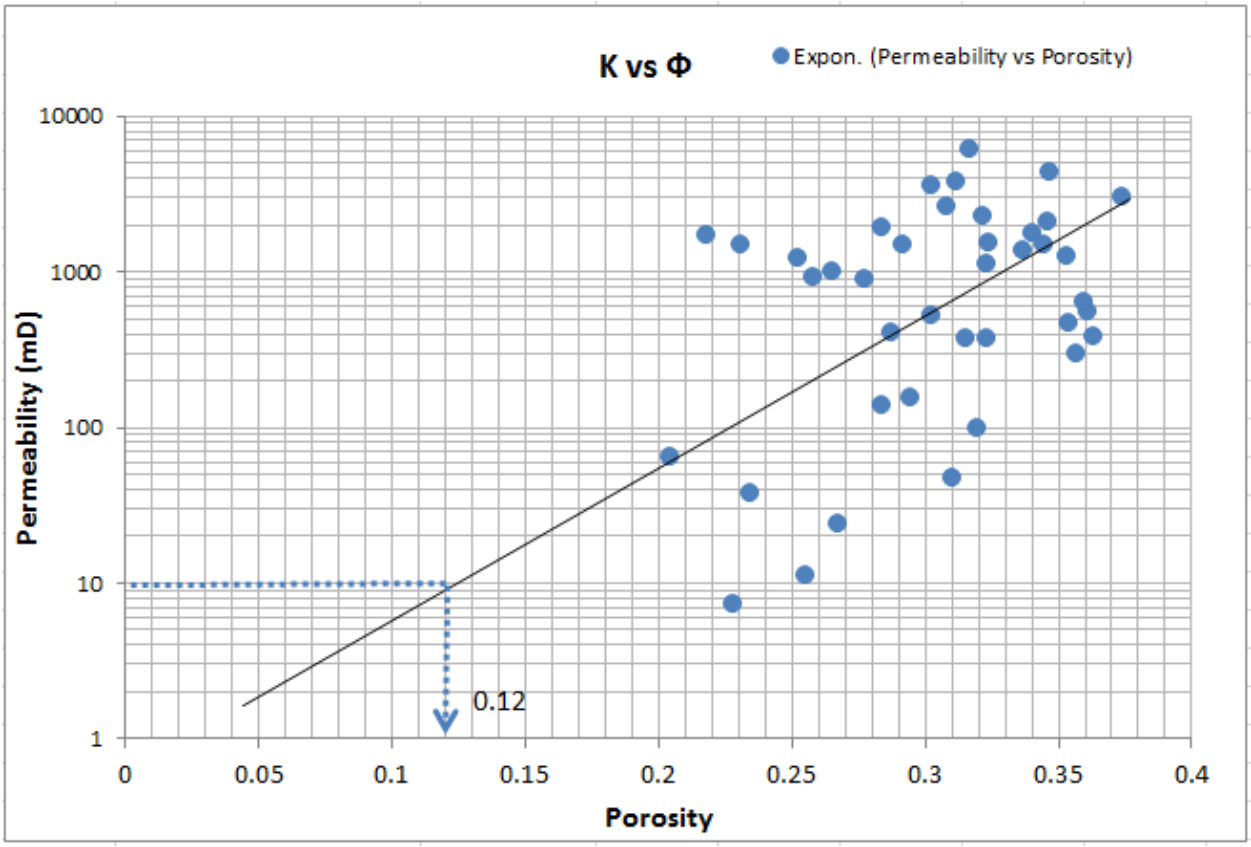

Figure 3.2: Graph showing the porosity cut-off determination for delineation of net pay

3.3.5 Permeability

The ability of fluid to migrate through the reservoir is largely controlled by the permeability. In the study of subsurface fluid movement, permeability is essential in the productivity of every reservoir. It is one of the most critical petrophysical parameters. This is because permeability contributes massively to the prediction of fluid flow patterns in a given reservoir. In the actual case, the permeability should definitely increase with increasing porosity, average grain size as well as improved packing and sorting in sandstone or clastic reservoirs.

The fact that the permeability is an essential parameter, it cannot be obtained directly from well logs. It is therefore estimated primary from indirect methods such as the use of applicable empirical and well-established correlations. In this study, the Timur (1968) equation, Coates and Denoo (1981) as well as the Morris Biggs (1967) Oil equation are adopted to estimate the permeability. The averages of the values of permeability were obtained from these correlations or methods. The equations employed in the permeability determination are as follows:

Timur Equation

$$K = 8581 * \frac{\Phi^{4.4}}{S^2} \quad \text{..... (3.6)}$$

Morris Biggs Oil Equation

$$K = 62500 * \frac{\Phi^{6}}{S^2} \quad \text{..... (3.7)}$$

Where:

K = permeability

$\Phi = \Phi_e$ = effective porosity

$S = S_{wi}$ = irreducible water saturation

3.4 Cores

Accurate delineation of flow unit depends on the availability of core data from the wells in the study area. Basically, core data is used to calibrate data obtained from well logs. They are usually used as a reference point to substantiate the lithology interpretation from wire-line logs. Cores allow determination of parameters which in essence provide a better understanding of wire line logs.

In this study, the core and log data for porosity is used to establish the relationship between these two data sources for quality control purposes. Core data was only available for well 1, well 2 well 3 and well 4. The core porosities were plotted against the respective log porosities to establish a relationship between these parameters. A line of best fit was established to determine the correlation coefficient from the relationship between the core and log data. The coefficient was first determined to be 0.77, representing 77% correlation between the plotted data. The data was re-calibrated. This improved the correlation between the dataset. The plot of the core versus log porosities gave an adjusted R^2 of 0.8918.

The figure below shows the results of the log calibration using core data from well 1.

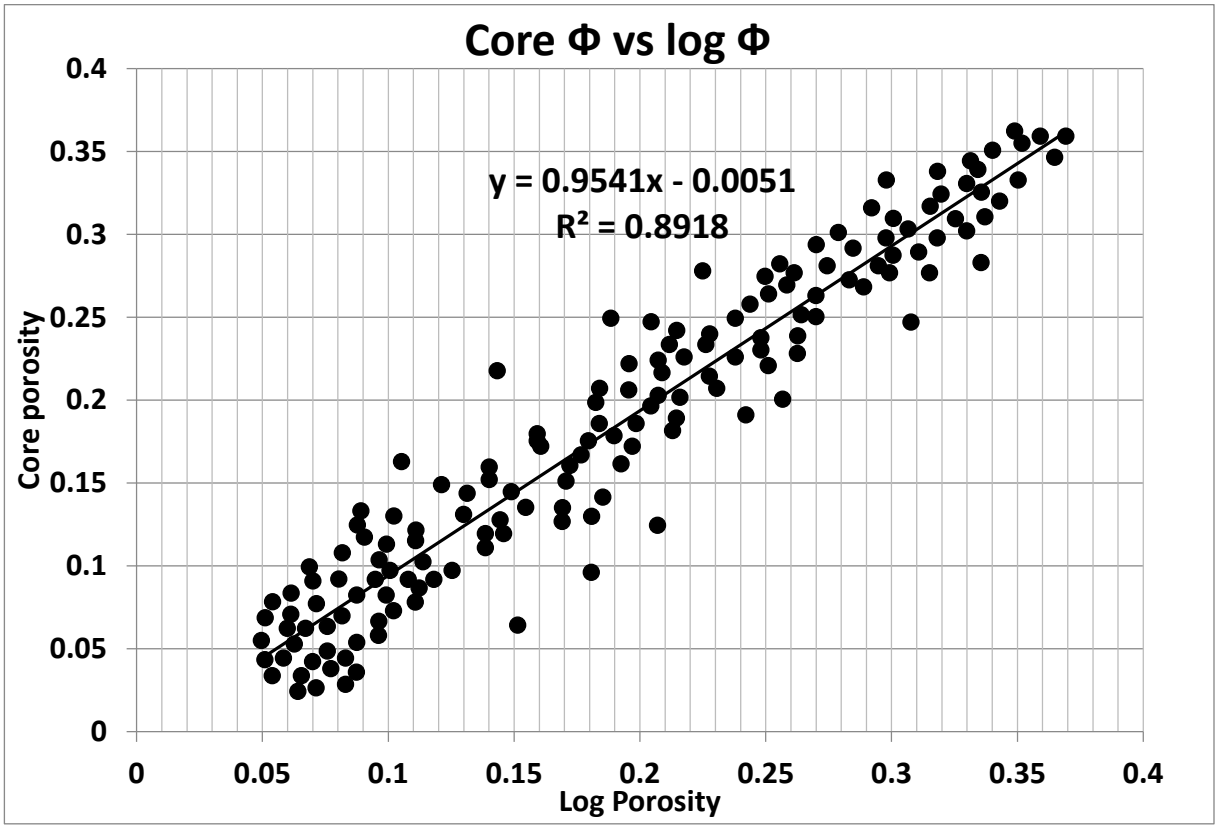

Figure 3.3: Relationship between core data and log data for quality assessment

CHAPTER 4

DATA PROCESSING AND ANALYSIS

4.1 Process of Evaluation

For the purpose of this research work, petrophysical evaluation of flow units for six wells in the Agbada-Akata petroleum system is carried out. The reservoir of interest designated reservoir X, is one of the deepest reservoirs in zone D3000 with six active wells present. All the necessary environmental correction aimed at removing the effect of variable hole-size was performed.

Normalization was carried out at scaling the various well logs for all wells to a reference well 1, to provide a homogeneous dataset. A detailed petrophysical evaluation was conducted for wells 1, 2, 3, 4, 5 and 6 respectively. The interpretation of the logs was also performed and shale volume, net thickness, and effective porosity were computed.

The next stage of the analysis involved the delineation of the flow units and finally building static models of the reservoir properties using geostatistical technique. Some of the parameters required in the evaluation are discussed below.

4.1.1 Reservoir Quality Index (RQI)

The concept of reservoir quality index was introduced by Amaefule *et al.* (1993). Therefore for a given reservoir unit, this concept is used to establish a relationship between porosity and permeability. It takes into account the pore and grain distribution, pore-throat attributes, and other macroscopic parameters. Permeability is always expressed in millidarcies and porosity as a fraction in using this particular method. RQI is mathematically expressed as below:

$$RQI = 0.0314\sqrt{\frac{K}{\Phi_e}} \quad \text{..... (4.1)}$$

4.1.2 Flow Zone Index (FZI)

The RQI versus normalized porosity plot defines the FZI. The intercept of a straight line on RQI axis at a normalized porosity value of 1, is the FZI. Samples will lie on other parallel lines if they have different FZI values. However, samples with similar pore throat attributes will lie on the same straight line and therefore, constitute a flow unit. Straight lines of gradient equal to unity should be expected primarily in clean sandstone formations whereas shaly formations are indicated at a gradient greater than one.

The flow zone indicator (FZI) is a special parameter that describes the architecture of the pores in terms of the shape factor or geometry, texture and mineralogical composition on all distinctive facies within a given rock layer. Generally, rocks containing pore filling and pore occlusions, authogenic pore lining, as well as poorly sorted nature with fine-grained sands have the tendency to exhibit high tortuosity, high surface area and consequently low FZI values. On the contrary, higher FZI values indicate less shaly, coarse-grained and well-sorted sand with low shape factor, lower surface area, and lower tortuosity.

The geometry of the reservoir and consequently the flow zone index is controlled by different depositional environments and diagenetic processes (Tiab, D. 2004).

4.1.3 Tiab Hydraulic Flow Unit (H_T)

Hydraulic flow unit refers to a continuous body within specific volume of the reservoir that basically possesses constant fluid and petrophysical properties and uniquely characterizes both the static and dynamic communication with the wellbore. The technique for delineating and characterizing a formation having similar hydraulic qualities, or flow units, based on the measurements of rock core samples at the microscopic level was developed by Tiab *et al.* (1993). This technique is solely a modification of the Carman-Kozeny (1938) equation and the mean hydraulic radius concept.

For this project work, the hydraulic flow units are obtained from the equation below. This equation is used to describe hydraulic flow units on a macroscopic scale:

$$H_T = \frac{1}{FZI^2} \quad \text{..... (4.2)}$$

4.1.4 Normalized Reservoir Quality Index (nRQI)

The plot of depth against cumulative normalized values of RQI gives the normalized RQI plot. Generally, the bottom of the reservoir is used as the starting point for the normalization and summation of the RQI values.

In the normalized RQI plot, consistent zones are defined by straight lines with the gradient of the line indicating the overall quality of the reservoir within a particular depth interval. The lower the gradient, the better is the reservoir quality.

The equation below is used in generating the cumulative normalized RQI‘s at different depth intervals within the study reservoir.

$$nRQI = \frac{\sum_{x=1}^{i} \sqrt{\frac{K_i}{\Phi_i}}}{\sum_{x=1}^{n} \sqrt{\frac{K_i}{\Phi_i}}} \quad \ldots\ldots (4.3)$$

4.1.5 Normalized Porosity (Φ*z*)

The normalized porosity is a representation of the pore volume to the grain volume of the rock. It should, however, be emphasized that the hydraulic quality of a rock depends on the geometry of the pores. The normalized porosity in this study is obtained using the equation below:

$$\Phi_z = \frac{\Phi_e}{1-\Phi_e} \quad \ldots\ldots (4.4)$$

4.1.6 Stratigraphic Modified Lorenz Plot (SMLP)

Stratigraphic Modified Lorenz Plot for a given reservoir describes the storage and flow capacity within a specific depth interval. This is obtained by calculating on a foot-by-foot basis the percent storage (porosity–thickness, Φh) and percent flow capacity (permeability-thickness, kh). Subsequently, the flow capacity is usually plotted against the respective storage capacity. The flow and storage qualities of the reservoir are revealed by the shape of the Stratigraphic Modified Lorenz Plot curve. These are grouped accordingly as follows:

- A high percentage of reservoir flow capacity is represented by sections with steep slopes and therefore, a high production potential is expected.

- Storage capacity, but little flow capacity is typically reservoir baffles which are normally represented by sections with flat behavior.
- Seals are represented by sections with neither flow nor storage capacity.

Calculations of the flow capacity and storage capacity were done using the equations below:

$$\phi h = \frac{\sum_{i=1}^{L} \phi_i \, h_i}{\sum_{i=1}^{n} \phi_i \, h_i} \qquad L = 1,2 \ldots\ldots,n \ldots\ldots (4.5)$$

$$kh = \frac{\sum_{i=1}^{L} k_i \, h_i}{\sum_{i=1}^{n} k_i \, h_i} \qquad L = 1,2 \ldots\ldots,n \ldots\ldots (4.6)$$

Where:

n is the total number of reservoir layers i

Φi is the porosity of layer i

ki is the permeability of layer i, and hi is the net thickness of layer i.

The layers are numbered in order from the shallowest layer i = 1 to the deepest layer i = L

4.1.7 Dykstra-Parsons Coefficient (V_k)

Reservoir heterogeneity is best determined using the coefficient of variation or Dykstra-Parsons coefficient. Dykstra-Parsons coefficient is principally a dimensionless measure of dispersion or sample variability. The ratio of the standard deviations to the mean of a given sample data defines the coefficient of variation.

The coefficient of variation provides an assessment of permeability heterogeneity which is often applied in engineering and geological studies. The mean and standard deviation for data from different populations often tend to change together such that the coefficient of variation stays relatively constant.

The Dykstra-Parsons coefficient of permeability variation used in this research is determined using the equation below:

$$V_k = \frac{K_{50} - K_{84.1}}{K_{50}} \ldots\ldots (4.7)$$

Where:

K_{50} is the permeability at 50% cumulative probability plot of permeability

$K_{84.1}$ is the permeability at 84.1% cumulative probability plot of permeability

The heterogeneity of the reservoir can be classified base on the range of index below:

$V_k = 0$, ideal homogeneous reservoir

$0 < V_k < 0.25$, slightly homogeneous reservoir

$0.25 < V_k < 0.50$, heterogeneous reservoir

$0.5 < V_k < 0.75$, very heterogeneous reservoir

$0.75 < V_k < 1.0$, extremely heterogeneous reservoir

$V_k = 1.0$, perfectly heterogeneous reservoir

4.2 Log Analysis for Wells of Reservoir X

4.2.1 Analysis of Well 1

The logs revealed that well 1 is characterized by unconsolidated sand with minor shale intercalations in some units. Field wide correlatable clean sand sequence and shales exist within its depositional system. However, the volume of sand is relatively dominant in this well compared to the shale thickness. The well log analysis classified well 1 as a good to moderate well. It exhibits high reservoir quality with good permeable zones (good porosity and permeability). The effective porosities vary while the estimated permeabilities remain constant with the reservoir quality index. This indicates that the reservoir rock in well 1 is more porous to accommodate fluids. Three different flow units can be defined along this depth within the zone of interest (see figure 4.1). The possible reason for the presence of three flow units identified in this well may be attributed to low volume of shale since more clean sand-stones were delineated, as much as the gamma ray log signature increased towards the sand-line. The volume of shale has less impact on the average porosity and permeability in this well.

Figure 4.1 shows the results of the log interpretation for well 1.

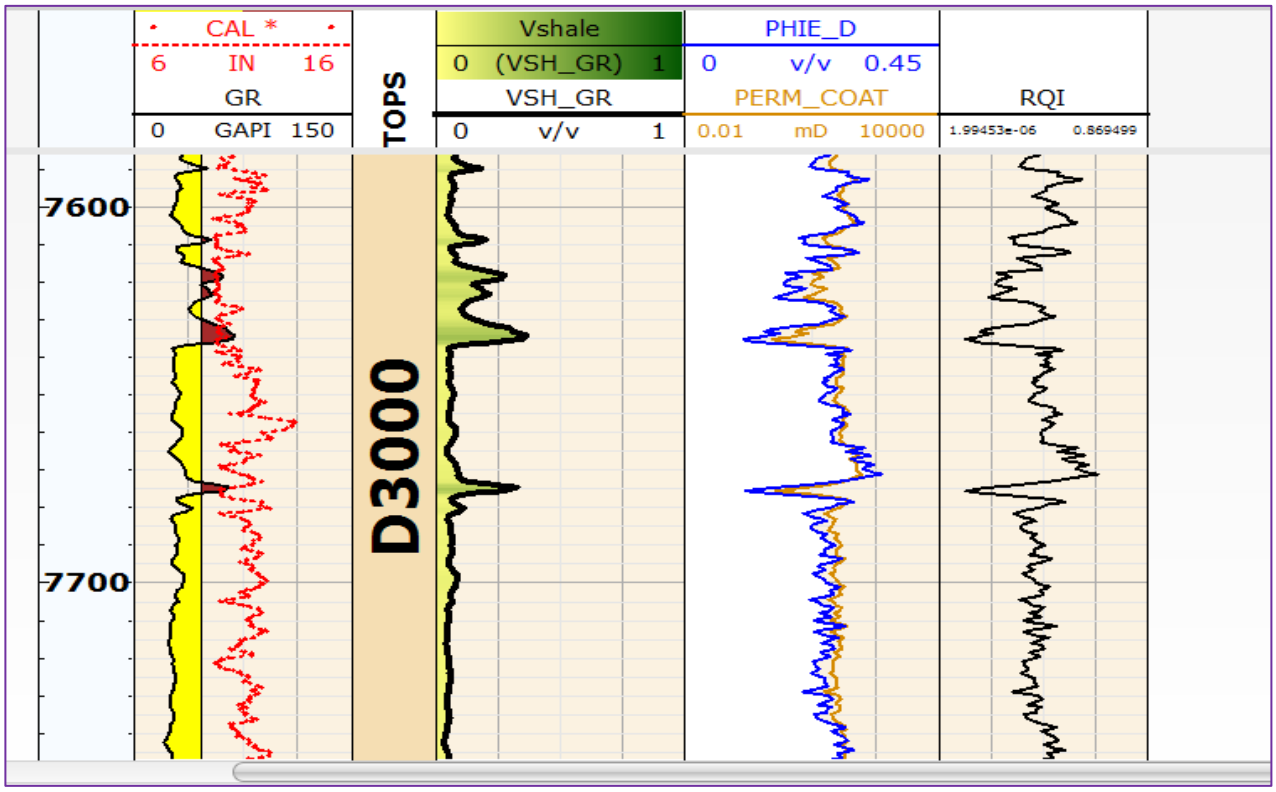

Figure 4.1: Log view of petrophysical parameters for Well 1

4.2.2 Analysis of Well 2

The well logs classified well 2 as, a good to moderate well (good porosity and permeability) which is characterized by unconsolidated sand with minor shale baffles. Correlatable clean sand stones and shales exist within its depositional system. The thickness of sand is dominant in this well compared to the shale. The well exhibits good reservoir quality and good permeable zones. The estimated permeabilities remain constant with the reservoir quality index, while the effective porosities vary significantly. The logs indicate more dense porous sandy formation in the depth region. This shows that the reservoir rock in well 2 is more porous and therefore has the ability to store and transmit more fluids.

Two different flow units can be defined along this interval within the zone of interest (see figure 4.2). The identification of two flow units in this well may possibly be due to the presence of some shale baffles and truncations, which might cause permeability barriers. The volume of shale in some units can hamper the free flow of fluid in the reservoir rock of this well.

Figure 4.2 shows the results of the log interpretation for well 2.

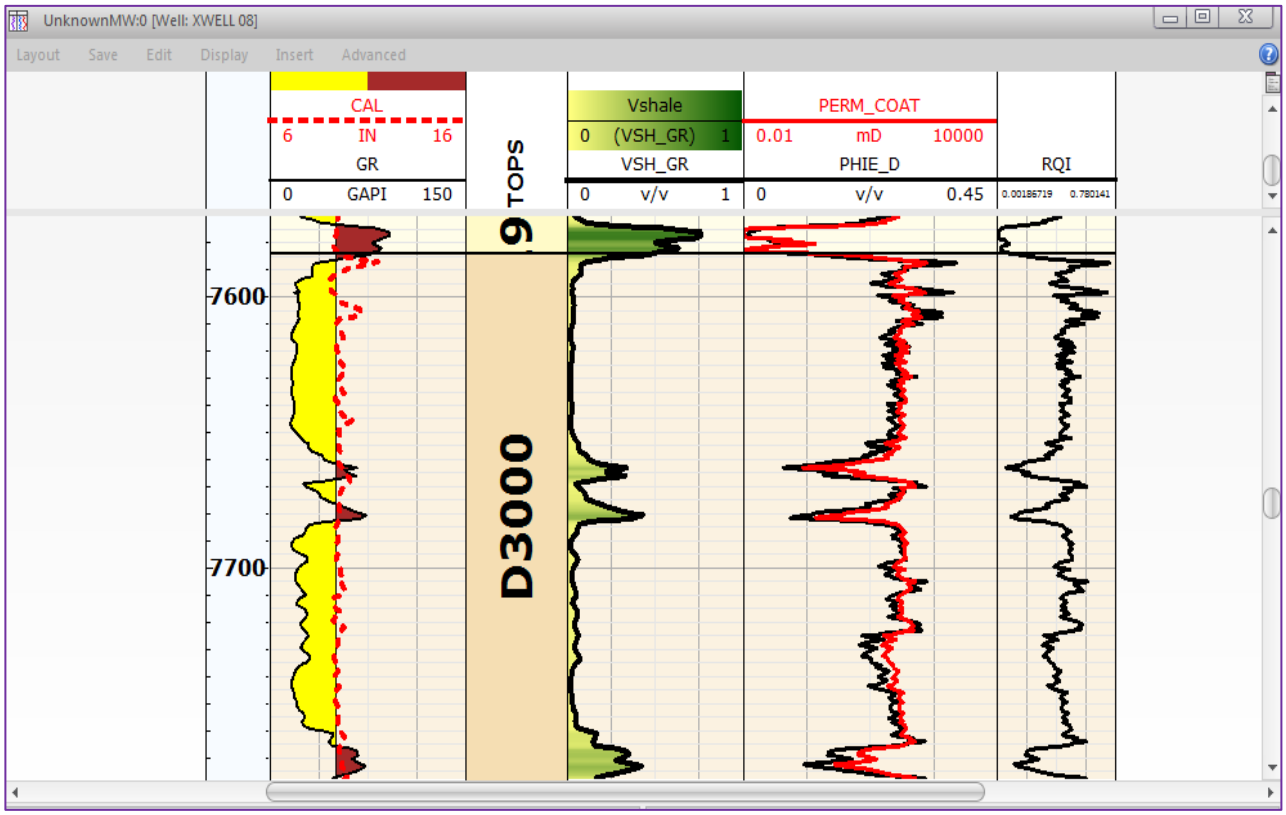

Figure 4.2: Log view of petrophysical parameters for Well 2

4.2.3 Analysis of Well 3

The gamma ray log delineates into sections with two lithofacies, namely sandstones and shale. This well is characterized by minor shale intercalations, and continuous clean sand bodies within its depositional system. The base of this well consists basically of thick shale sequence and a minor amount of sand. The volume of shale at the base of this well is dominant compared to the sand thickness. This suggests that the reservoir is not too clean. Good permeable zones are delineated in this well. The reservoir quality index remains constant with the estimated permeabilities while the effective porosity varies.

This shows that the reservoir rock in this well is more porous to store and transmit fluids. Three distinct flow units can be defined along well depth (see figure 4.3).

The reason for three flow units occurring in this well may possibly be due to the presence of low shale baffles, and high clean sands being delineated as the GR log signature increased towards the sand-line.

Figure 4.3 shows the results of the log interpretation for well 3.

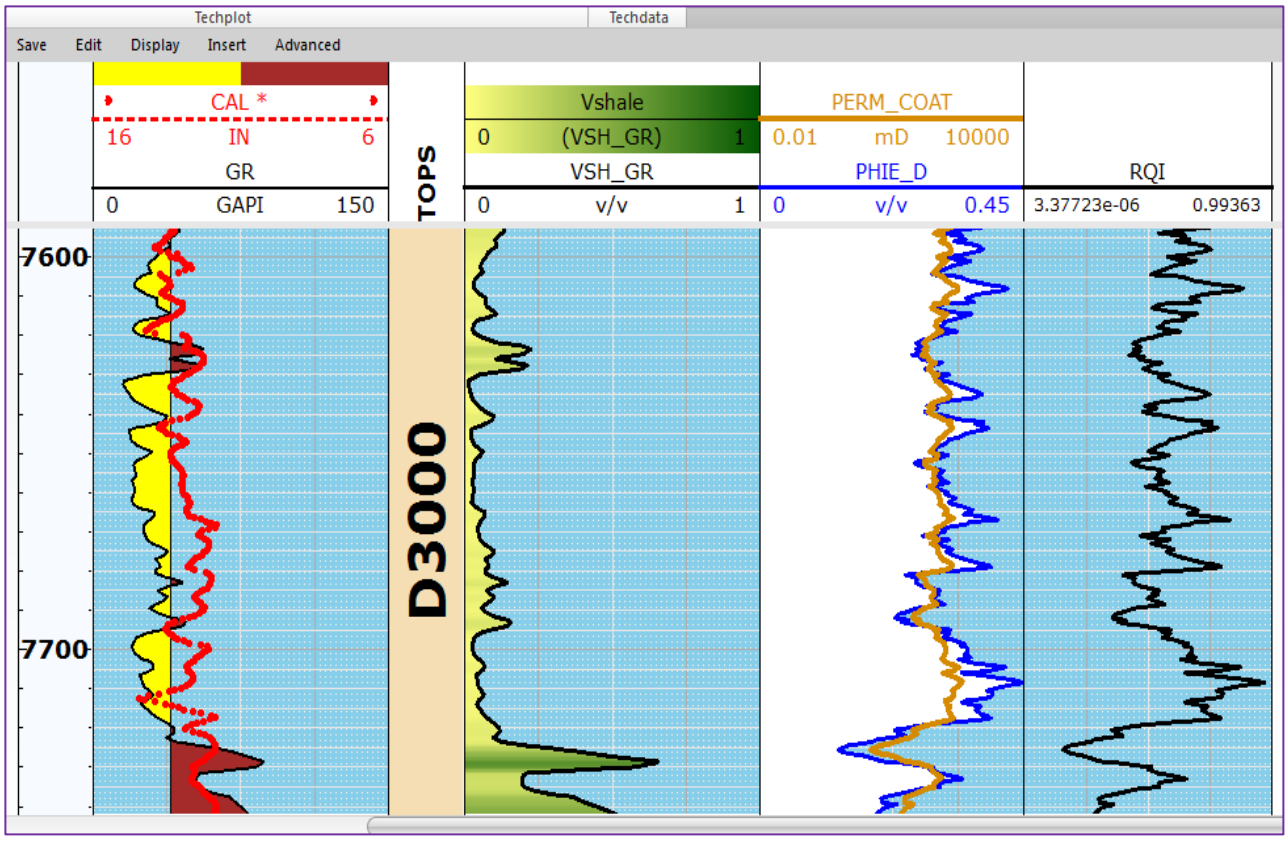

Figure 4.3: Log view of petrophysical parameters for Well 3

4.2.4 Analysis of Well 4

Well 4 indicated a very good identification of flow units compared to the other wells. Two lithofacies namely, sandstones and shale are delineated in this well by the gamma ray log. Minor shale baffles and clean sand zones exist within its depositional system. The thickness of sand compared to the shale thickness is very high, as much of the gamma log signature increased towards the sand-line than the shale-line. The reservoir quality index varies with the effective porosities and remains constant with estimated permeabilities. Four distinct flow units can be defined along the depth of this well (see figure 4.4) within the zone of interest.

This shows that the reservoir rock in this well has very a good storage capacity to accommodate more fluids. The average porosity and permeability are very good for this particular well. The identification of four flow units in this well may be due to the presence of low shale volume, high porosity, and permeability.

Figure 4.4 shows the results of the log interpretation for well 4.

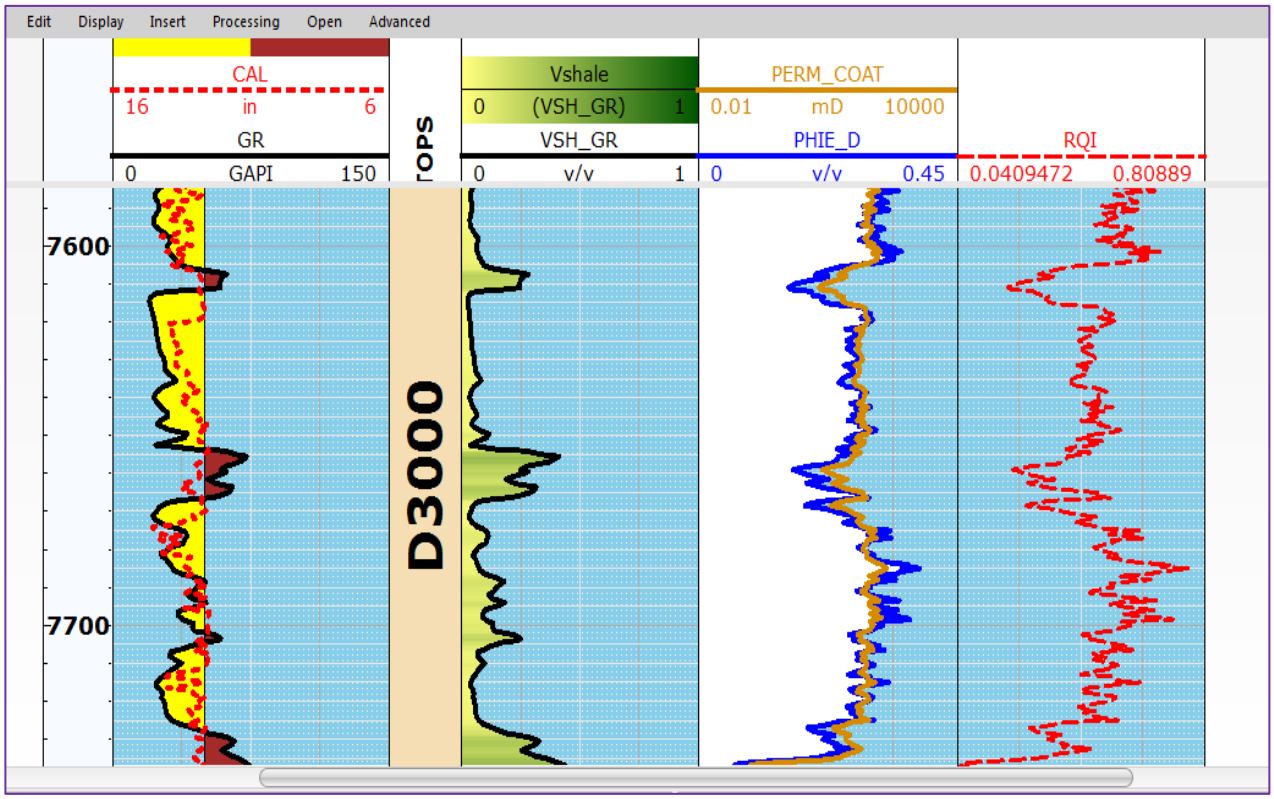

Figure 4.4: Log view of petrophysical parameters for Well 4

4.2.5 Analysis of Well 5

The log classified well 5 as a good to moderate well, which is characterized by correlatable clean sands and minor shale intercalations within its depositional environment. Two lithofacies, shale, and sand are delineated by the gamma ray log. The sand sequence is dominant in this well compared to the shale, as the much of the gamma log signature increased towards the sand-line. The well exhibits good reservoir quality and good permeable zones. The reservoir quality index varies with the effective porosities and remains constant with estimated permeabilities.

Two different flow units can be defined along this interval (see figure 4.5). The identification of two flow units in this well could possibly be due to the presence of shale baffles and truncation of other flow units, which can cause vertical permeability barrier in that part of the reservoir. The shale volume can relatively affect the average porosity and permeability to obstruct the free flow of fluids.

Figure 4.5 shows the results of the log interpretation for well 5.

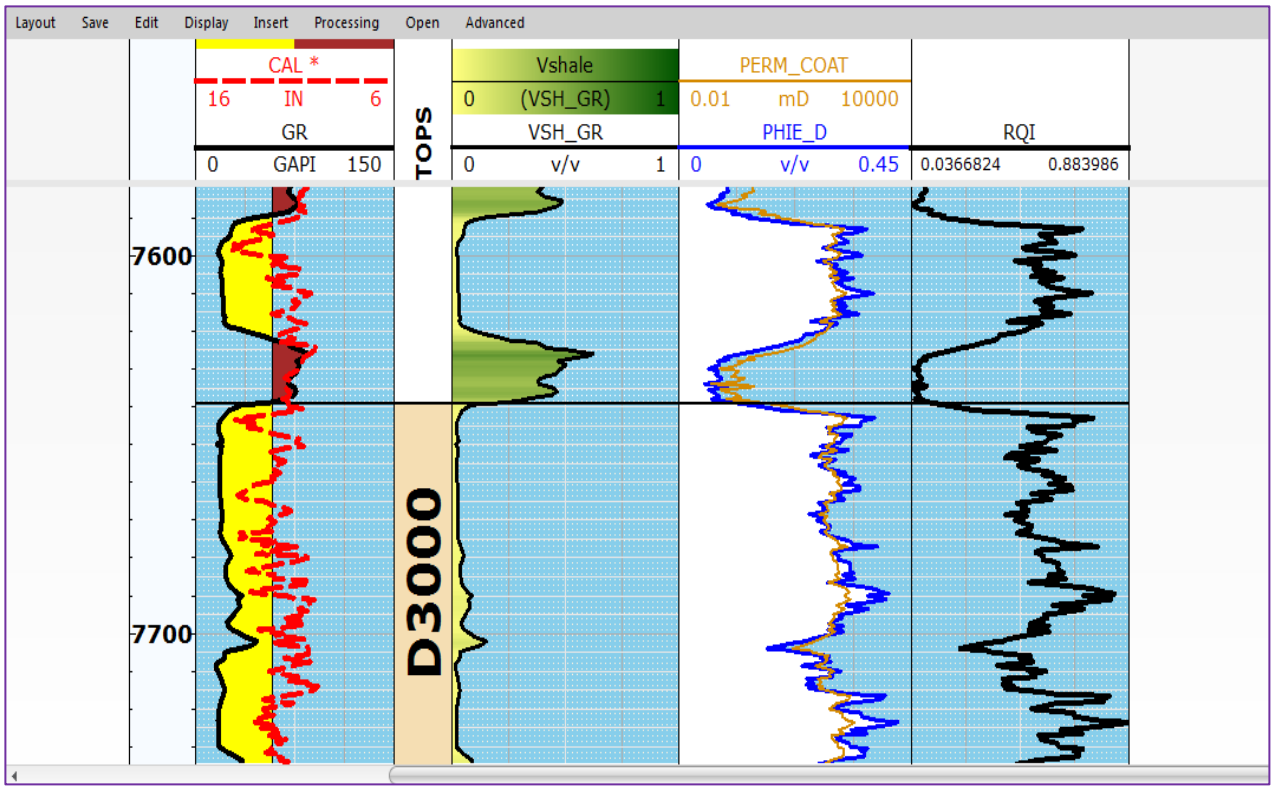

Figure 4.5: Log view of petrophysical parameters for Well 5

4.2.6 Analysis of Well 6

Well 6 indicated a very good identification of flow units as in well 4. Shale and sandstones are the two main lithofacies delineated by the gamma ray log. The reservoir rock in this well consist of massive, highly porous, clean bearing sands-stones localized with minor shale intercalation which increases towards the base of the formation. Four distinct flow units can be defined in the reservoir sand of this well (see figure 4.6). The thickness of sand compared to the shale thickness is relatively very high. This well exhibits high reservoir quality and good permeable zones. The effective porosity varies, while the estimated permeability is constant with the reservoir quality index. The average porosity and permeability is very good for this particular well. The reason for four flow units occurring in this well may possibly be due to the presence of low shale baffles and high clean sands being delineated, as much of the GR log signature increased towards the sand-line than the shale-line. This clearly reveals that the reservoir rock in this well has very good storage capacity to accommodate more fluids.

Figure 4.6 shows the results of the log interpretation for well 6.

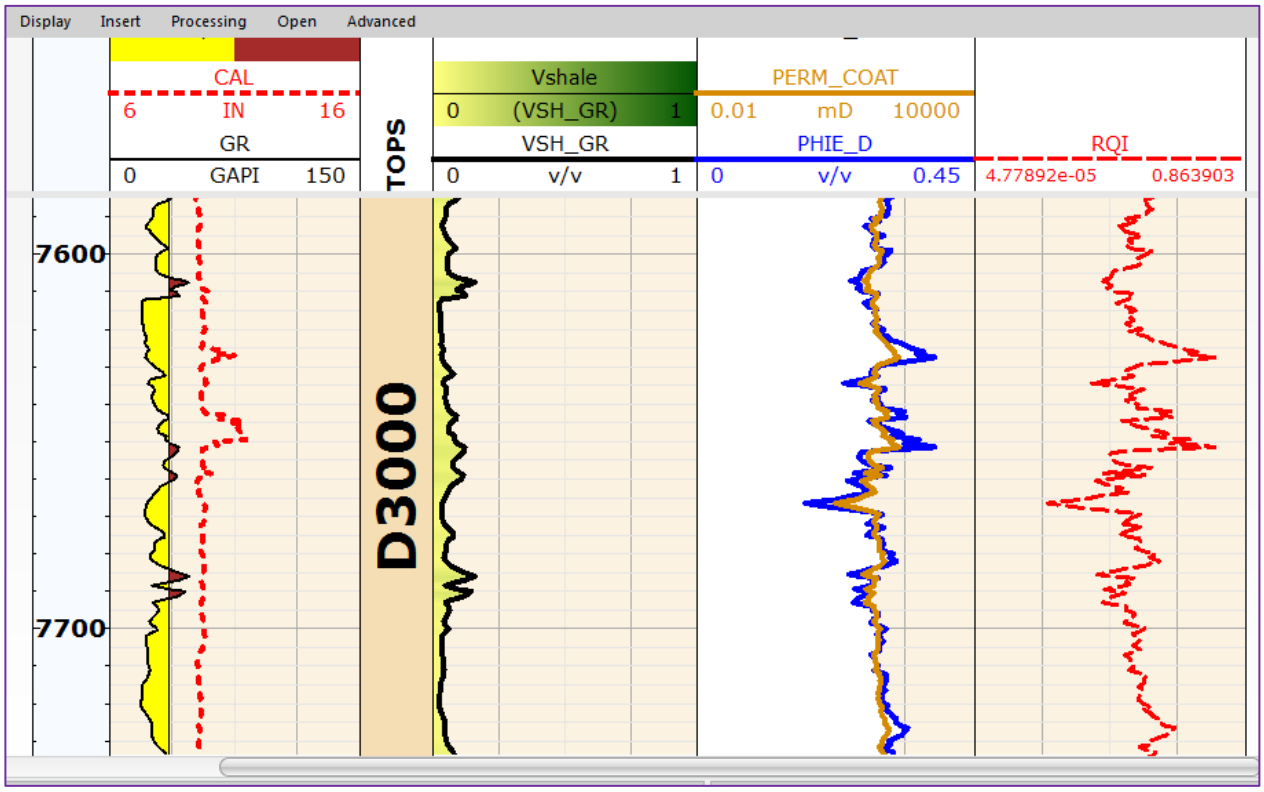

Figure 4.6: Log view of petrophysical parameters for Well 6

4.3 Well Correlations

The architecture of the reservoir is essential in describing the lithology, stratigraphy as well as the flow characteristics of the reservoir. In this research, the various wells of interest in the sector of the study were correlated to evaluate the various petrophysical parameters, and to establish a reference depth for a common base sand and shale volume. The well logs were normalized using quantile normalization by linear transformation at 5% and 95% percentiles. After normalization, the minimum and maximum percentile values were subsequently calibrated to typical sand and shale peak gamma ray readings of 10 API and 100 API units respectively. Well 1 was used as the calibration logs for the well to well correlation process because it has the most consistent signature. Having normalized the logs of all the wells, an average cut-off of 55 API was used across the field. The corrected and processed logs were used in the petrophysical analyses of the wells of interest, and in the construction of Reservoir X static models of the various flow properties (permeability and porosity).

The well to well correlation shows that various wells for Reservoir X generally thin from the north to south towards the basin signifying a prograding sequence. The reservoir is elongated since it is a barrier type deposit and is of good continuity.

Figure 4.7 depicts the Lithologic cross section for Reservoir X (Sector of Study).

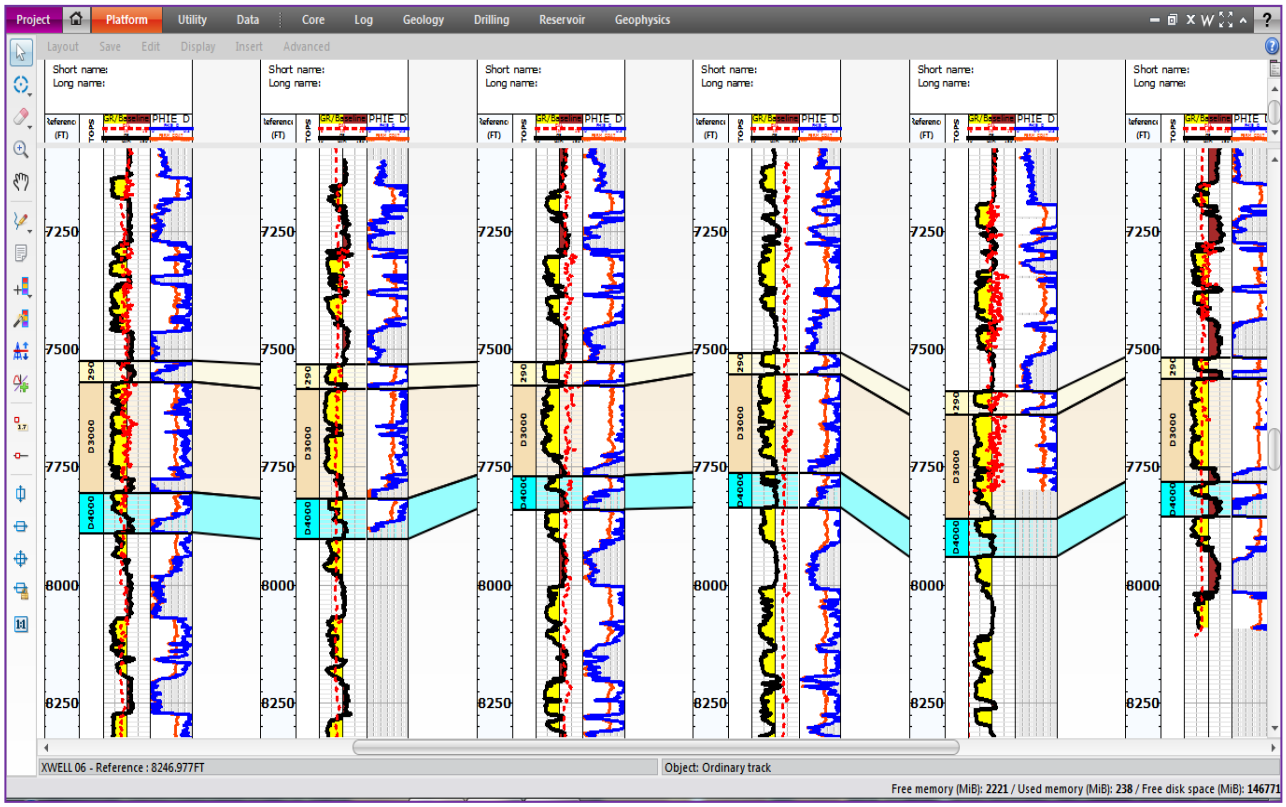

Figure 4.7: Six well logs showing the structural correlation for Reservoir X

4.4 Analysis of Flow Units in Wells of Reservoir X

The flow units for the six wells within the reservoir were delineated using three different techniques. These included, Reservoir Quality Index versus Normalised Porosity graphs, Normalised Reservoir Quality Index graph, and Stratigraphic Modified Lorenz Plot. The results observed in the first graph were validated using the last two methods. The various wells in the reservoir of interest were analyzed as described below:

4.4.1 Analysis of Well 1

This well is localized with minor shale intercalations and intercepts reservoir sands present in the reservoir of interest (Reservoir X). Log records were present for most of the upper portions of this well. The identified reservoir sands are within this logged zone. This is because the upper portions of this well were delineated in the zone of interest (D 3000). It is observed from the graphs of RQI versus Normalized Porosity, Normalized RQI, and Stratigraphic Modified Lorenz Plot that well 1 intercepts three distinct flow units identified in the reservoir of interest.

The probable causes for these observations vary but the most likely reason is due to the diagenetic setting of this clastic system. The variation in clay groups as a function of depth within this system, suggest that the diagenetic overprint affecting the clastic rocks of the Niger Delta are both of environmental and sedimentary origin.

It is observed from the log analysis that the reservoir unit thins out completely from well 1 towards well 2. They may be sand pinch outs within some portions in the reservoir. Some of the other flow units might have been truncated and therefore were not present in this well. Also, the possible explanation for having fewer flow units in the reservoir in well 1 compared to well 2 may be due to the nature of the depositional environment in which the reservoir was originally formed. The Agbada-Akata environments according to Weber (1971) exhibit various intrinsic complexities. Therefore, the flow units delineated in one well may be significantly different from the other wells within the same reservoir.

It is observed from the graph (see figure 4.9) that, minor shale intercalations exist within the flow paths identified in this well. The normalized RQI and SMLP graphs reveal little flow barriers in the layers.

The quality of the reservoir flow units can be determined from the various plots below. The gradient of the flow unit in the normalized porosity plot indicates the quality of the flow unit. Poor reservoir quality is characterized by high gradient whereas lower gradient indicates a better reservoir quality.

Table 4.1 shows the FZI's, gradient, regression coefficients and the wells of occurrence for each of the flow units identified in reservoir of interest.

Table 4.1: Table showing flow units present in Well 1 and their properties

Flow Unit	Gradient	FZI	H_T (µm^2)	R^2	Wells of Occurrences
A	2.02	10.05	9.90E-3	0.87	1,2
B	2.05	3.95	6.41E-2	0.90	1,3
C	2.10	1.56	4.11E-1	0.95	1,4

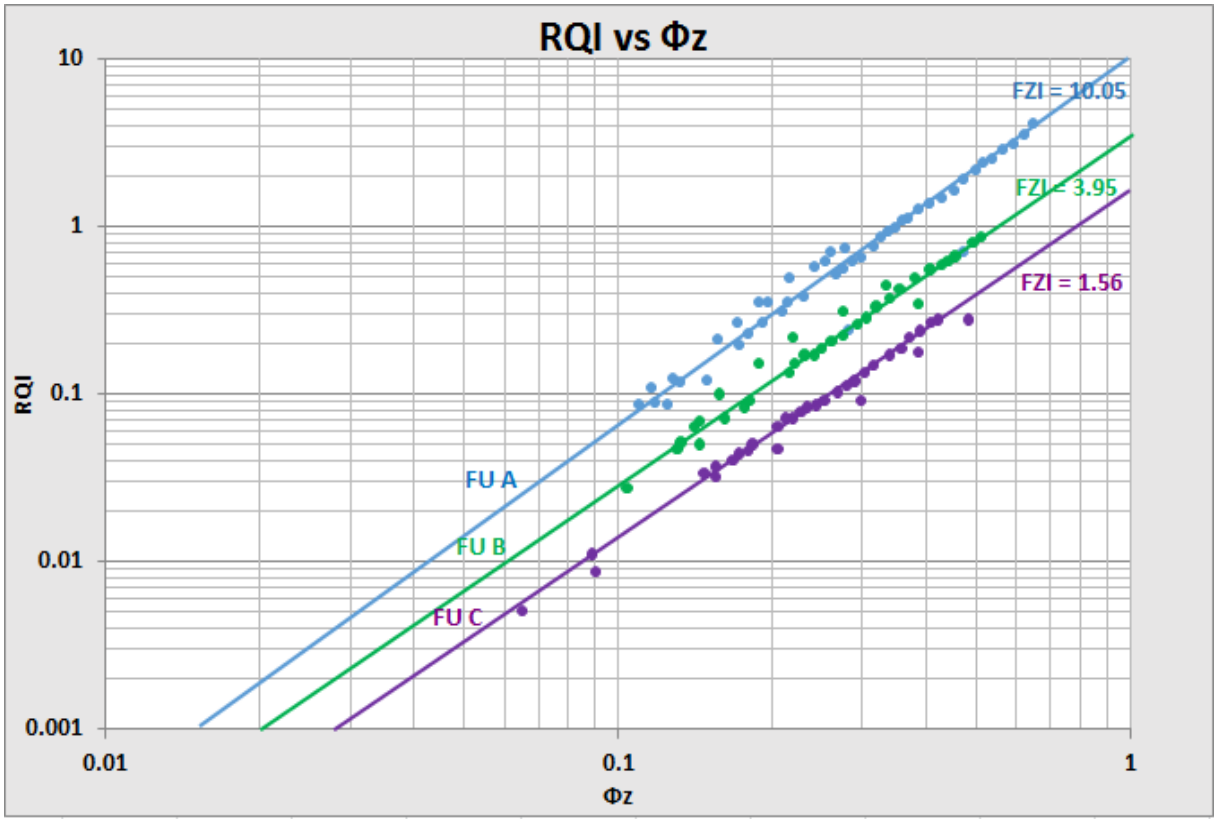

Figure 4.8: Graph of RQI versus Normalized Porosity of reservoir for Well 1

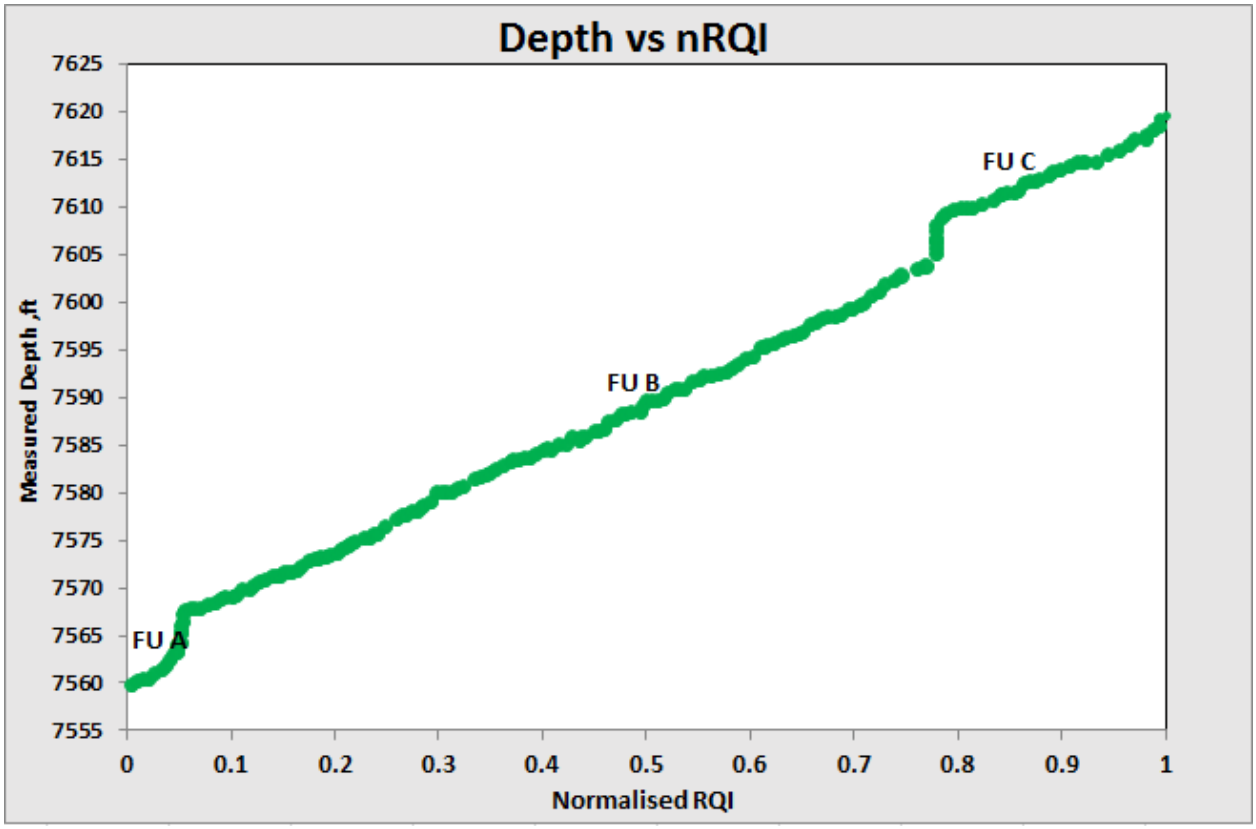

Figure 4.9: nRQI plot of the reservoir of interest for Well 1

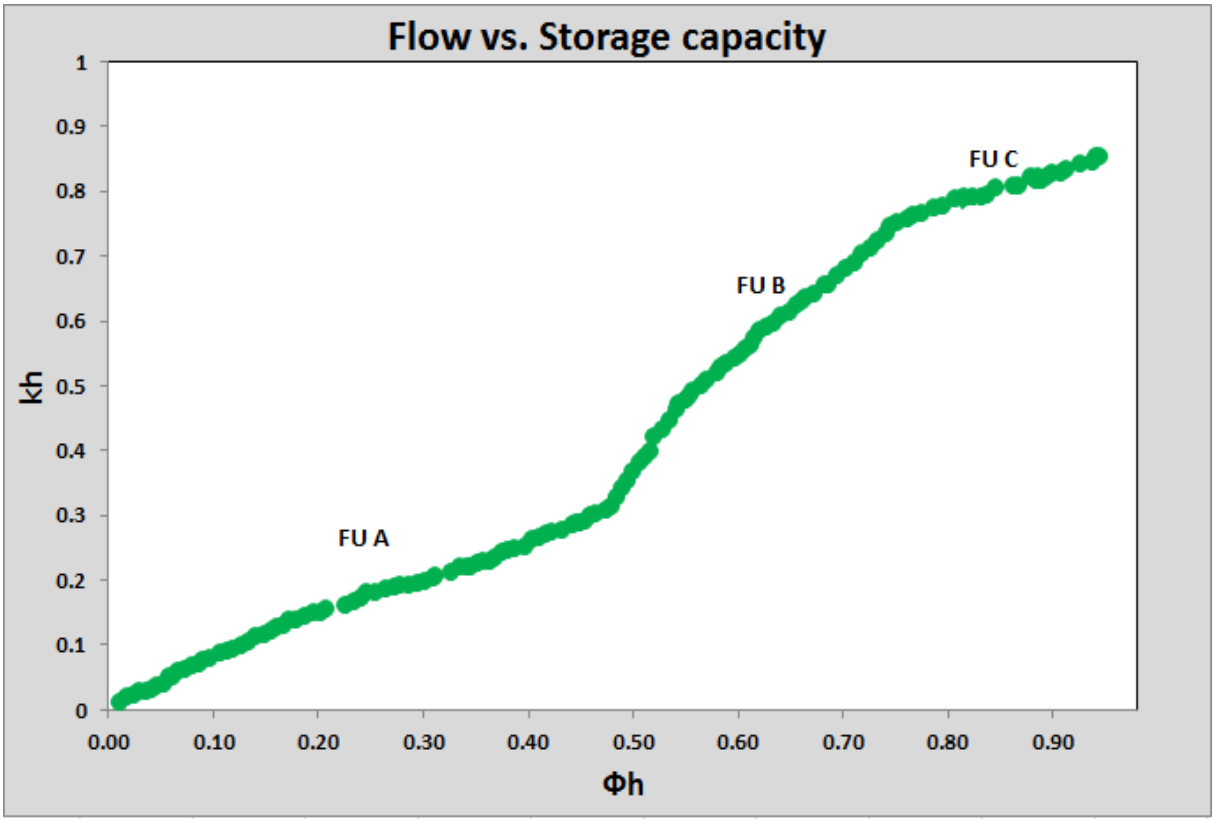

Figure 4.10: SMLP of the reservoir of interest for Well 1

4.4.2 Analysis of Well 2

The data available indicates that well 2 has two distinct flow units identified in the reservoir sands within zone D3000. There were detailed log records present for the upper part of the well. However, there were no logs present for some lower portions of the well. It is possible that, this portion for which there were no log data intercepts the other reservoirs that were not delineated within the zone of interest. The RQI versus Normalized Porosity, Normalized RQI, and Stratigraphic Modified Lorenz graphs indicate that this well contains two flow units in the reservoir of interest (Reservoir X). The Agbada-Akata environments exhibit high spatial heterogeneity which is solely responsible for the truncation of some other flow units in the reservoir. The reservoir sand unit may have been gradually pinching towards the direction up to the point where well 2 intercepts it, that many flow units were delineated in well 3 with fewer flow units identified in well 2 can be explained by the truncation of the some of the flow units. The environment of deposition and its nature may also be the possible cause for having only two flow units in the reservoir at the point well 2 crosscuts the observed reservoir.

Another remarkable cause of what is happening in this well may be due to the existence of an unconformity or bounding surface between the point of well 3, and well 2. This may have led to the thinning out of some of the areas being occupied by the other flow units present in well 3 thereby eliminating them. The other flow units defined in well 3 may therefore not be continuous to well 2. The Agbada-Akata environment considering the way they were originally formed, are complex in mineralogical composition and pore attributes. This means greater variation exist between the two locations for the same lithologic unit relative to a less erratic depositional environment. Therefore it is highly possible for this well to exhibit different characteristics compared to the other wells for the same reservoir sand unit. The quality of the reservoir flow units can be determined from the plots below. The gradient of the flow unit in the normalized porosity plot describes the flow unit quality. High gradient characterize poor quality whereas lower gradient is indicative of better reservoir quality.

Table 4.2 shows the FZI's, gradient, regression coefficients and the wells of occurrence for each of the flow units identified in reservoir of interest.

Table 4.2: Table showing flow units present in Well 2 and their properties

Flow Unit	Gradient	FZI	H_T (μm^2)	R^2	Wells of Occurrences
C	2.74	10.00	1.00E-2	0.92	2,3
D	2.12	4.85	2.06E-1	0.95	2,4

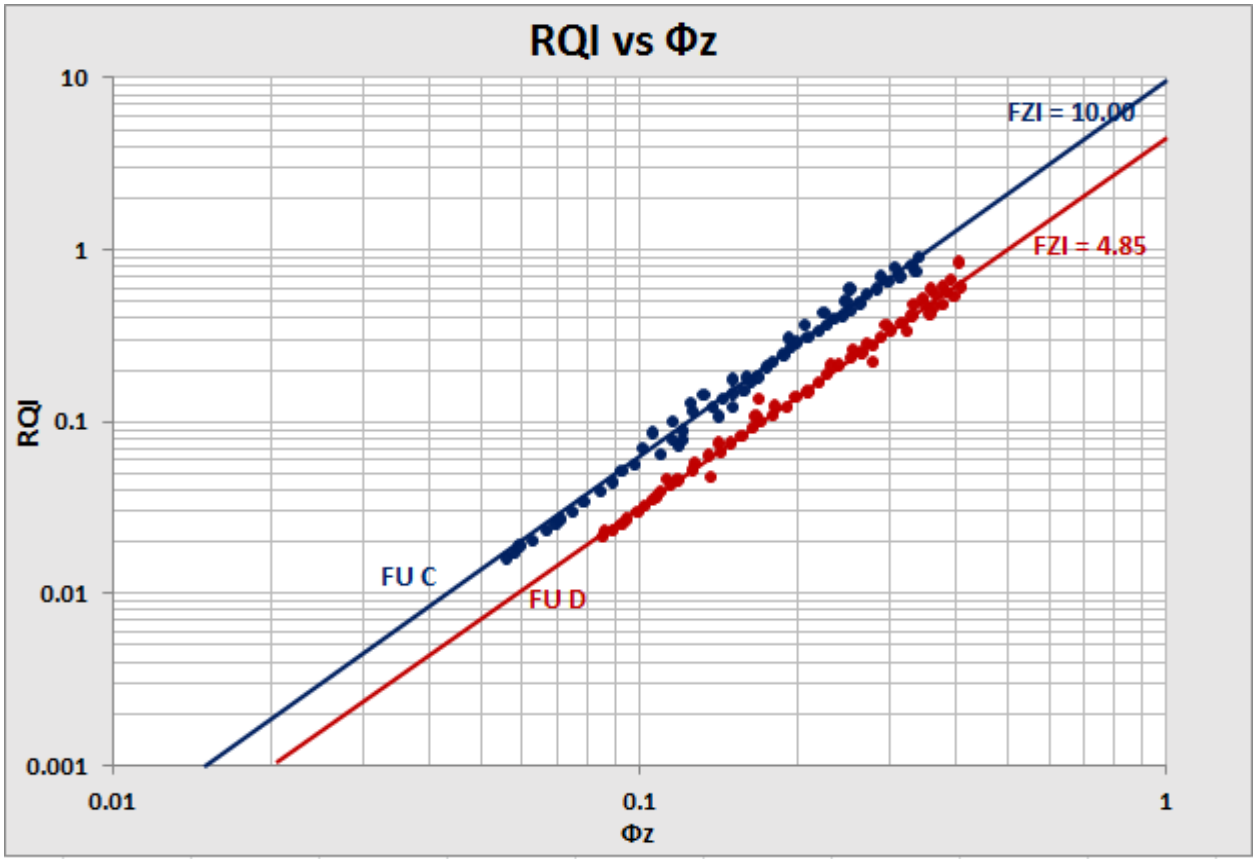

Figure 4.11: Graph of RQI versus Normalized Porosity of reservoir for Well 2

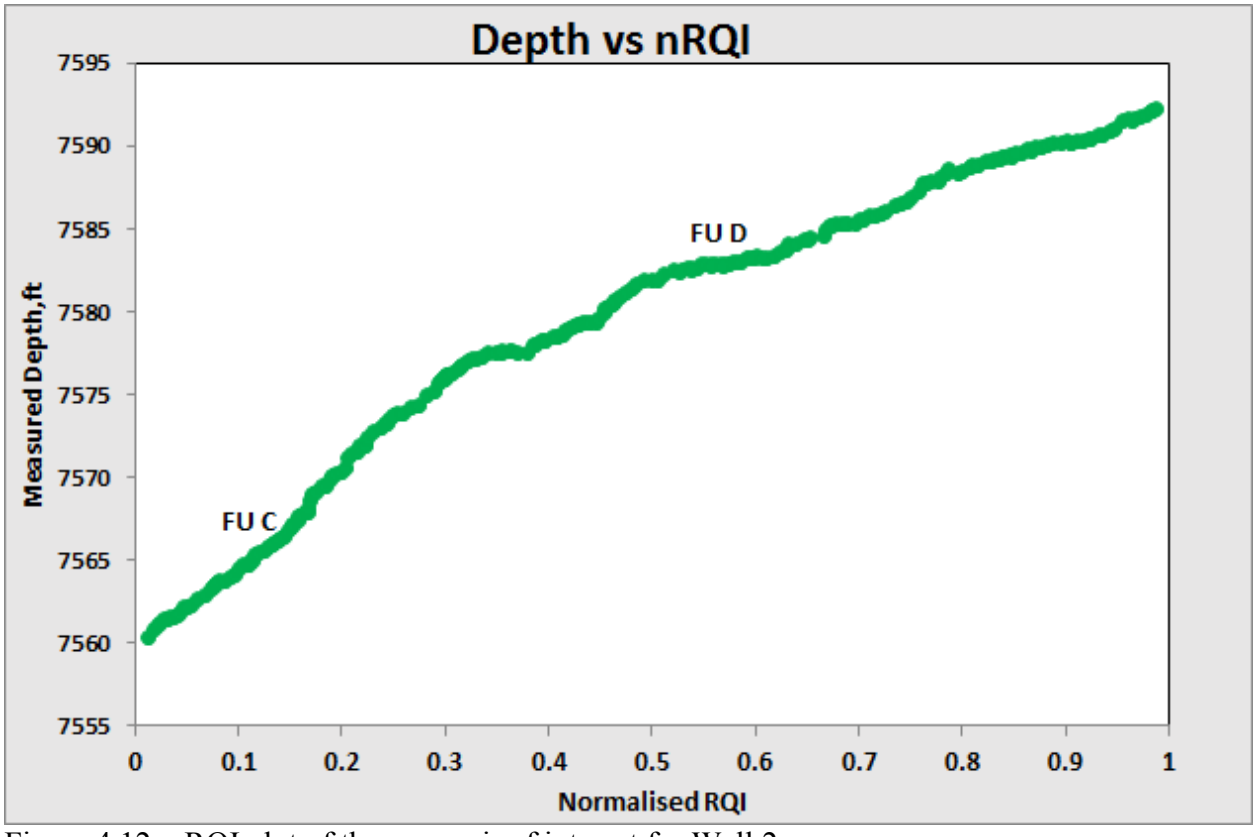

Figure 4.12: nRQI plot of the reservoir of interest for Well 2

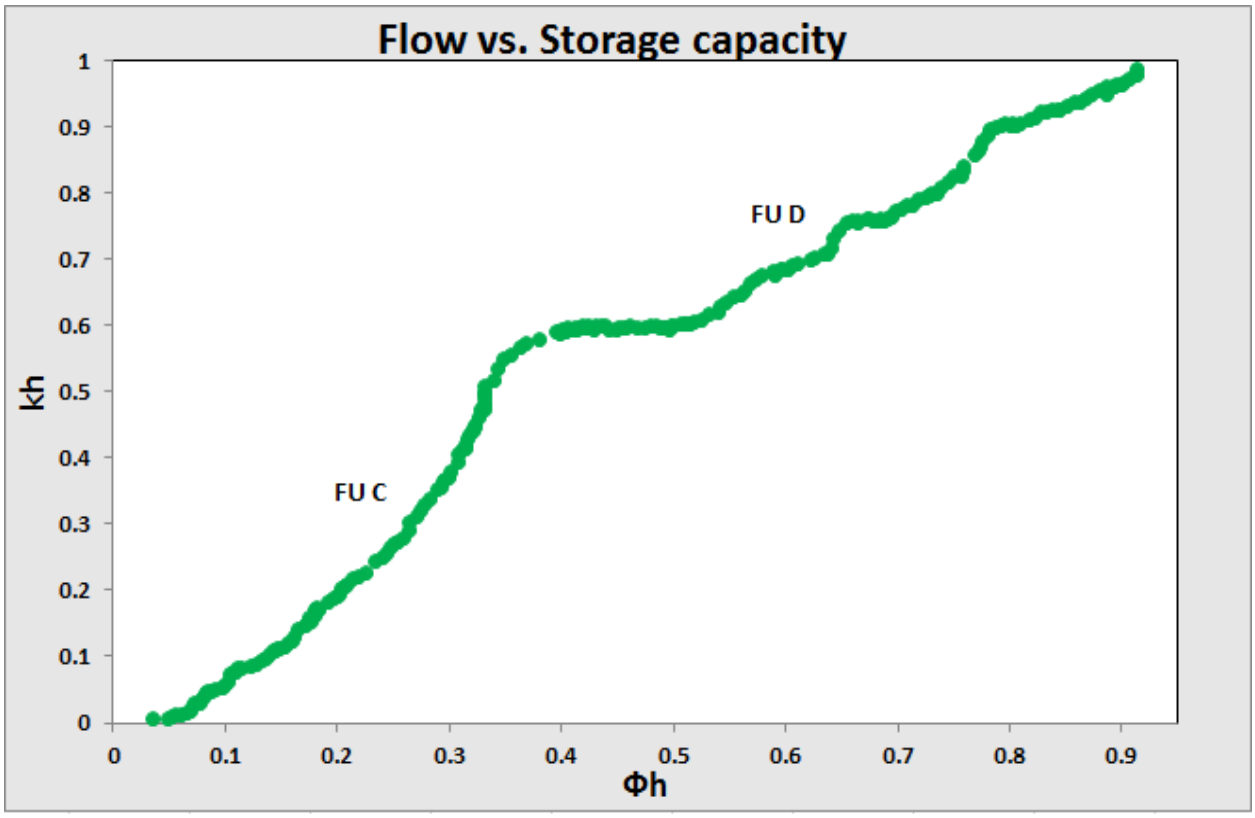

Figure 4.13: SMLP of the reservoir of interest for Well 2

4.4.3 Analysis of Well 3

There were log records for the top most portion of this well. The logs indicate that the well intercepts the reservoir sands present within the specified zone (D3000). It is observed from the graphs of RQI versus Normalized Porosity, Normalized RQI, and Stratigraphic Modified Lorenz Plot that this well contains three flow units out of the four flow layers delineated in the reservoir of interest (Reservoir X).

The tendency of different number of flow units in reservoir sands of the Agbada-Akata formations lies in the nature of their deposition and the diagenetic imprint. Therefore, there is the possibility of experiencing various flow barriers and baffles at deeper depth in this clastic system where the over burden pressure increases with temperature.

The log revealed that this well is associated with high volumes of shale. The existence of high shale volume within, coupled with the complex structure of pores in the reservoir units can lead to truncations of some flow units. The truncation of flow units in certain parts of the reservoir may cause the absence of flow units in some of the wells.

However, high content of shale can also affect the average porosity and permeability thereby petitioning divisions of the reservoir into different flow layers. The quality of the reservoir can be observed from gradient of the RQI against normalized porosity graph. Poor quality is characterized by high gradient whereas lower gradient is indicative of better reservoir quality.

Table 4.3 shows the FZI's, gradient, regression coefficients and the wells of occurrence for each of the flow units identified in reservoir of interest.

Table 4.3: Table showing flow units present in Well 3 and their properties

Flow Unit	Gradient	FZI	H_T (µm^2)	R^2	Wells of Occurrences
A	2.05	10.03	9.94E-3	0.84	1,3
B	2.11	4.05	6.09E-2	0.87	2,3
C	2.08	1.95	2.63E-1	0.82	1,2,3

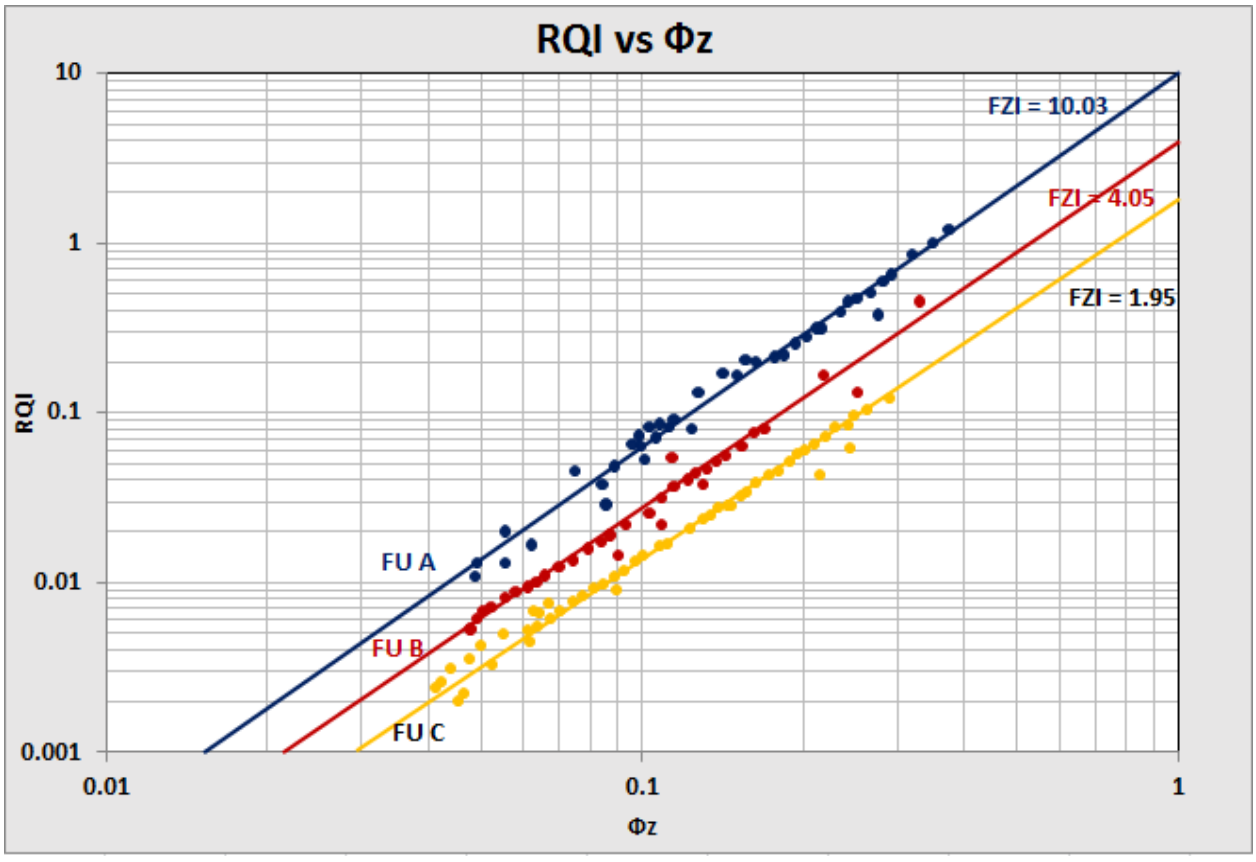

Figure 4.14: Graph of RQI versus Normalized Porosity of reservoir for Well 3

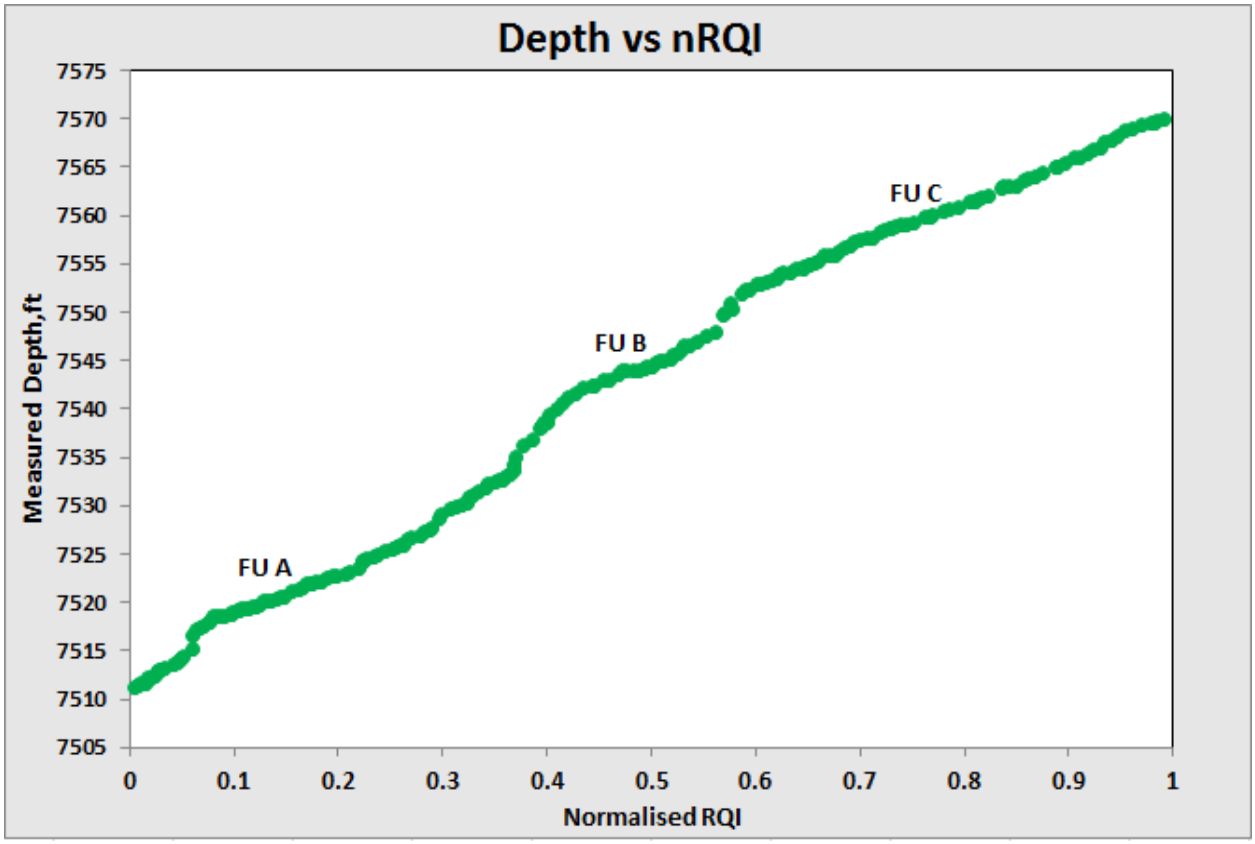

Figure 4.15: nRQI plot of the reservoir of interest for Well 3

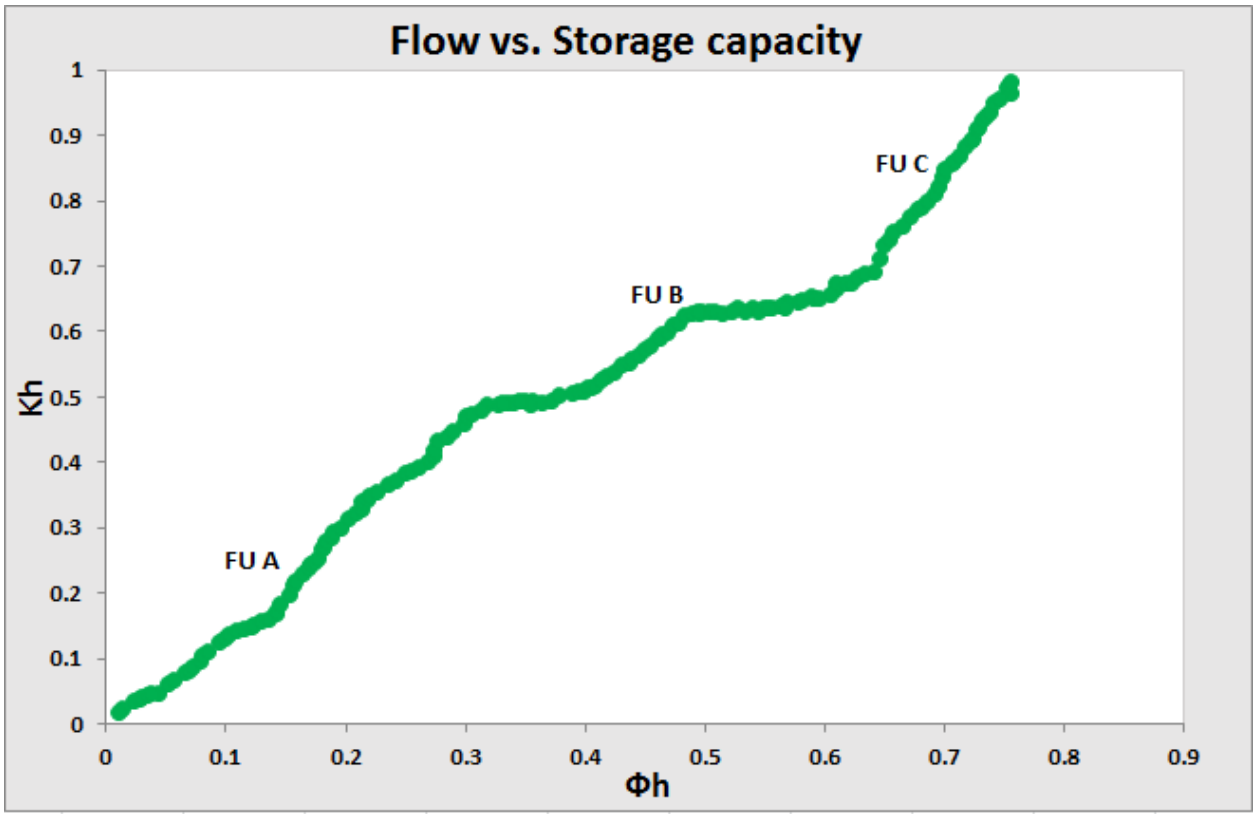

Figure 4.16: SMLP of the reservoir of interest for Well 3

4.4.4 Analysis of Well 4

Like the other wells, this well had log records for the upper most portions. The RQI versus Normalized Porosity, Normalized RQI, and Stratigraphic Modified Lorenz Plot reveal that, this well contains four flow units in the reservoir of interest (Reservoir X).

It is observed from the logs (see figure 4.7) on the petrophysical analysis software that, this well exhibits various geological interruptions within the reservoir. The correlated wells demonstrated the presence of a down-throw side displaced between well 4 and well 5 in the reservoir. This indicate that, there might be the presence of a fault or a fold occurring between well 4 and 5 which can throttle the movement of fluid in the reservoir with four flow layers delineated in this well. The well is displaced relative to well 5 in the east direction and also intercepts the reservoir sands at a point where many flow paths were delineated. The heterogeneous nature of the reservoir units in this well can cause different flow zones to exist within the reservoir sands in different directions and at different locations.

The well cross-cuts the highest thickness of the reservoir of interest and therefore the highest amount of hydrocarbons is expected.

The quality of the reservoir flow units can be determined from the plots above. The gradient of the flow unit in the normalized porosity line indicates the flow unit quality. High gradient characterize poor reservoir quality whereas lower gradient indicate better reservoir quality.

Table 4.4 shows the FZI's, gradient, regression coefficients and the wells of occurrence for each of the flow units identified in reservoir of interest.

Table 4.4: Table showing flow units present in Well 4 and their properties

Flow Unit	Gradient	FZI	H_T (μm^2)	R^2	Wells of Occurrences
B	2.02	22.04	2.06E-3	0.83	1,4
C	2.30	12.03	6.91.E-3	0.87	2,3
D	2.32	6.02	2.75E-2	0.89	2,4
E	2.36	3.05	1.07E-1	0.85	3,4

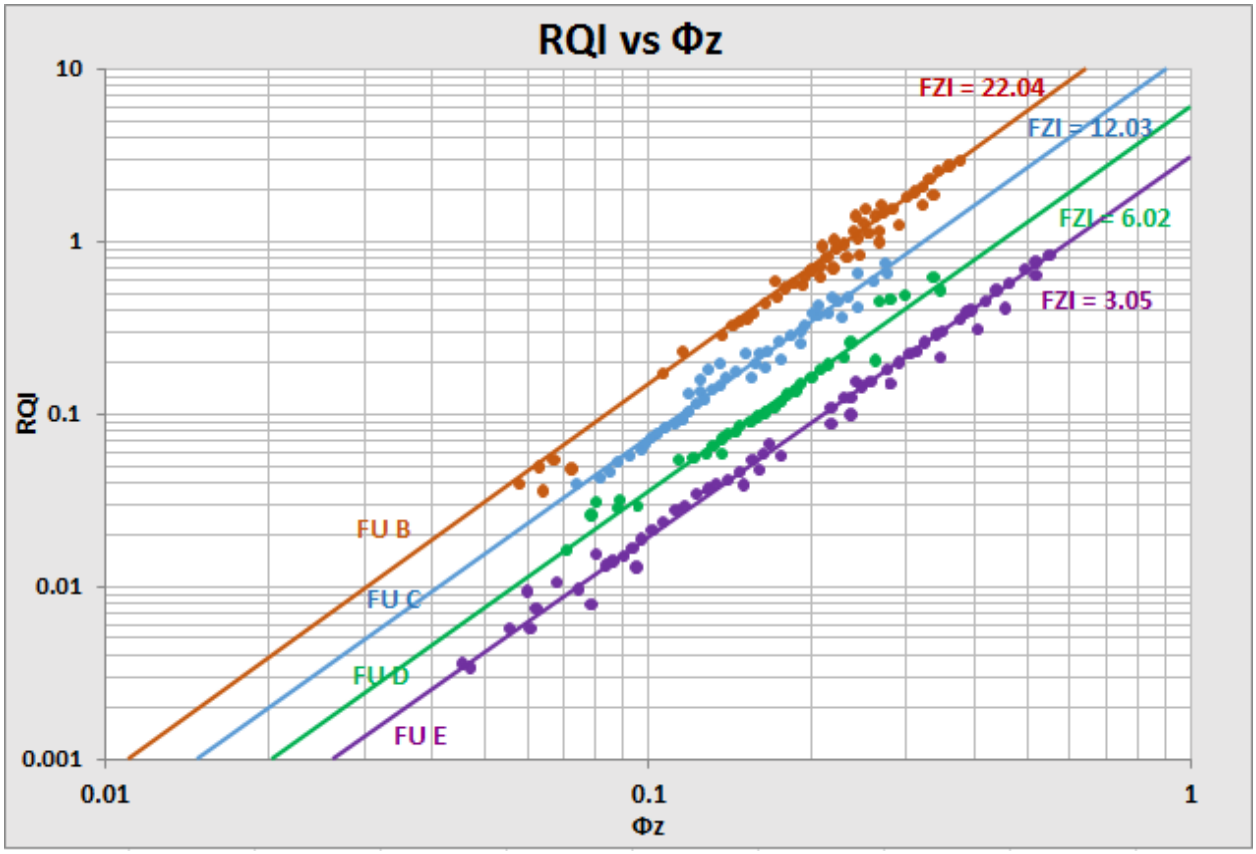

Figure 4.17: Graph of RQI versus Normalized Porosity of reservoir for Well 4

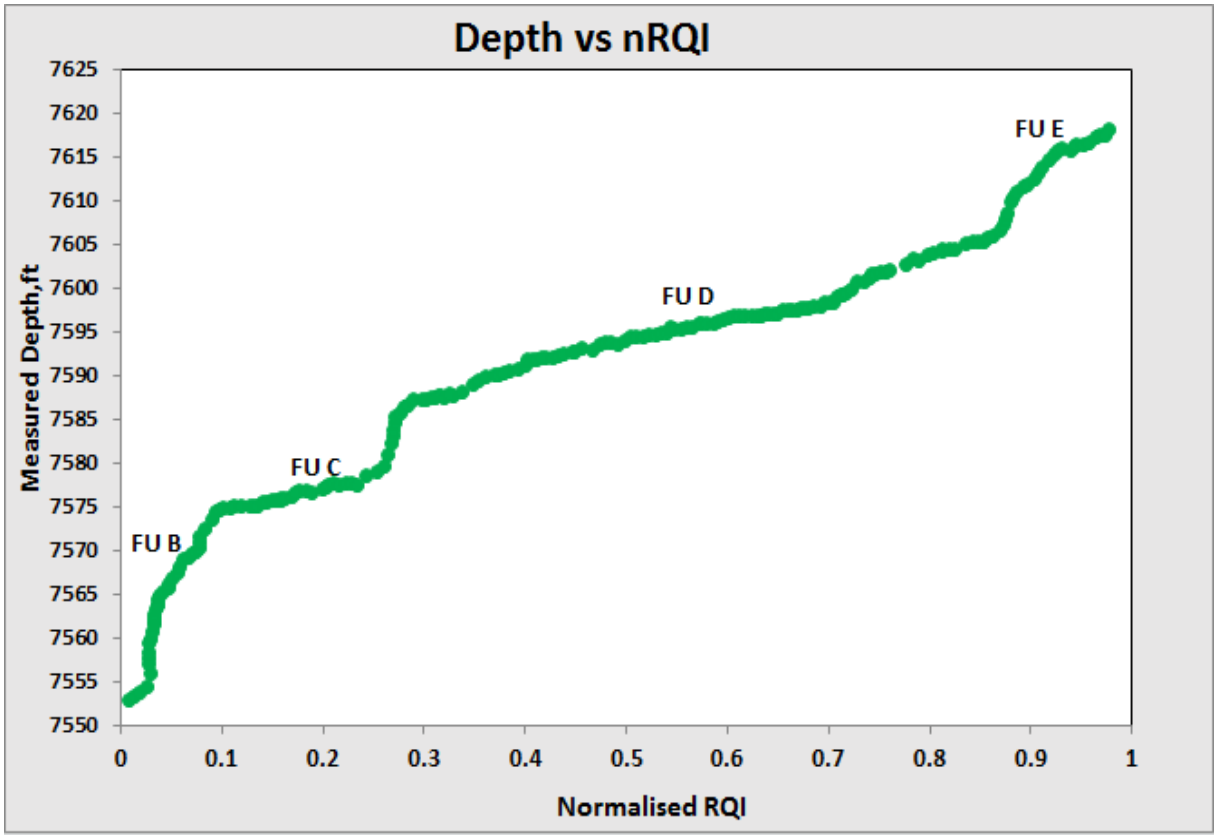

Figure 4.18: nRQI plot of the reservoir of interest for Well 4

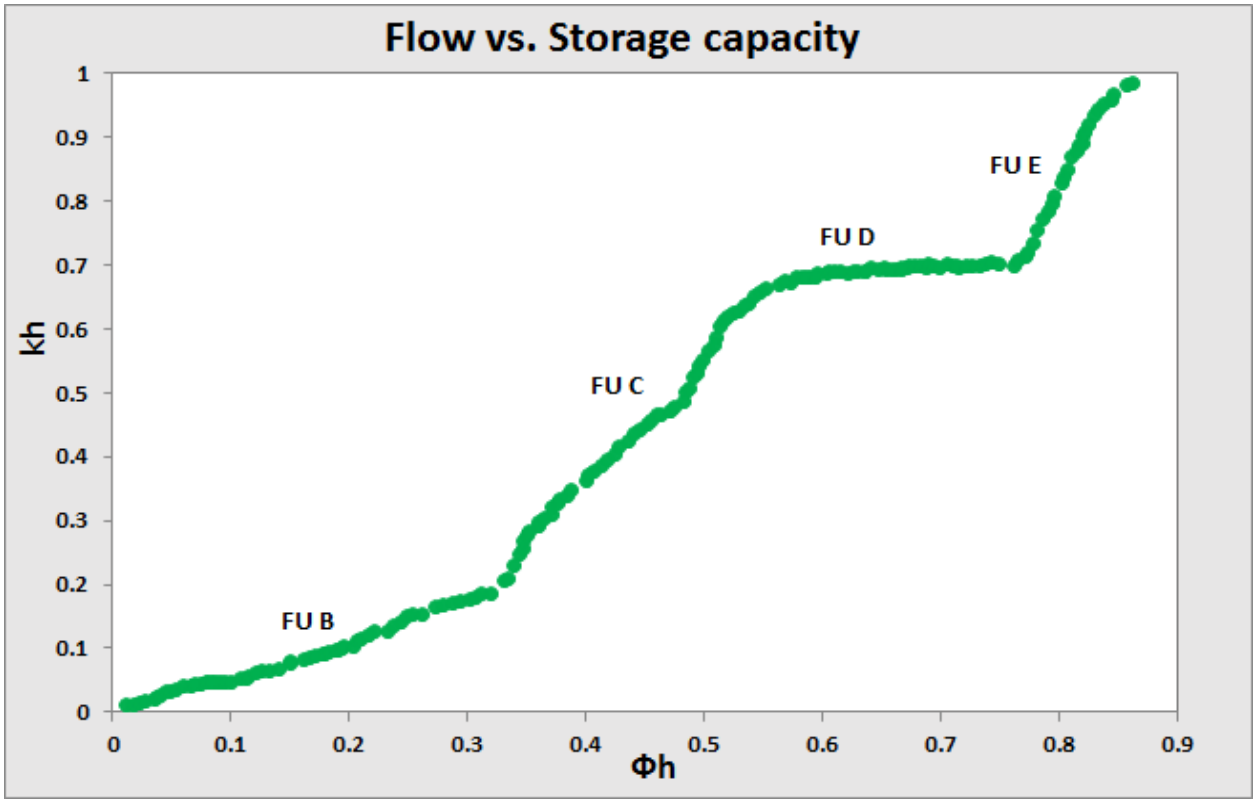

Figure 4.19: SMLP of the reservoir of interest for Well 4

4.4.5 Analysis of Well 5

The available data indicated that there were log records for the upper part of this well within the reservoir sands. However, there were no logs for some lower portions of the well. It might be possible that this part for which there were no logs intercepts the other reservoirs that were not delineated. The observations made from the respective graphs of RQI versus Normalized Porosity, Normalized RQI, and Stratigraphic Modified Lorenz Plot revealed that, well 5 basically contains two distinct flow zones out of the four flow layers which contribute to fluid flow in the reservoir of interest (Reservoir X). These may be due to pinch out, truncations as well as high spatial heterogeneity of the reservoir rock properties occurring at deeper depths. The reservoir sand exhibits different flow units at different points in all the wells. The presence of many flow units in well 4, with fewer flow units in well 5, is caused by truncation of the some of the flow units. The nature of the depositional setting may also be the probable cause for having only two flow units out of the four flow layers in the reservoir at the point where well 5 intercepts the reservoir under investigation.

The Agbada-Akata formations are associated with variations in the geological properties of the reservoir rock which is responsible for the truncation of some other flow units. There might be the presence of an unconformity between the point of well 5 and well 6, as the established baseline indicates an up-throw side towards the direction where well 6 intersect the reservoir sands.

This may have led to the blockage of other flow paths defined within some portions in well 5, thereby terminating them. Therefore the flow may not be continuous in this well compared to the other wells.

Considering the nature of the depositional environment within the Agbada-Akata petroleum system, it is, therefore, possible for well 5 to exhibit different properties relative to the other wells for the same reservoir sand unit. The quality of the reservoir flow units can be determined from the plots below. The gradient of the delineated flow unit in the normalized porosity graphs describes the flow unit quality. High gradient characterize poor reservoir quality, whereas lower gradient is indicative of better reservoir quality.

Table 4.5 shows the FZI's, gradient, regression coefficients and the wells of occurrence for each of the flow units identified in reservoir of interest.

Table 4.5: Table showing flow units present in well 5 and their properties

Flow Unit	Gradient	FZI	H_T (μm^2)	R^2	Wells of Occurrences
F	2.16	22.09	2.05E-3	0.91	3,5
E	2.25	42.06	5.65E-4	0.89	4,5

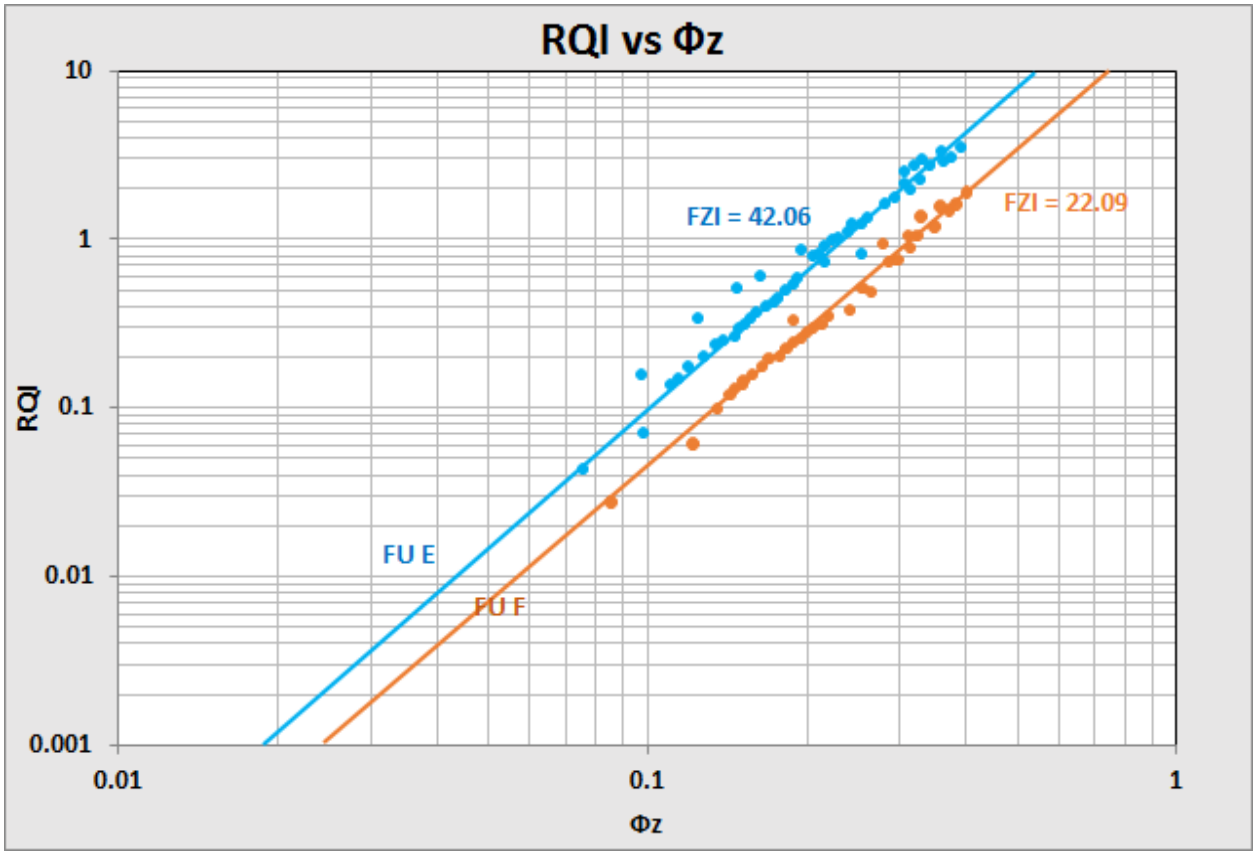

Figure 4.20: Graph of RQI versus Normalized Porosity of reservoir for Well 5

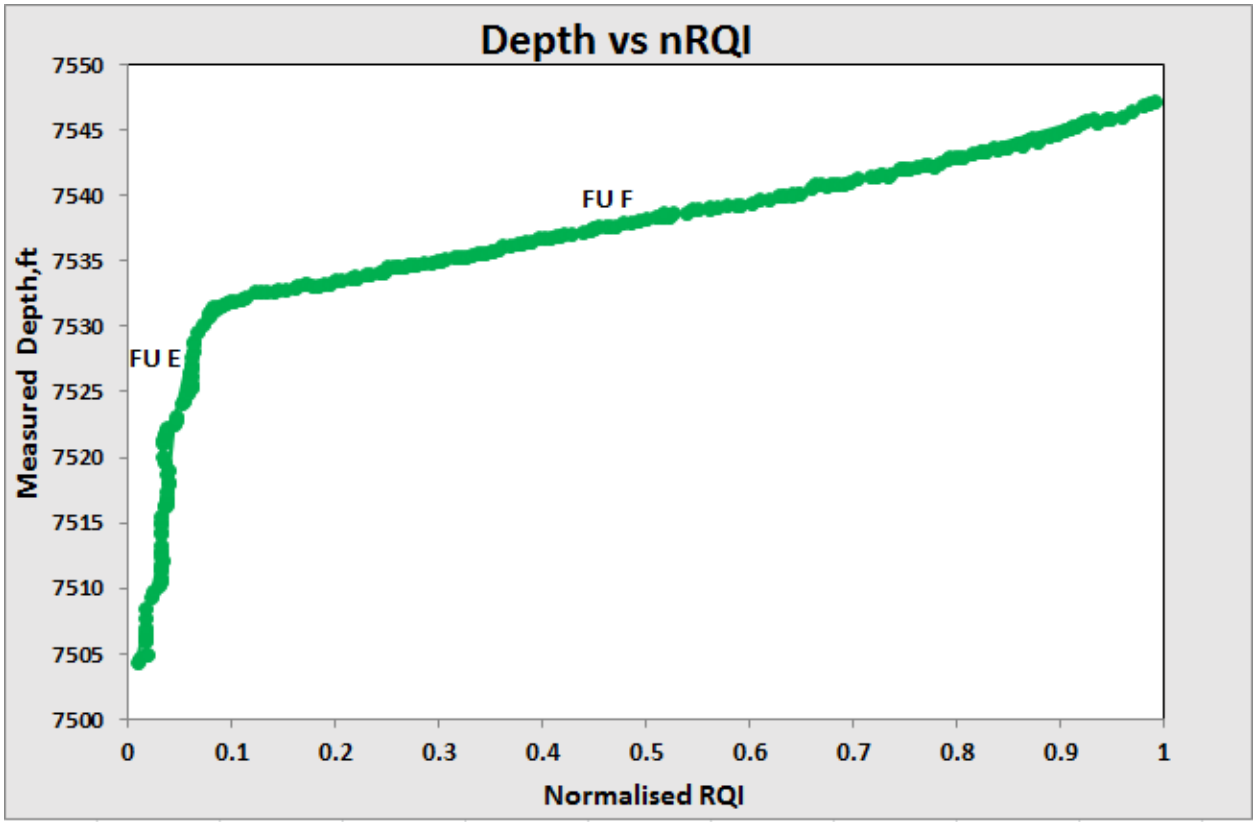

Figure 4.21: nRQI plot of the reservoir of interest for Well 5

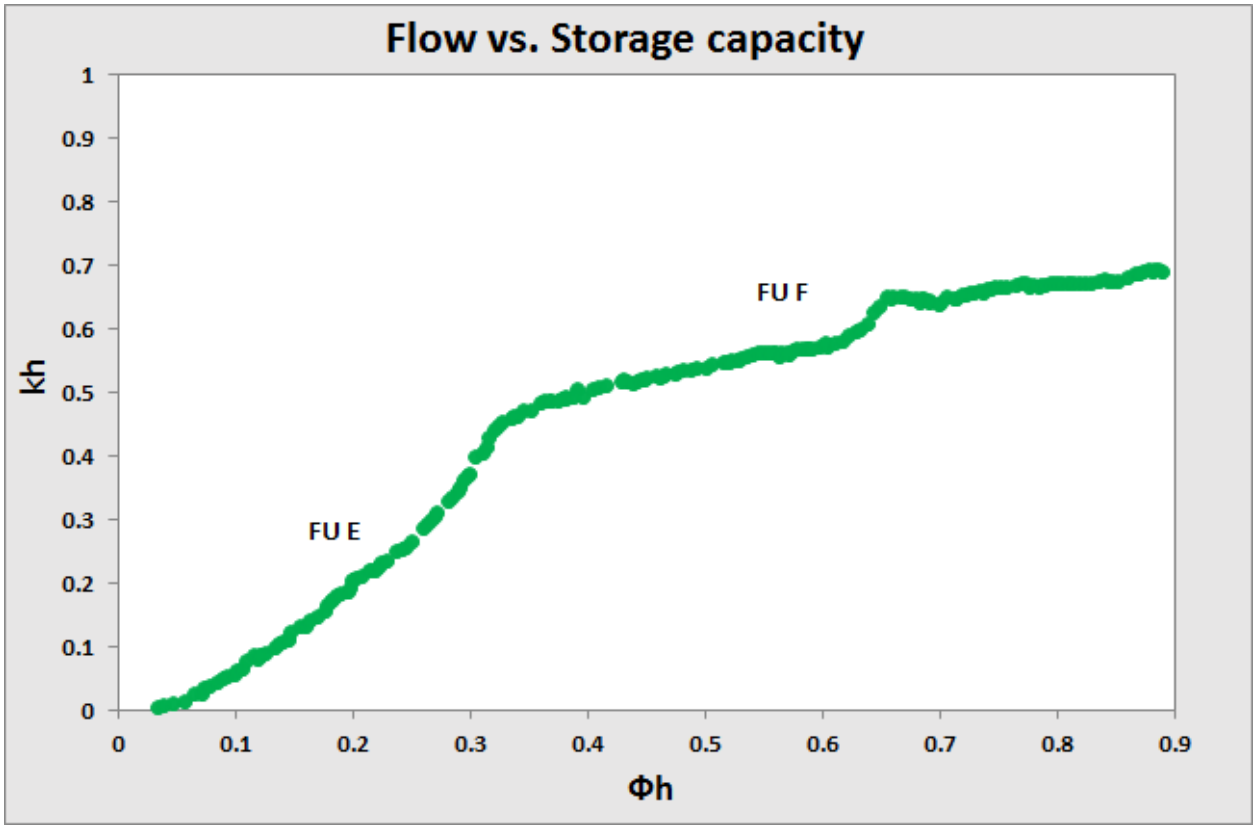

Figure 4.22: SMLP of the reservoir of interest for Well 5

4.4.6 Analysis of Well 6

This well intersects the reservoir sands present in the zone of interest (D 3000). No log records were present for some lower portions of this well. The unidentified portions may be within this unlogged zone. This is because some portions of the reservoir sand were not delineated in this well by the logs. Comparing the number of flow units in this reservoir, Well 4 and Well 6 have the highest number of flow units which show a better reservoir quality. The graphs of RQI versus Normalized Porosity, Normalized RQI, and Stratigraphic Modified Lorenz Plot reveal that, this well intersects four out of flow units present in the reservoir. The causes for this observation vary from well to well within the entire reservoir. It is observed from the log view on petrophysical analysis software that the reservoir unit thins out gradually from well 5 towards well 6. Much of the reservoir unit may have different flow units at the different portions, for which well 6 intersected the reservoir sand at the point where four flow zones significantly exist. The other flow units that were not present in this well might have been truncated.

The high spatial heterogeneous nature of the depositional environment may also be a possible explanation for having four distinct flow units in the reservoir at well 6. This well may, therefore, intersect the reservoir at the point where different zonations occur relative to the other wells being observed.

The quality of the reservoir flow units can be obtained from the various plots below. The gradient of the flow units in the normalized porosity plots explains the flow unit quality. High gradient characterize reservoir poor quality, whereas lower gradient is indicative of better reservoir quality.

Table 4.6 shows the FZI's, gradient, regression coefficients and the wells of occurrence for each of the flow units identified in reservoir of interest.

Table 4.6: Table showing flow units present in well 6 and their properties

Flow Unit	Gradient	FZI	H_T (μm^2)	R^2	Wells of Occurrences
A	2.03	22.03	2.06E-3	0.85	2,6
B	2.15	12.08	6.85E-3	0.86	4,6
C	2.26	5.03	3.95E-2	0.88	3,6
D	2.18	2.13	2.20E-1	0.87	5,6

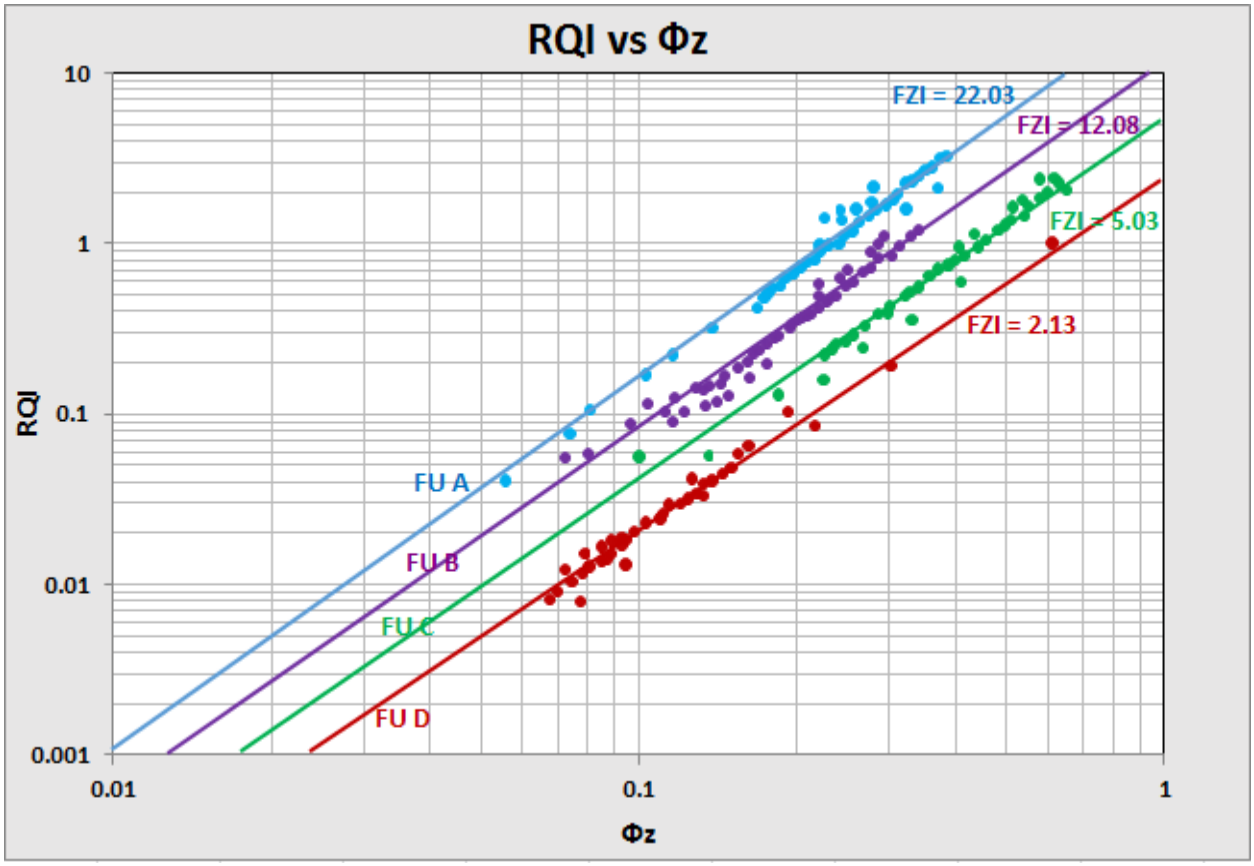

Figure 4.23: Graph of RQI versus Normalized Porosity of reservoir for Well 6

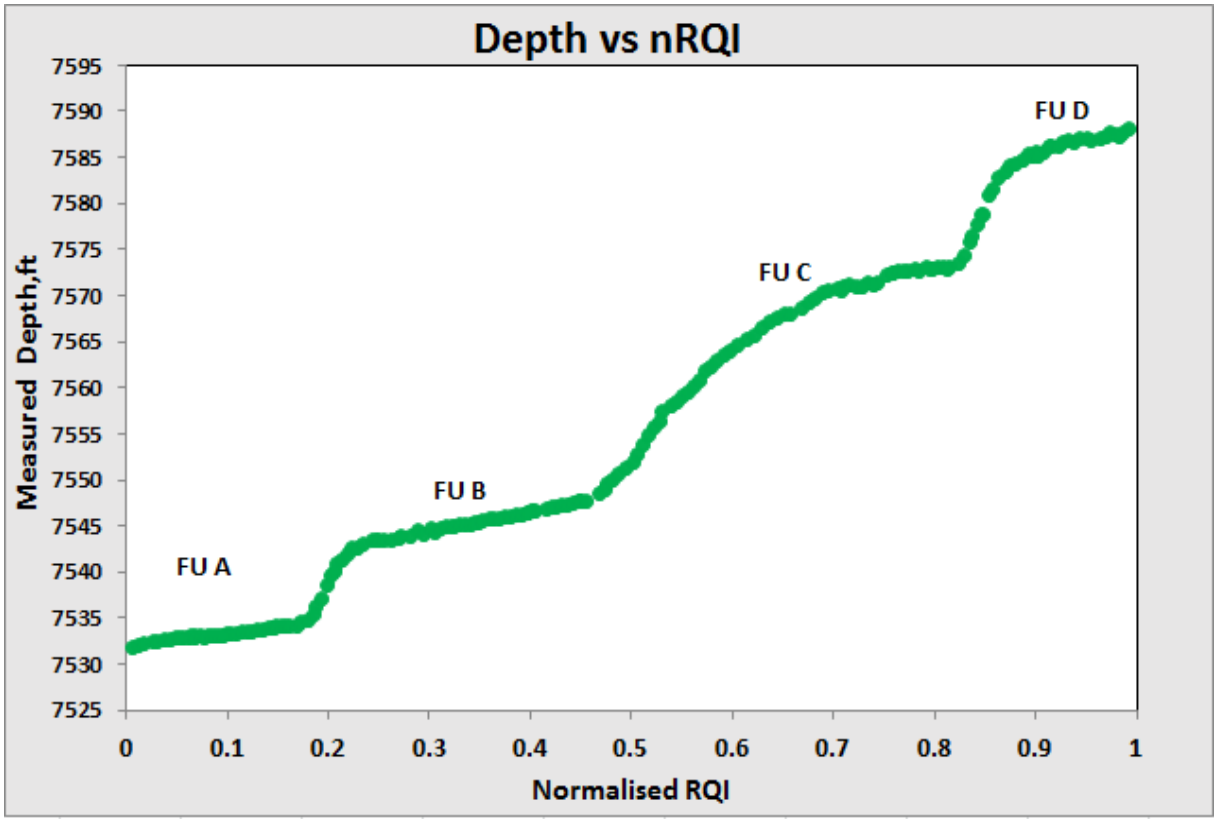

Figure 4.24: nRQI plot of the reservoir of interest for Well 6

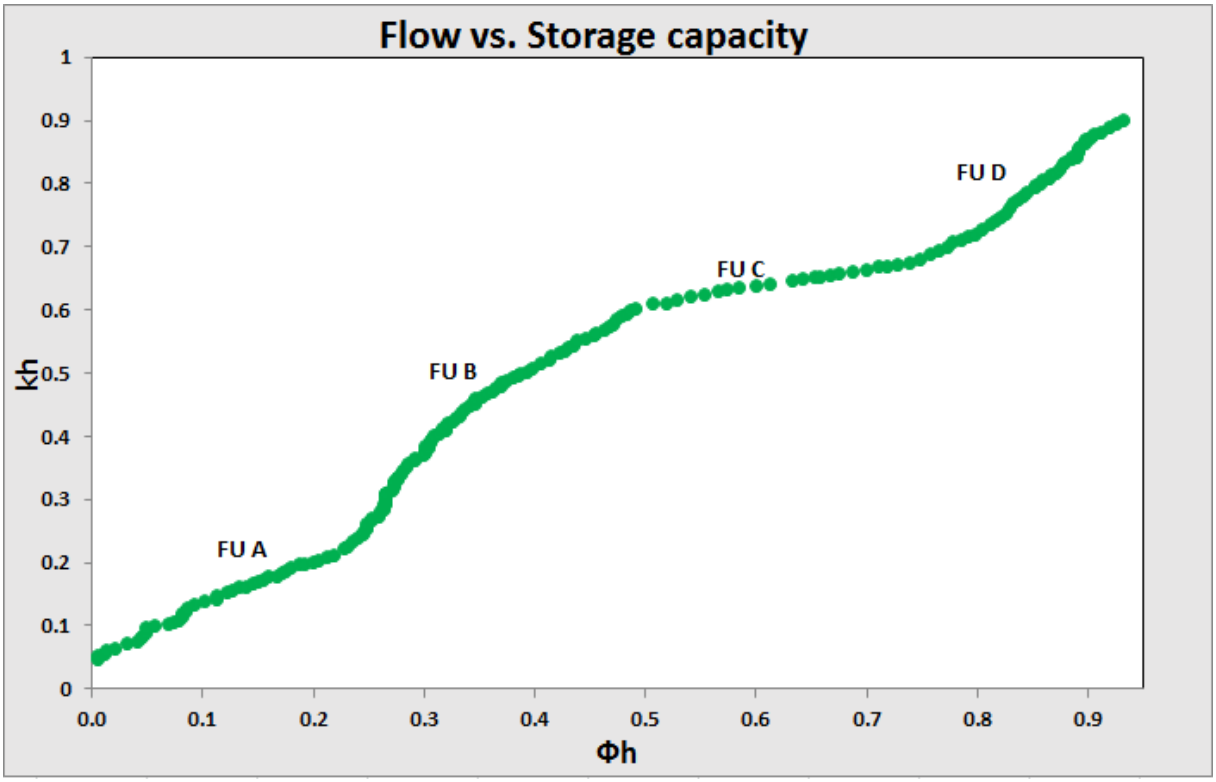

Figure 4.25: SMLP of the reservoir of interest for Well 6

The table below is a summary of the petrophysical parameters of the six wells in Reservoir X.

Table 4.7: Shows Petrophysical Sums and Averages for Reservoir X

Reservoir X	Top Sand MD (ft)	Base Sand MD (ft)	Net MD (ft)	Perm. (mD)	Total Porosity (Φ_T)	Eff. Porosity (Φ_e)	Shale Volume (Vsh)
Well 1	7500.32	7714.92	214.60	1056.234	0.3641	0.2264	0.1405
Well 2	7555.48	7710.78	155.30	2542.372	0.3583	0.2360	0.2716
Well 3	7505.05	7703.60	198.10	2618.545	0.3203	0.1823	0.1563
Well 4	7550.78	7716.48	165.70	1961.352	0.3154	0.1974	0.1376
Well 5	7500.89	7701.39	200.50	2342.944	0.3015	0.2203	0.2294
Well 6	7525.90	7712.10	186.20	3465.648	0.3185	0.2554	0.2643

4.5 3D Static Reservoir Modeling

Reservoir rocks are rarely found to be homogeneous in nature in terms of physical properties. They usually possess some variations in geologic processes of erosion, deposition, lithification, folding, and faulting among many others, which makes the reservoir rock heterogeneous and nonuniform. Therefore, adequate description of the lateral variations of these properties is essential to characterize the reservoir. In view of this, it was necessary to build static models of the reservoir properties to describe its flow characteristics. Modern geostatistical methods were incorporated to describe the spatial distribution of the reservoir flow parameters and also to assess how these properties are significantly affected by certain geological facies such as shale.

A cell size of 96 x 96 x 20 was selected in building the 3D Grid, being enough to capture all the details of the reservoir. The total number of 3D grid cells came up to 184320. Static models of the various flow properties for the Agbada-Akata formation were built by integrating relevant petrophysical data. The porosity and permeability from calibrated logs were used to build the models. The SGEMS (Version 2.1) suite was used in building the static models.

4.5.1 Property Modeling

This is the process whereby the cells of the grid are filled with continuous (petrophysical) or discrete (facies) properties including porosity, permeability and facies.

The property modeling was distributed stochastically within the constructed 3D grid using Sequential Gaussian Simulation, Sequential Gaussian Cosimulation, Sequential Indicator Simulation and Kriging Algorithms. The dataset was imported into SGEMS with all the property logs (validated with core data). These logs were then calibrated and scaled up. The well logs are scaled up by sampling the various property values from the well logs into three dimensional grid such that each grid cell will be assigned a single value for each property to be modeled.

The methods adopted are described as follow:

i. Defining region of stationarity

The maximum and minimum values of the x and y coordinates were used to estimate the region of stationarity as shown in Table 4.8.

Table 4.8: Shows computed values used to define region of stationarity

Xmin	621359.554 ft		Ymin	4416890.171 ft
Xmax	623285.703 ft		Ymax	4418816.317 ft
ΔX	1926.149 ft		ΔY	1926.146 ft
No. of X Cells	96 ft	No. of Y Cells	96 ft	No. of Z Cells = 20 ft
Size of each cell along x-direction	20 ft	Size of each cell along x-direction	20 ft	Size of each cell along z-direction = 10 ft

ii. Spatial modeling of sampled data

The SGEMS modeling software was first used to generate histogram plots and descriptive statistics for the data from the sampled porosity, permeability, and facies. This was followed by generating a series of experimental variograms and corresponding modeled variograms, from which the ones with the best fit data points were chosen for kriging and simulation.

iii. Estimation of variables (property values) at unsampled locations

Simple kriging (SK), Ordinary kriging (OK) and Cokriging were carried out on the selected variogram models (Gaussian models for porosity, permeability and facies) to estimate porosity, permeability and to assess the effect of shale facies on these properties at the unsampled locations within the flow layers delineated. Sequential Gaussian Simulation was equally carried out on the various models for porosity with different realizations. Sequential Gaussian, Sequential Gaussian Cosimulation, and Indicator Simulation were equally carried out on the variogram models for permeability and facies with different realizations. The maps generated from kriging and simulations are shown in the figures below and the results discussed.

4.6 Porosity Models

The total porosity was estimated majorly from density logs using a *rho-matrix* value of 2.65 g/cm^3 and *rho-fluid* value of 1.0 g/cm^3 from PVT data. The effective porosity was then deduced by substituting shale volume into the equation .The effective porosities obtained were validated using core data from well 1 in the reservoir. The deduced effective porosities from the petrophysical analysis software compare well with the core porosity. The equation above (3.4.3) was used in the computation. These effective porosities within the identified flow units were modeled to describe the flow characteristics of the Agbada-Akata formations.

The figures below show the porosity maps generated from Kriging and Sequential Gaussian Simulation.

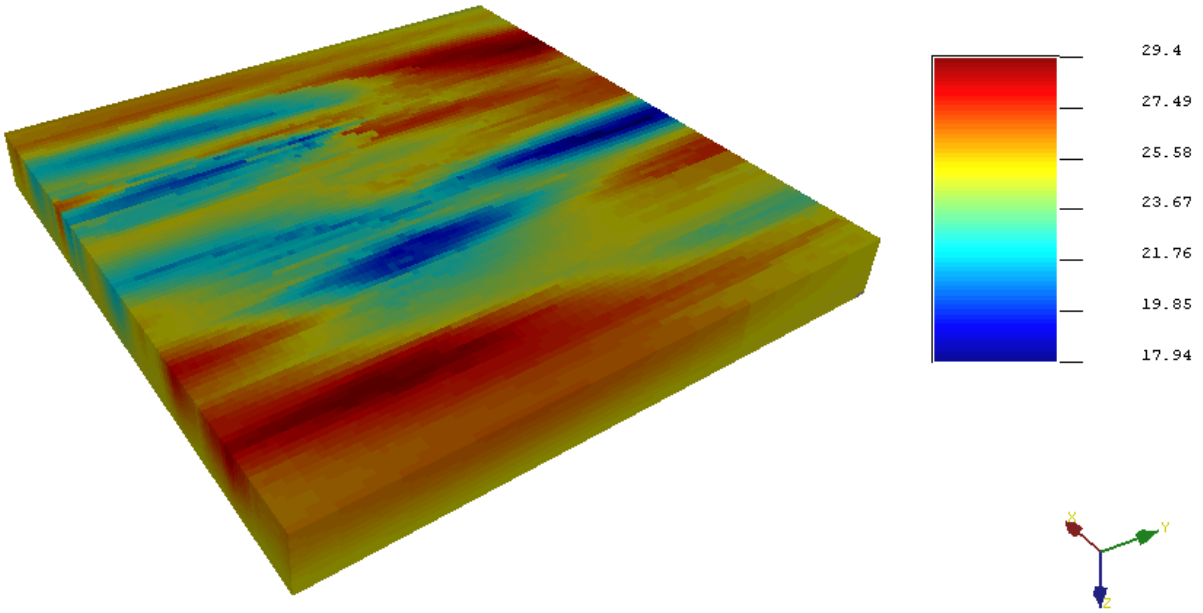

Figure 4.26: Porosity model (all wells) from Simple Kriging

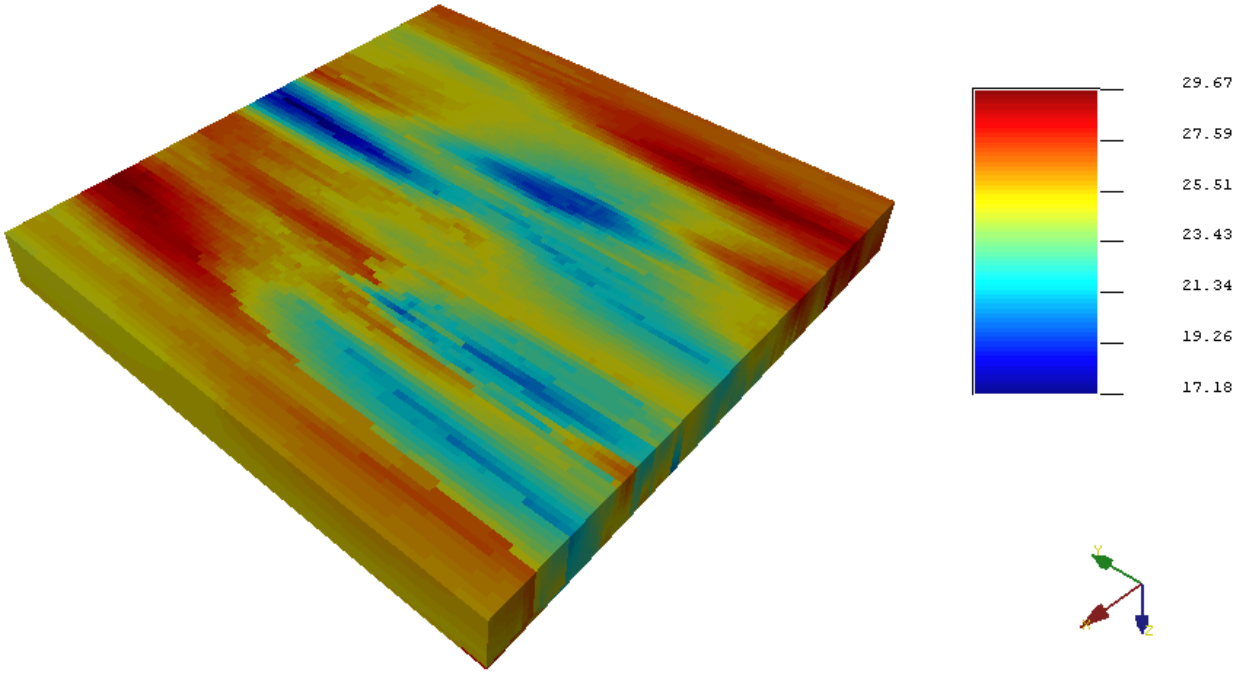

Figure 4.27: Porosity model (all wells) from Ordinary Kriging

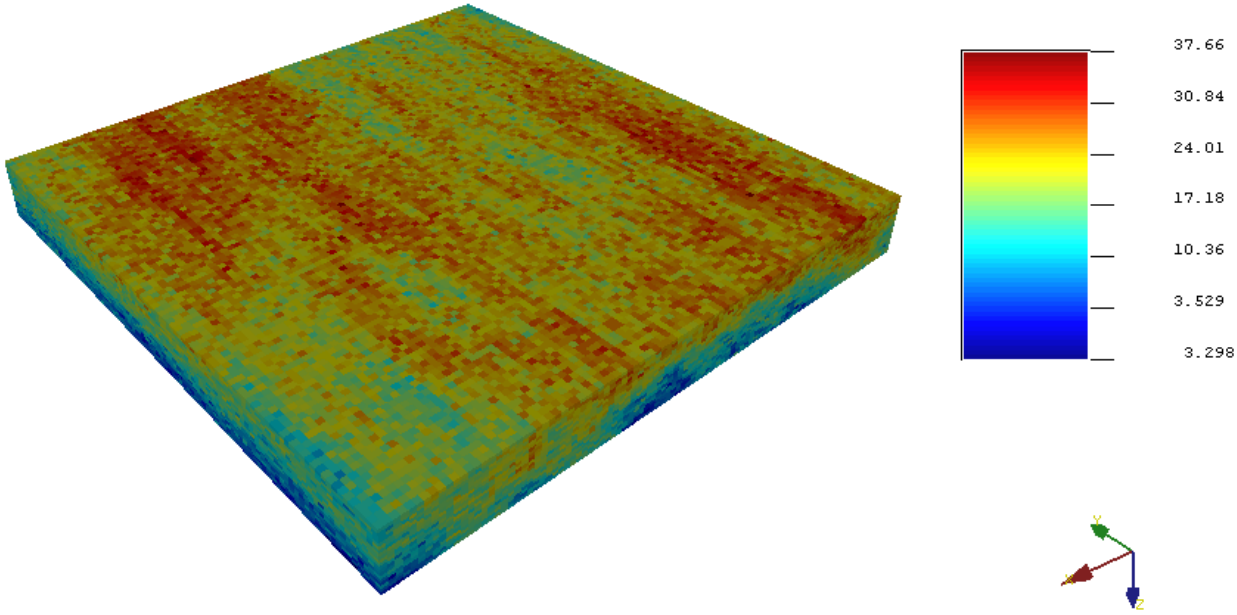

Figure 4.28: Porosity model (all wells) from Sequential Gaussian Simulation

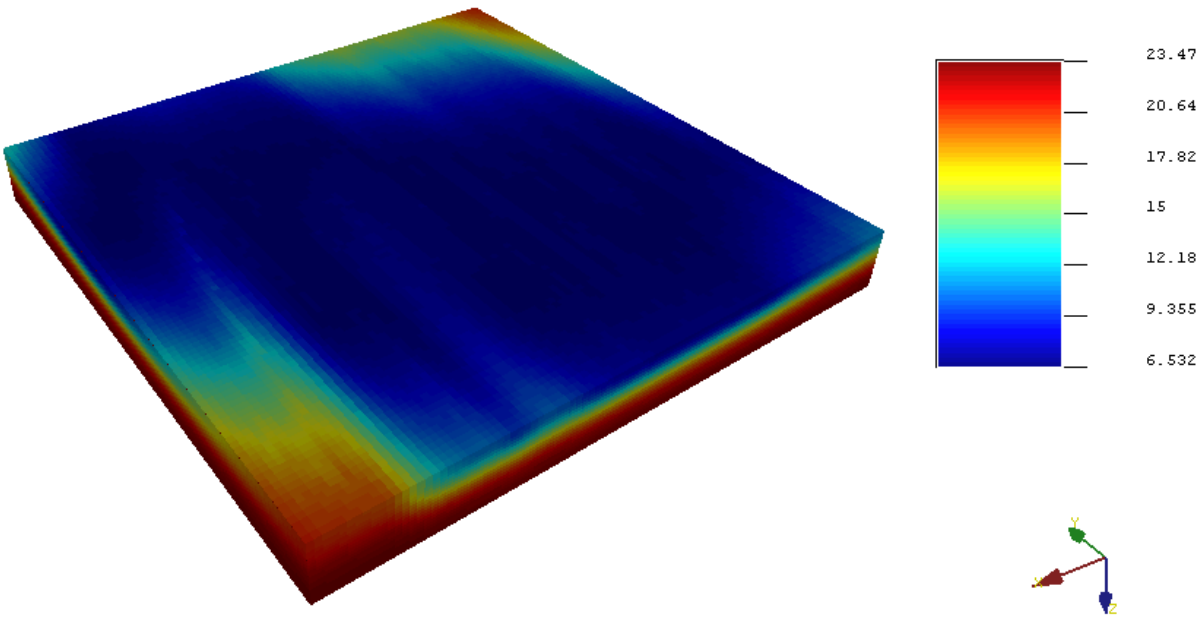

Figure 4.29: Porosity model (all wells) from Simple Kriging Variance

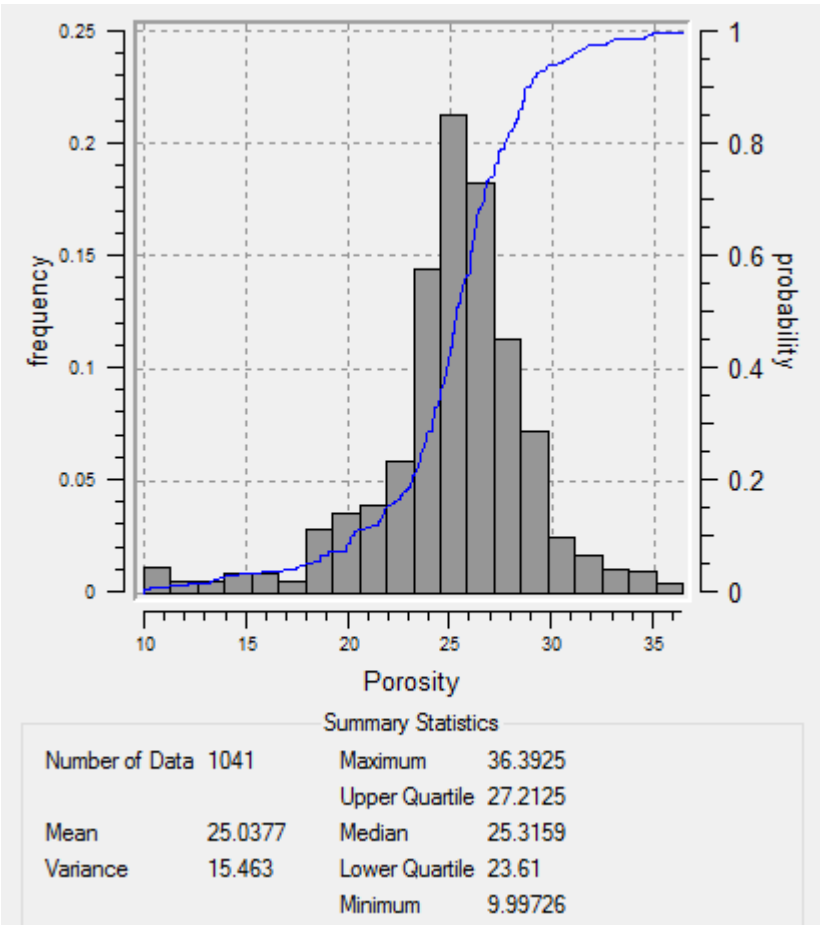

Figure 4.30: Histogram of porosity distribution (all wells)

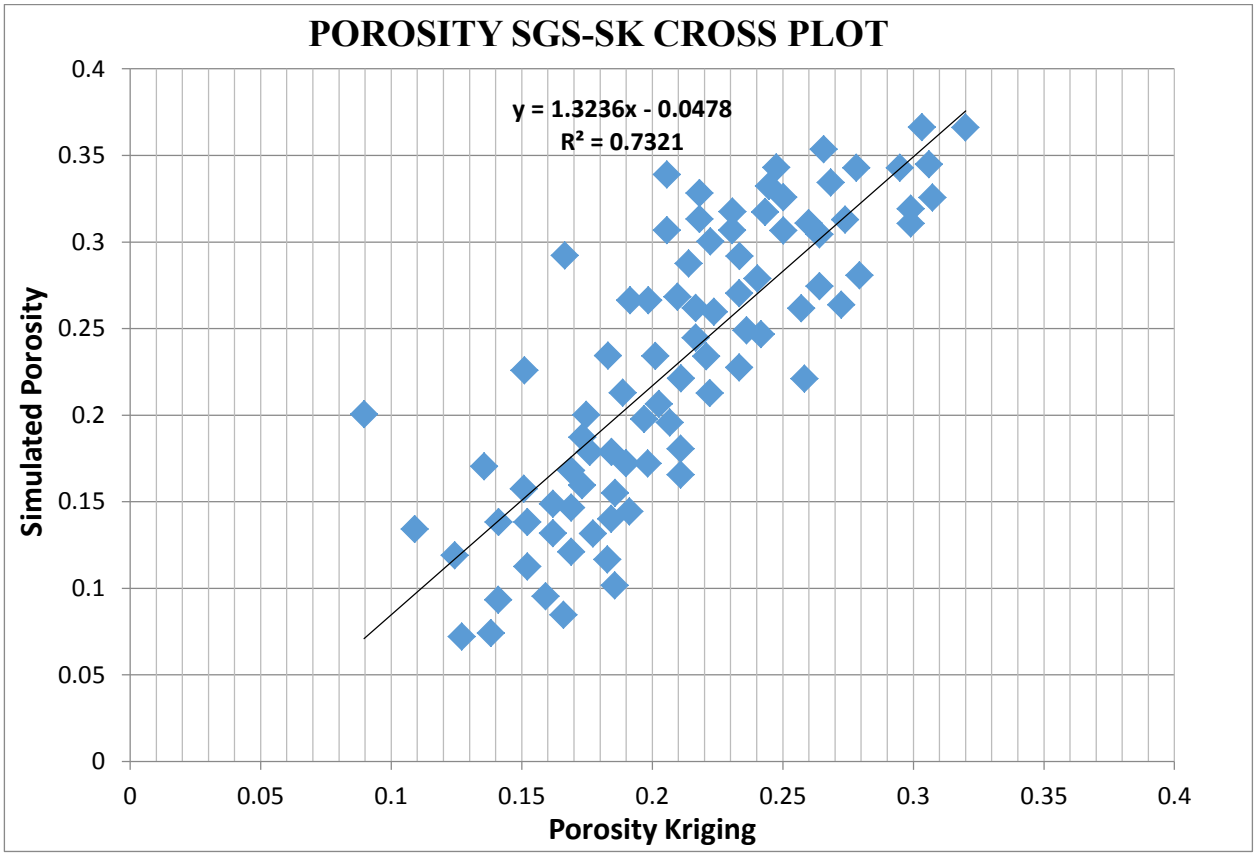

Figure 4.31: Porosity SGS – SK Cross Plot

4.6.1 Analysis of Results

The porosities for both the simple and ordinary kriging maps have smooth appearances indicating a good spatial continuity of porosity distributions in the flow units of the reservoir which corresponds to the principal direction of the variogram. The estimation variance could be low as 6.532 at where the grid block is close to the sample data. However, the estimation variance could be as large as 23.47%. The mean and median value of porosities data from the histogram are 25.03% and 25.31% respectively. They are very close to each other indicating symmetry in the distribution of these properties. The average porosity range is between 9.99%-36.39% across the entire reservoir. The porosity values in the reservoir fall within good porosity. These values indicate that the reservoir rocks in the wells have enough pore space to accommodate fluids. Realizations of porosity were generated using Sequential Gaussian Simulation which used a normal transform to turn the porosity values at the wells into several sets of values which constantly gives a standard normal distribution with a unit standard deviation and zero mean.

From figures 4.26 and 4.27, it can be seen that the distribution trend of the simulated porosities is quite similar to that from the simple kriging estimation as well as the ordinary kriging estimations. Higher porosities are experienced when moving towards the peripherals of the grid area. This indicates that there are high porosity locations spreading from the middle to the corner portion of the reservoir.

Noticeably, in the grid corners, the simulated values of porosity are relatively higher at the central portion of the reservoir than either of the results estimated from the two kriging techniques. The linear regression line fitted on the cross plot of Sequential Gaussian simulation porosity versus simple kriging gave a correlation coefficient (R^2) of 0.7321 indicating a good correlation and similarity between the two.

4.7 Permeability Models

Empirical correlation was used to predict the permeability of the reservoir. Coates Method (1981) was employed in this study for that purpose. Since core data was present for some of the wells in Reservoir X, the estimated permeabilities were validated using core data from well 1 in the study reservoir.

The deduced permeabilities from Techlog compare well with the core permeability. These permeabilities within the identified flow units were modeled to describe the flow characteristics of the Agbada-Akata formations.

The figures below show the permeability distribution maps generated from Kriging, Sequential Gaussian Simulation and Sequential Indicator Simulation.

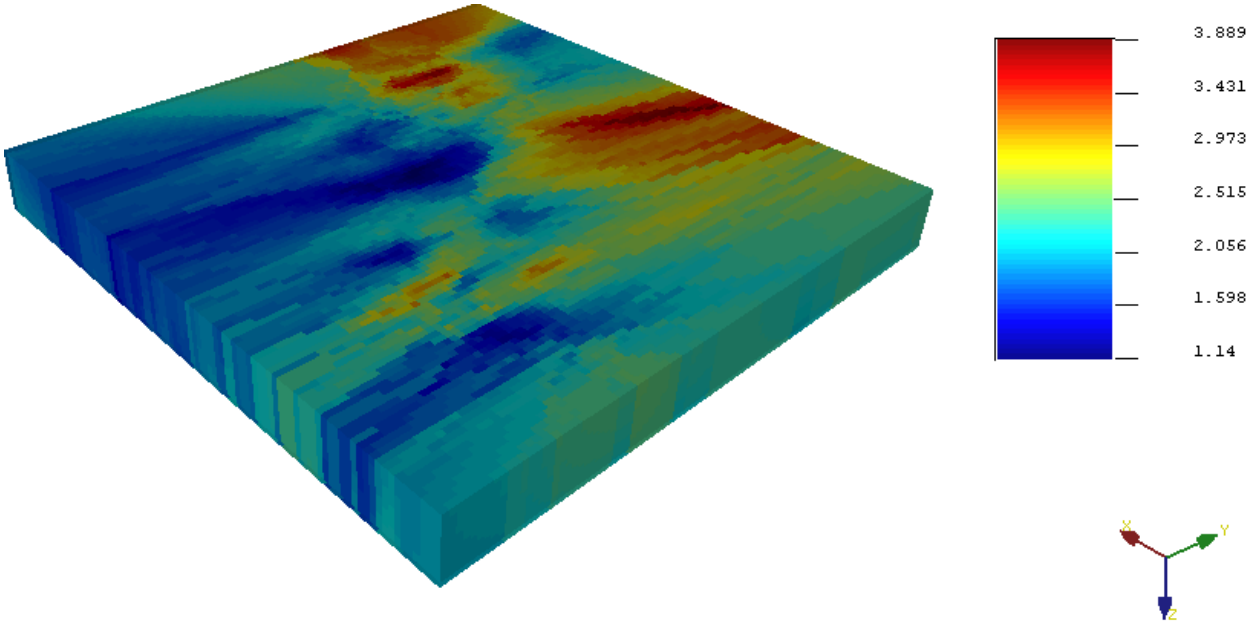

Figure 4.32: Permeability model (all wells) from Simple Kriging

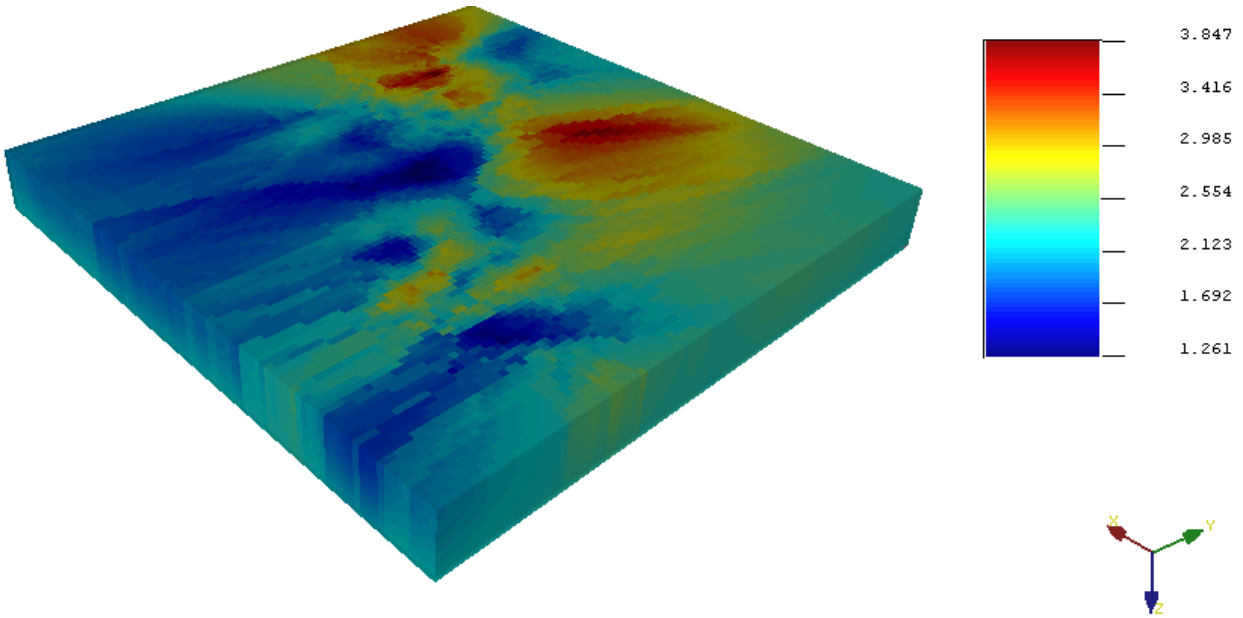

Figure 4.33: Permeability model (all wells) from Ordinary Kriging

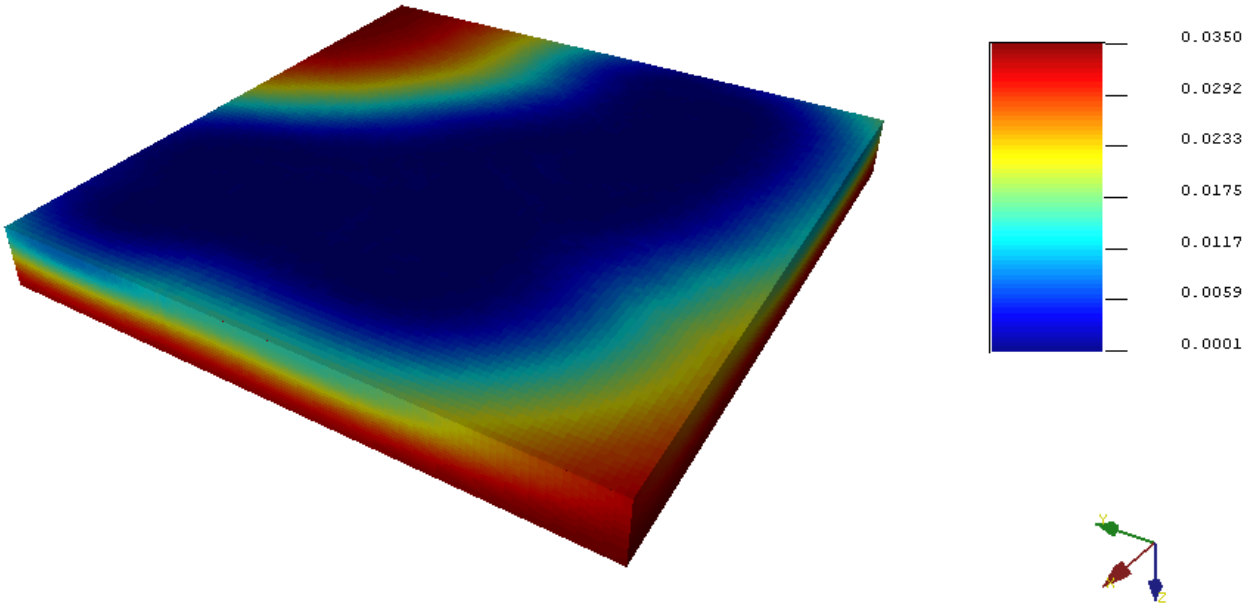

Figure 4.34: Permeability model (all wells) from Simple Kriging Variance

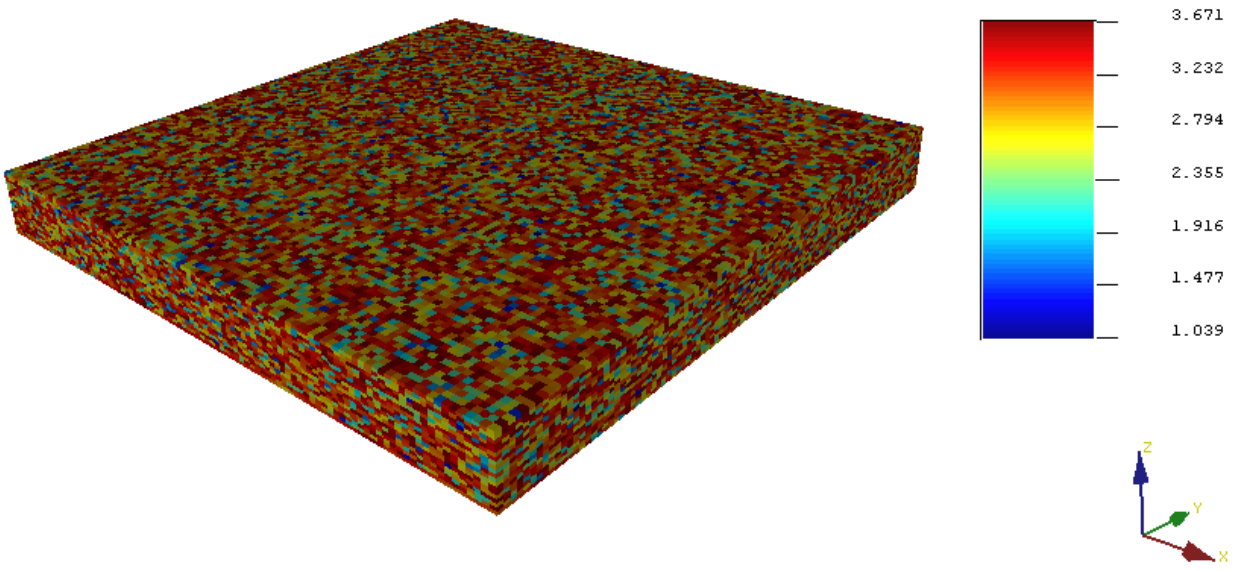

Figure 4.35: Permeability model (all wells) from Sequential Indicator Simulation

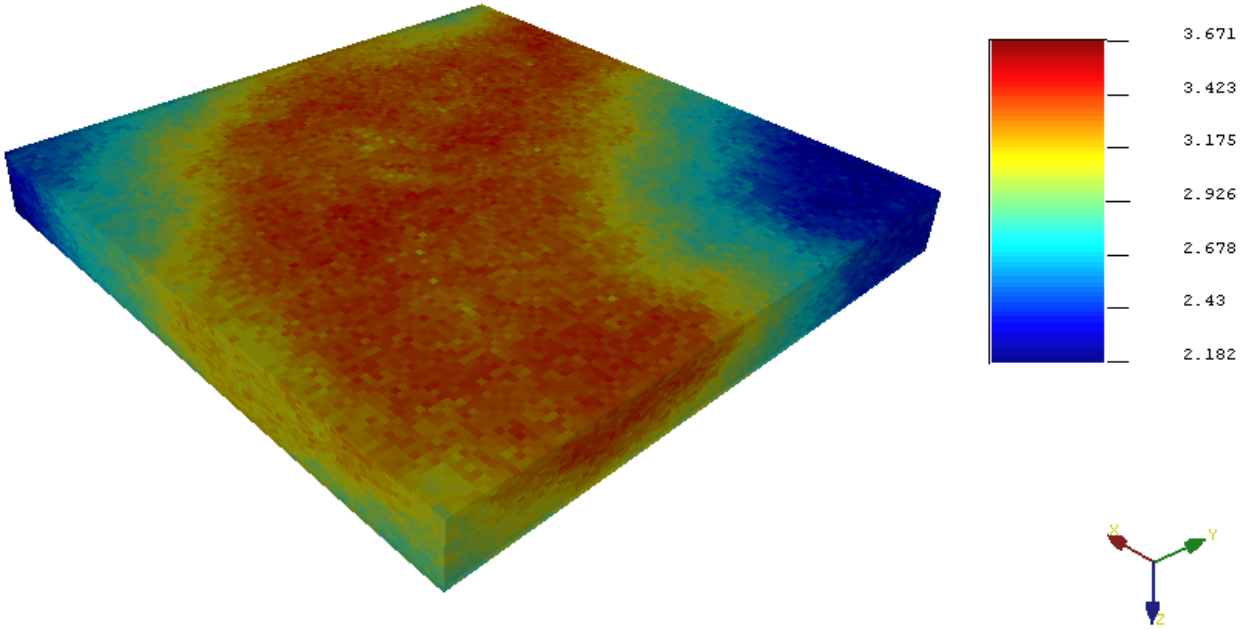

Figure 4.36: Permeability model (all wells) from Sequential Gaussian Simulation

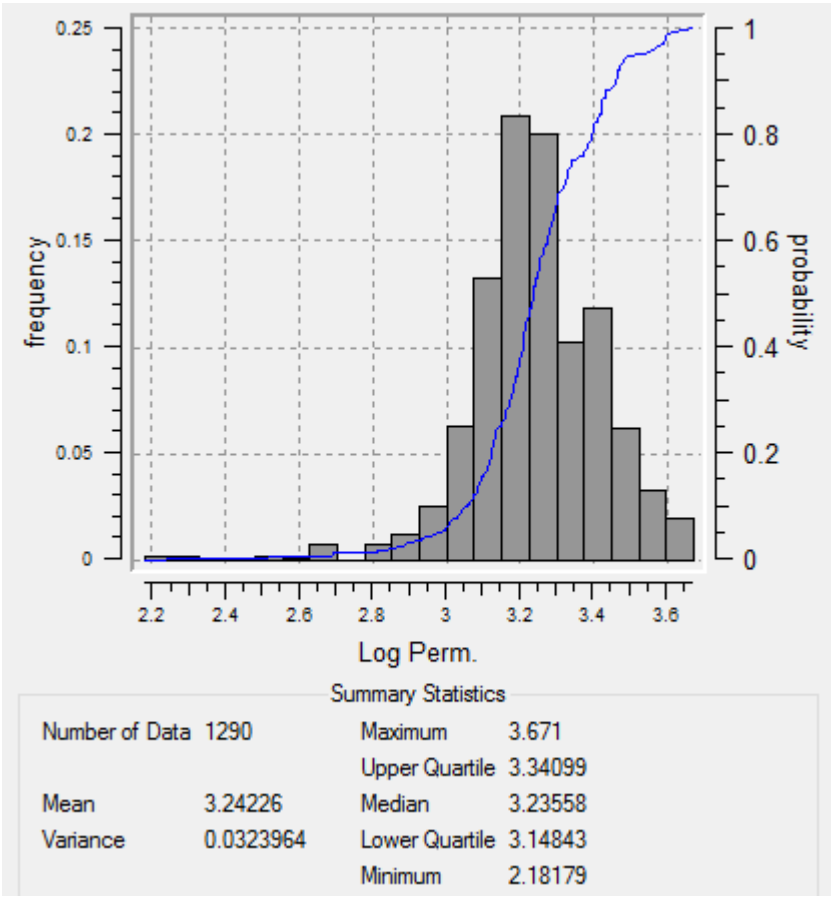

Figure 4.37: Histogram of permeability distribution (all wells)

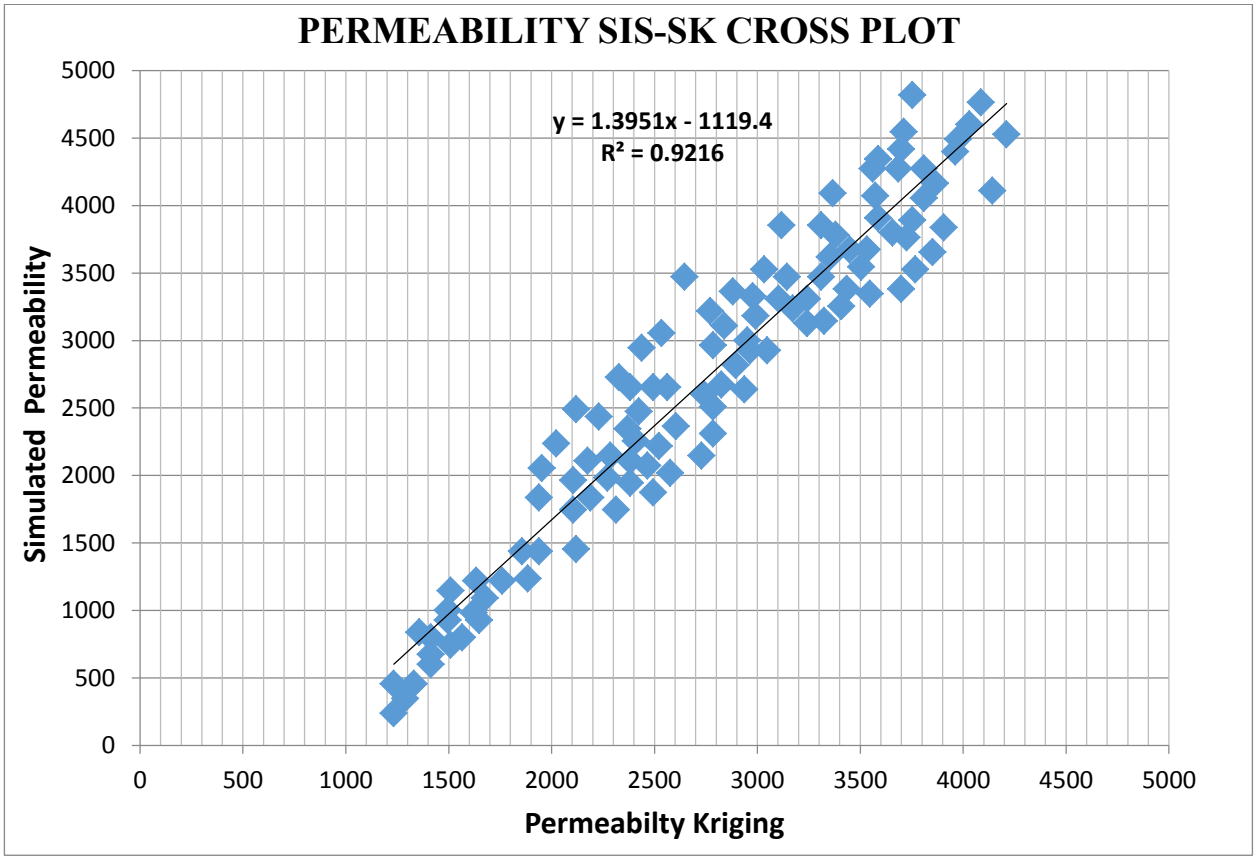

Figure 4.38: Permeability SIS – SK Cross Plot

4.7.1 Analysis of Results

Considering permeability, the mean and median values (from figure 4.37) are 1931.70mD and 1736.94mD. They are closely related indicating that, the estimated distribution of the permeability in the reservoir is symmetrical. This means they are uniformly distributed throughout the reservoir with some few variations. The permeability peaked at 4688mD with the minimum value occurring at 248.87mD respectively. The average permeability ranges between 248mD-5000mD across the entire reservoir. The permeability values in the reservoir fall within high to very high permeability. These values indicate that the reservoir rocks in the wells are more permeable to transmit fluids. Both the simple and ordinary kriging shows a similar trend in spatial continuity which corresponds to the principal direction of the variogram model. Higher permeability values are experienced in the flow units from the north-west corner of the reservoir. The yellow and red areas represent the portions of which the permeability is relatively higher, whereas the blue represents portions with relatively lower permeabilities.

Several realizations of permeability were generated using Sequential Indicator and Gaussian Simulation, which used a normal transform to turn the permeability values at the wells into a set of values that gives a standard normal distribution with a unit standard deviation and zero mean. The estimation variance could be low as 4.301E05 at specified locations where the grid block is in proximity with the sample data, and could be as large as 6.997E05. However, the realizations of permeability generated using indicator simulation demonstrated permeability values which are closer to the values from the Simple and Ordinary kriging techniques. A cross plot of sequential indicator simulation (SIS) permeability, versus simple kriging (SK) with a linear correlation fitted for them (R^2 = 0.9216), indicates a better correlation and similarity between the two techniques. In all, the estimated permeability distribution in the various flow units matches the distribution in the study reservoir with very few significant variations.

4.8 Permeability Variations

The permeability variations within the flow layers identified were determined using Dykstra-Parson coefficient. The coefficient of variation is obtained from equation (4.1.7). The procedure for graphically determining the coefficient of variation is as follows:

a. Permeability data was sorted in decreasing or descending order as shown in Table 4.9

b. Index of rank data, j is obtained from sorted data indicating samples with larger permeability

c. Cumulative frequency distribution is the computed from the relation j/(N+1)

Where N is the number of sample data = 16

d. The standard normally distributed variables, Z- values were calculated using:

Column 5 = NORMSINV(G5)

Where G5 = Cumulative frequency distribution

e. A graph of Z-values versus sorted permeability data was plotted

f. K_{50} and $K_{84.1}$ were read from the Z- values versus permeability graph

g. The Coefficient of variation was computed using the relation

$V_{DP} = (K_{50}-K_{84.1})/K_{50}$

h. The data was fitted using straight line through them, with more emphasis placed on data points in the middle portion where the cumulative frequency is approximately 50%. This straight line provides a qualitative, as well as a quantitative, measure of the heterogeneity of the reservoir rock.

Table 4.9: Calculated parameters for the permeability variation measure

Permeability to air (mD)	Sorted Perm	Number of Samples with Larger Permeability	Cumulative Frequency Distribution	Z-Values
620.6	1094.5	0	0	0
455.4	1093.9	1	0.058823529	-1.5647
602.0	1040.4	2	0.117647059	-1.1868
716.2	947.5	3	0.176470588	-0.9289
408.3	903.3	4	0.235294118	-0.7215
633.1	798.9	5	0.294117647	-0.5414
947.5	770.0	6	0.352941176	-0.3774
903.3	756.6	7	0.411764706	-0.2230
798.9	752.6	8	0.470588235	-0.0738
770.0	716.2	9	0.529411765	0.0738
752.6	633.1	10	0.588235294	0.2230
1093.9	620.6	11	0.647058824	0.3774
1040.4	602.0	12	0.705882353	0.5414
1094.5	595.0	13	0.764705882	0.7215
756.6	455.4	14	0.823529412	0.9289
595.0	408.3	15	0.882352941	1.1868
362.3	362.3	16	0.941176471	1.5647

4.8.1 Analysis of Results

The permeability variation of the study reservoir is approximately 0.35. This shows that the Agbada-Akata formations are heterogeneous systems. The average permeability variation range for this reservoir is $0.25 < V_k < 0.50$. Therefore, for the purpose of minimizing errors in reservoir simulation, the reservoir can be approximated with a homogeneous model. In this case, the numerical simulators should then be run efficiently with the concept of maintaining a heterogeneous reservoir model if the heterogeneity index is closer to 0.50.

The reason for the permeability variations in the reservoir may be attributed to the geologic processes of deposition and accumulation of sediments. This is because the amount of cementing materials or seal to flow e.g. shale, is always high for low permeability values, and relatively low for high permeability values. In this case, the geometric averaging technique would be applicable for the permeability determination in this clastic reservoir.

Figure 4.39 shows the heterogeneity measure of the Agbada-Akata formations.

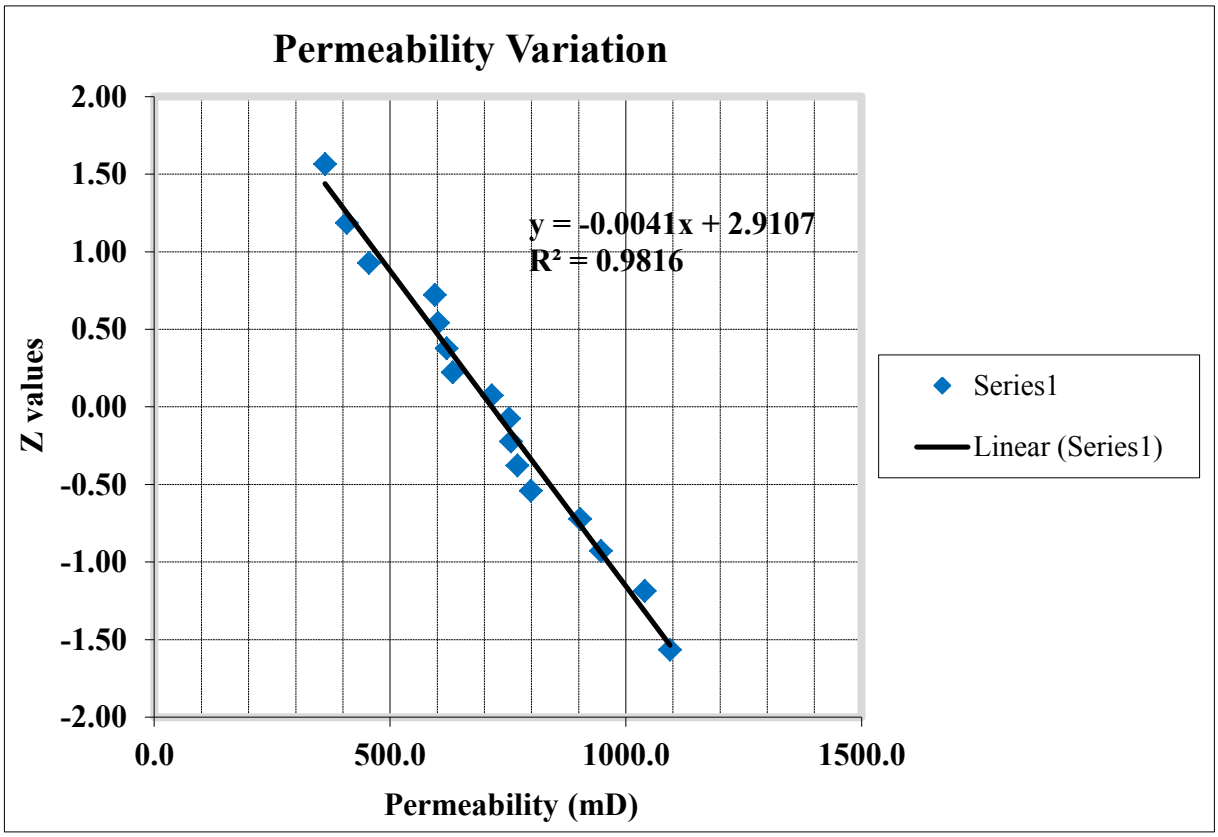

Figure 4.39: Graph of permeability variations for reservoir X

Table 4.10: Shows the results of permeability variation for reservoir X

Parameters	Calculated	Eye Ball from Straight line
At Z = 0, K50 =	709.9268 mD	700 mD
At Z = 1, K84.1 =	465.1219 mD	450 mD
VDP=(K50-K84.1)/K50	0.34483	0.35714

4.9 Effect of Shale on Permeability and Porosity

The percentages of shale volume to sands were estimated using gamma logs. The results were achieved by applying Larionov's (1969) Tertiary Rock equation for clastic reservoirs. The Gamma log curves were used in the evaluation process because all the six active wells have gamma logs. The Larionov's (1969) Tertiary Rock equation for clastic reservoirs was adopted simply because the Agbada-Akata petroleum system according to (Stacher, 1995) is a tertiary clastic formation in the Niger Delta Province.

Cokriging and Sequential Gaussian Cosimulation techniques were adopted to assess how shale adversely affects the permeability and porosity distributions within the identified flow layers of the Agbada-Akata formations.

The figures below show the maps of permeability distribution in shale facies generated from Cokriging and Sequential Gaussian Cosimulation.

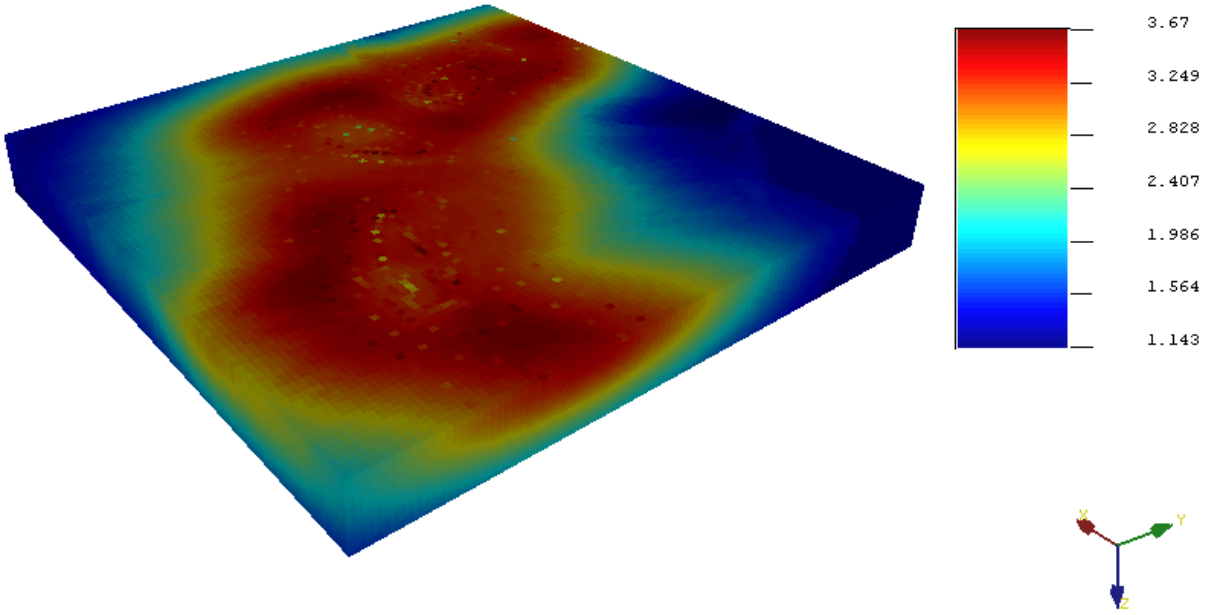

Figure 4.40: Permeability in shale model (all wells) from Cokriging

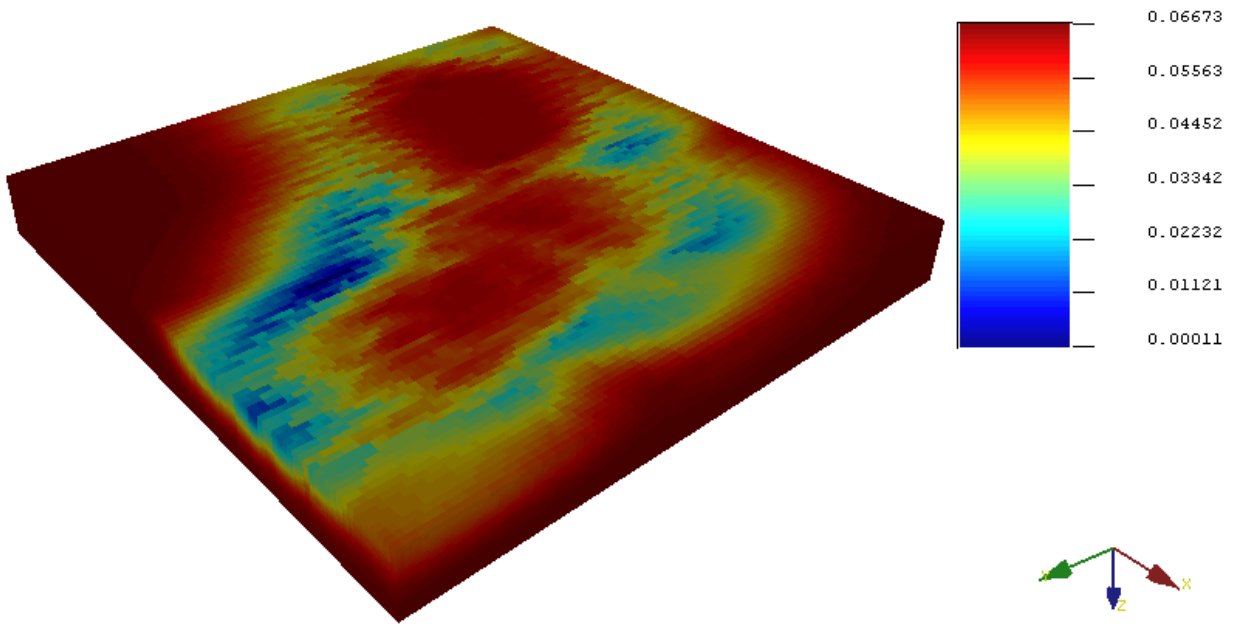

Figure 4.41: Permeability in shale model (all wells) from Cokriging Variance

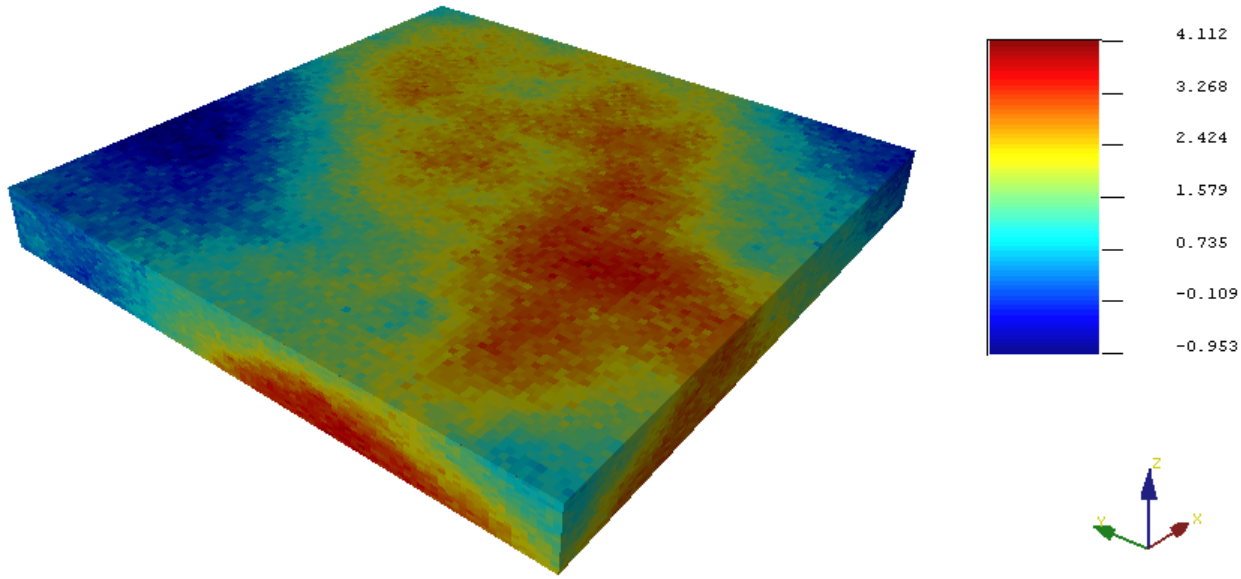

Figure 4.42: Permeability distribution in shale model (all wells) from Cosimulation

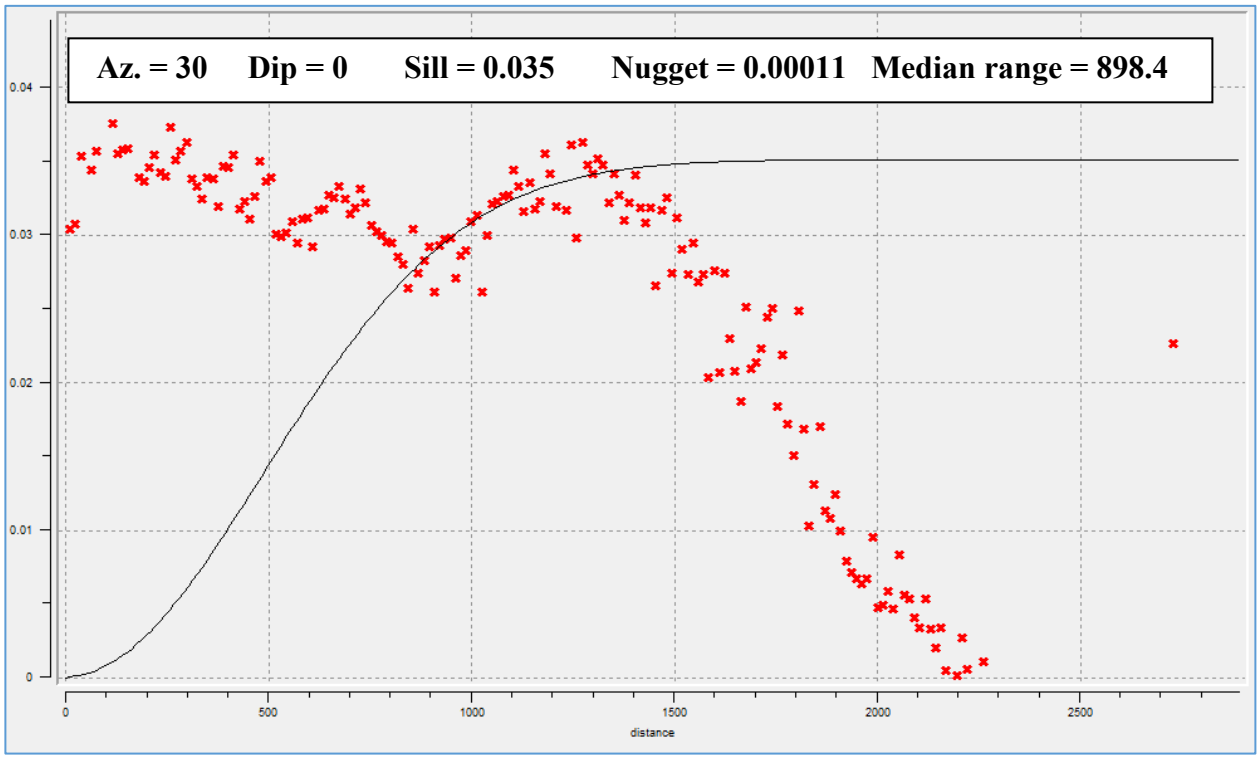

Figure 4.43: Anisotropic Cross Variogram model for Cokriging of permeability

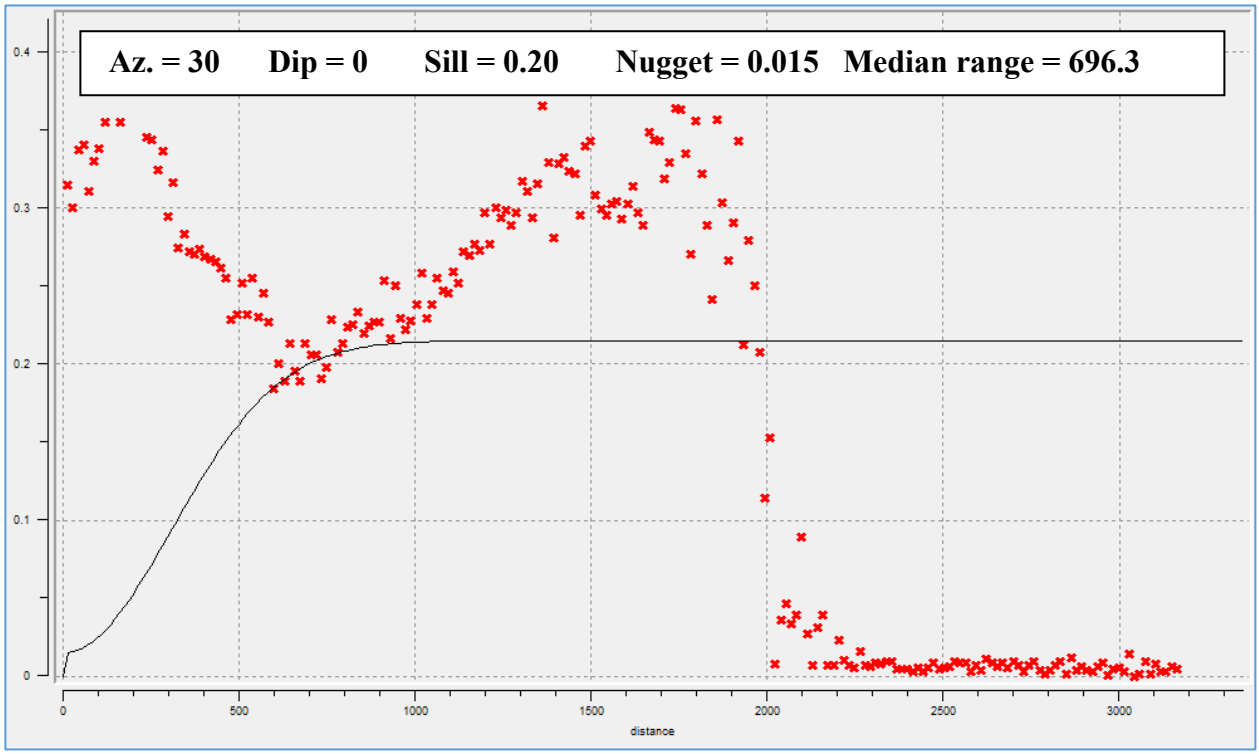

Figure 4.44: Anisotropic Perm-Perm Variogram model for Cokriging of permeability

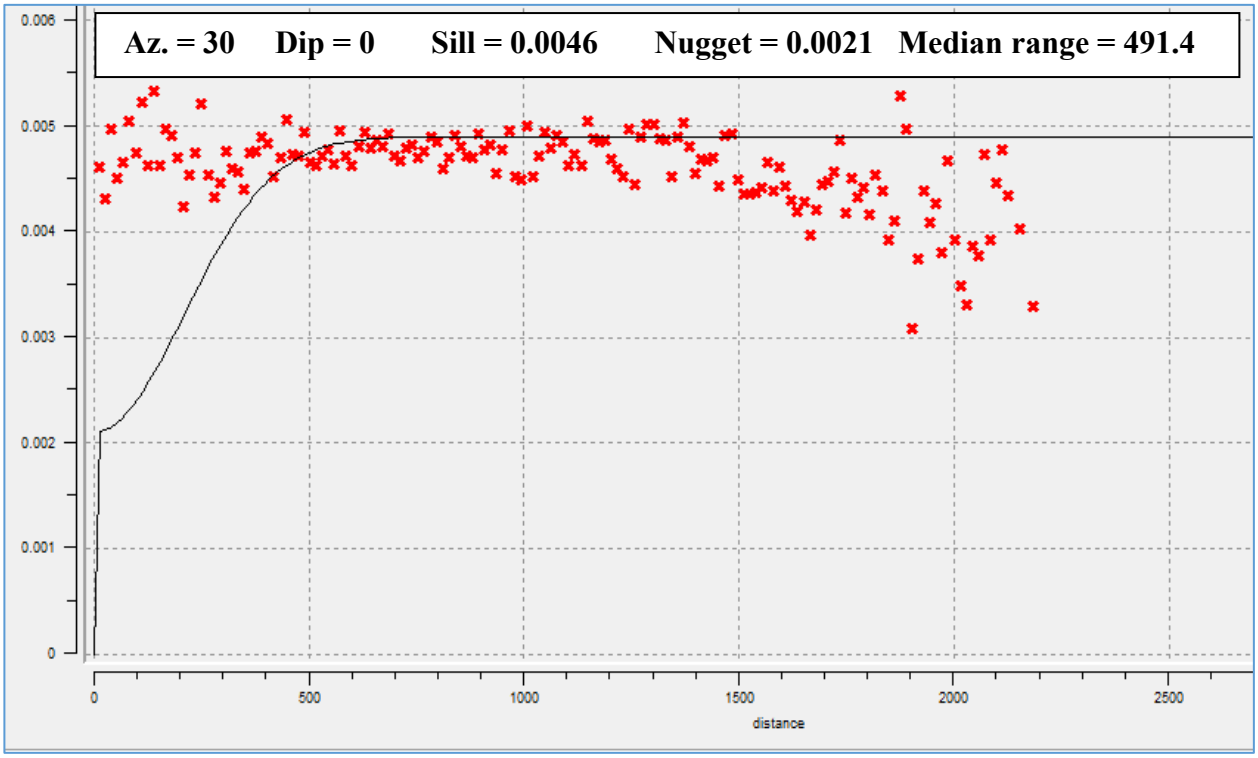

Figure 4.45: Anisotropic Shale-Shale variogram model for Cokriging of permeability

The figures below show the maps of porosity distribution in shale facies generated from Cokriging and Sequential Gaussian Cosimulation.

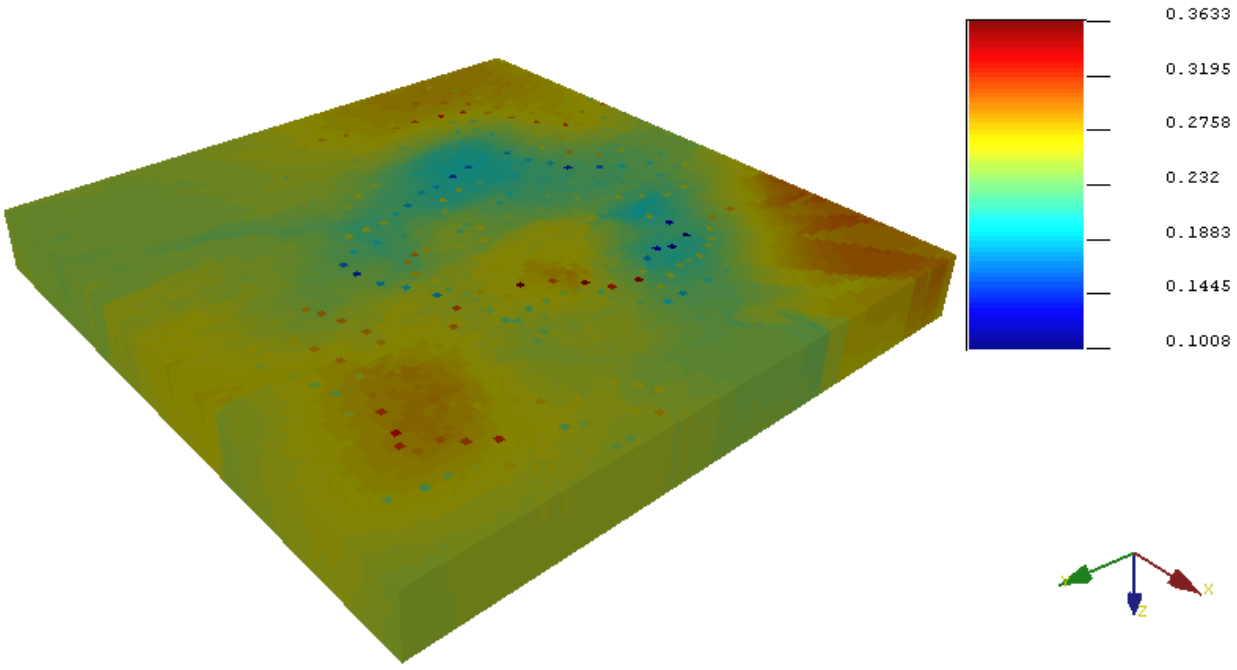

Figure 4.46: Porosity distribution in shale model (all wells) from Cokriging

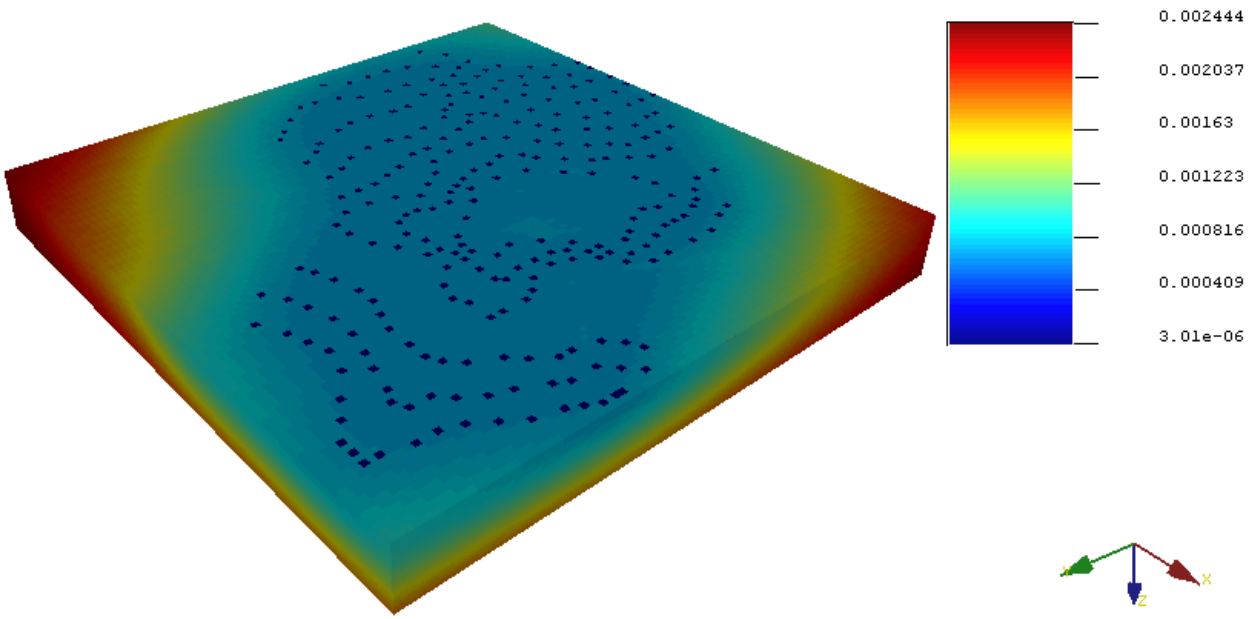

Figure 4.47: Porosity distribution in shale model (all wells) from Cokriging Variance

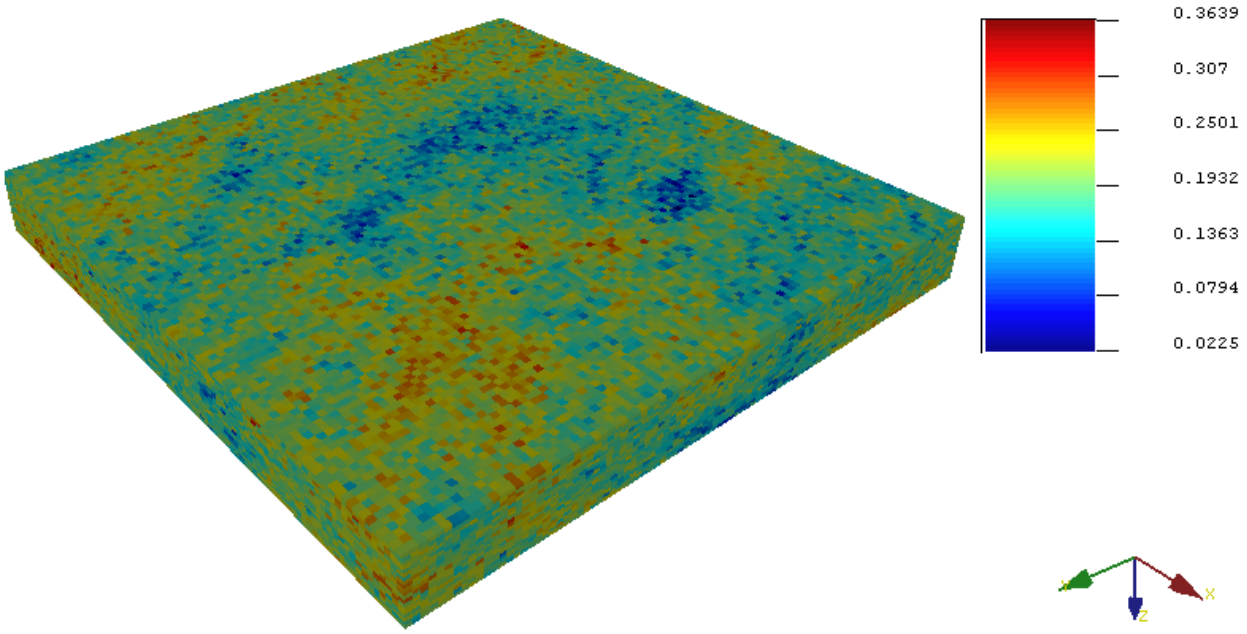

Figure 4.48: Porosity distribution in shale model (all wells) for Cosimulation

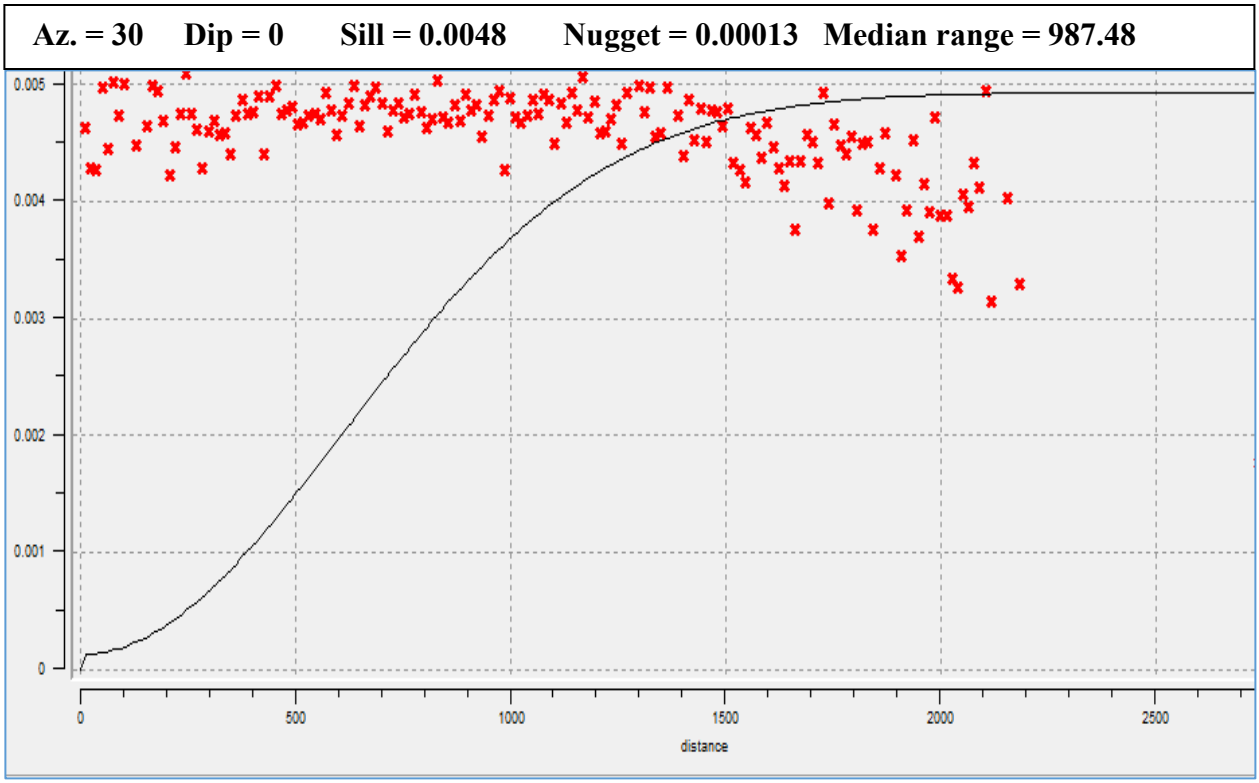

Figure 4.49: Anisotropic Cross Variogram model for Cokriging of porosity

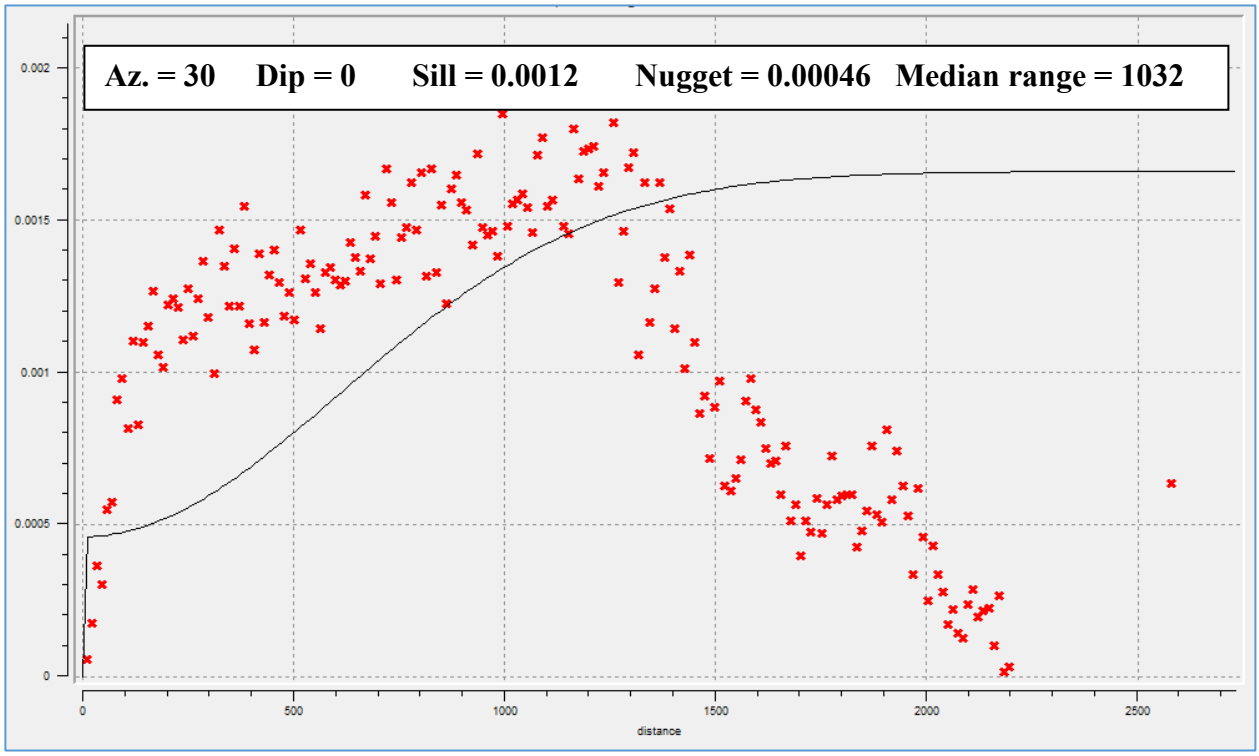

Figure 4.50: Anisotropic Porosity-Porosity variogram model for Cokriging of porosity

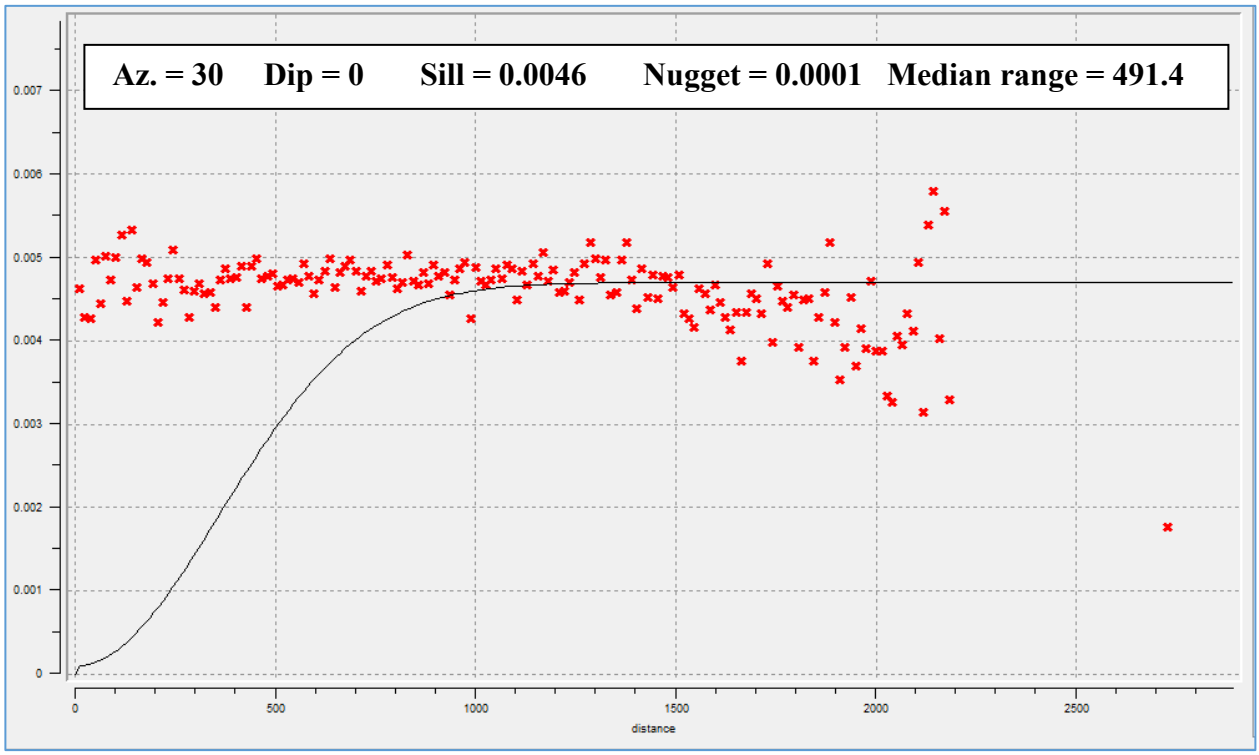

Figure 4.51: Anisotropic Shale-Shale variogram model for Cokriging of porosity

4.9.1 Analysis of Results

Models generated from the Cokriging and Cosimulation techniques (Figures 4.42 and 4.48) indicate that both good and moderate sand quality is found in the reservoir, which supports the properties from petrophysics in terms of porosity and permeability. Good facies are more than the poor facies in the reservoir rocks, which is an indication of low Shaliness and high clean sand-stones in the depositional system where the flow units exist.

Therefore it is possible for the wells in the reservoir to exhibit different flow units relative to the other wells for the same reservoir sand unit.

However, there are permeability and porosity variations within the identified flow layers which are extremely influenced by the nature of the shale distribution in the Agbada-Akata rock formations.

The estimation variance for porosity in the shaly regions could be as low as 3.01E-06 and as large as 2.44E-03, whereas the estimation variance for permeability could be as low as 6.67E-02 and as large as 1.10E-04.

This clearly depicts that low values of permeability and porosity were observed within the shaly regions where the flow paths were delineated.

The presence of shale within some portions of the reservoir sands decreases the permeability, as well as the pore spaces within the rock matrix.

This may affect the average permeability and porosity in completion design, particularly in choosing the phasing and vertical spacing of perforation. This indicates the heterogeneity of the study reservoir and its impact on fluid flow circulation along each defined flow channel.

CHAPTER 5

DISCUSSION, CONCLUSIONS AND RECOMMENDATION

5.1 Discussion

The nature of the depositional environment in the Tertiary Niger Delta Petroleum Province makes it challenging to delineate possible flow paths to predict what will happen with further development. The deposition of reservoir sands is heterogeneous that, it poses major problems to reservoir engineers in modeling certain parameters, logged and calculated using the conventional petrophysical methodologies. The incorporation of reservoir simulation is, therefore, necessary. This allows for the construction of a model whose behavior portrays the behavior of the actual reservoir. The simulation will provide much necessary information on the distribution of the reservoir rock properties to assess its performance during subsurface hydrocarbon development, and exploration activities within the Agbada-Akata system.

5.1.1 Flow Unit Identification

It is observed that, the reservoir of interest consist basically of clean sand zones that are intercalated with minor and major amount of shale. There is the existence of dirty sand zones having very high shale baffles which can cause permeability barriers. These characteristics can throttle the movement fluid within the flow layers delineated. The above mentioned properties are the possible cause for identifying many flow units within the reservoir of interest (reservoir X). The number of flow units varies from one well to another within the relatively thin reservoir. This dictates the complex nature of the Agbada-Akata formations in the Niger Delta Petroleum Province. The highest number of flow units (four flow units) is delineated in Well 4 and 6, whereas well 2 and 5 contain the least number of flow units (two flow units). This is an indication of the possibility of truncations of other flow units in the reservoir. As observed from the log view plot on the petrophysical analysis software, the reservoir under investigation is not perfectly continuous. There are some discontinuities in the reservoir even though the wells are displaced relative to each other, such that the various wells thin from the north to south towards the basin.

The intrinsic complexity within the reservoir‘s depositional setting and latter geological interruption result in very spatial high heterogeneity in the reservoir. This explains the need for reservoir simulation analysis to characterize the reservoir. This is because the producing, wells as well as injection wells if the need arise, requires proper placement and optimization, in order to produce efficiently from this reservoir. Therefore, detailed information about the various wells and reservoir rock properties is essential for proper well placement. However, the core analysis and well logs, with available information can make it easy to predict where the producing wells will be placed, either near the location of well 4 or well 6, in order to maximize production potential from reservoir X. Well 4 and 6 cross-cuts the reservoir of interest at the point where many flow paths exist and therefore the highest amount of hydrocarbons is expected from these wells in the reservoir. In this manner, perforations for production will not be located at the same level throughout the reservoir due discontinuities from one well to the other. Therefore, care must be taken when designing locations to perforate.

5.1.2 Modeling flow properties

The property value (both facies and petrophysical) were assigned to each grid cell at the well locations, and distributed realistically to preserve the heterogeneity of the studied reservoir. The variogram was used as an important tool to quantify the spatial distribution of the flow properties. Variograms were computed and models fitted for porosity and permeability data as well as facies data. It was used as input to infer the direction of maximum data continuity before generating each property‘s variogram model using various kriging algorithms. Sequential Gaussian Simulation method was used to calculate porosity distribution, whereas the Sequential Gaussian and Indicator Simulation methods were employed to calculate the permeability and facies distribution. The results from these two simulation techniques were then compared. Simple kriging and ordinary kriging were used to populate these properties. Sequential Gaussian and Indicator Simulation were considered reasonable for generating multiple equiprobable realizations because the method allows easy understanding of the spatial distribution of the reservoir properties to describe its flow characteristics.

5.2 Conclusions

Based on the study conducted on the reservoir, the following conclusions were made:

- The flow unit method subdivided the reservoir into various layers that have similar flow characteristics in terms of pore throats, reservoir quality index and mean hydraulic radius. This has established possible flow path of liquids during production, as well as the best intervals for perforation.

- Flow unit delineation by the RQI approach, adopted in this study, demonstrated a better understanding to predict the performance of the reservoir by identifying the layers that contribute massively to fluid flow in the reservoir.

- The simulation runs using geostatistical technique, demonstrated the effectiveness and ability of the flow unit concept to characterize heterogeneous clastic reservoirs.

- This study shows that the reservoir rock is characterized by a wide range of porosity and permeability values. It revealed that the reservoir falls within good porosity (9.99%-36.39%) and permeability (248mD-4688mD). This depicts that the formation is highly permeable and has very good storage capacity to accommodate more fluids.

- Good facies are more than the poor facies in the reservoir rocks which is an indication of low Shaliness and high clean sand zones in the depositional system where flow units exist. Both good and moderate sand quality is found in the reservoir within the region of interest (Zone D3000) where the currently known flow units were delineated. However, the shale facies is relatively high at the base of the formations compared with sand.
- The following is a summarized view of the characteristics of the flow units present in the reservoir; the slopes for all the flow units on the RQI versus normalized porosity are greater than one. This attests to the fact that, some minor shale intercalations exist in each flow unit and by extension some units within the studied reservoir.

This confirms the complex nature of the reservoir in the Agbada-Akata petroleum system. Comparing the flow unit quality using the three methods above, flow unit A is observed to exhibit the best reservoir quality in the reservoir under study. The identification of more flow units in Well 4 and 6 of the reservoir indicates that there is a higher possibility of obtaining better hydrocarbon recovery.

5.3 Recommendation

I strongly recommend for uncertainty analysis to be incorporated in this study since, different data sources, at different scales of measurement were integrated to estimating the petrophysical properties (porosity, permeability, and facies) of the study reservoir.

NOMENCLATURE

Sw = Water Saturation

Swi = Irreducible Water Saturation

Vsh = Shale Volume

Z = Atomic Number of Element

Φe = Effective Porosity

Φ_T = Total Porosity

Φ_{TD} = Total Porosity from Density log

BVW = Bulk Volume Water

FU = Flow Unit

K = Permeability

FZI = Flow Zone Index

Φh = Storage Capacity

kh = Flow Capacity

Eqn = Equation

Az = Azimuth

GR = Gamma Ray

$GRlog$ = Log reading for Gamma Ray

$GRmin$ = Minimum Gamma Ray reading

$GRmax$ = Maximum Gamma Ray reading

ρ_f = Fluid Density

ρ_{ma} = Matrix Density

ρ_{sh} = Shale Density

ρ_e = Electron Density Index

A =Atomic Weight of element

H_T = Tiab Hydraulic Flow Unit

I_{GR} = Gamma Ray Index

nRQI = Normalized Reservoir Quality Index

R^2 = Regression Coefficient

RQI = Reservoir Quality Index

Φz = Normalized Porosity

ρ_a = Apparent Density of Electron

ρ_b = Bulk Density

PVT = Pressure Volume Temperature

COKRIG = Cokriging

3D = Three Dimensional

PDF = Probability Density Function

SISIM = Sequential Indicator Simulation

COSGSIM = Sequential Gaussian Cosimulation

VDP = Dykstra-Parson Coefficient of Variation

SGSIM = Sequential Gaussian Simulation

SMLP = Stratigraphic Modified Lorenz Plot

SGS = Sequential Gaussian Simulation

OK = Ordinary Kriging

SK = Simple Kriging

SGEMS = Stanford Geostatistical Earth Modeling Software

HFU = Hydraulic Flow Unit

REFERENCES

1. Amaefule, J., M. Altunbay, D. Tiab, D. Kersey, and D. Keelan, (1993), "Enhanced Reservoir Description Using Core and Log Data to Identify Hydraulic Flow Units and Predict Permeability in Uncored Intervals/Wells": SPE, 26436, pp. 205 - 220.

2. Ameloko et al. (2013), "Petrophysical Characteristics and reservoir quality of the Inda field, Niger Delta, Nigeria", Journal of Poverty, Investment and Development: An Open Access International Journal, Volume 2, 2013.

3. Anon, (1972) "Schlumberger Log Interpretation", Schlumberger Ltd.,New York, 1. pp 113.

4. Anon, (2010), www.springerlink.com/content/p0537372874j7102/fulltext.pdf.Accessed:

21st March, 2016.

5. Anon, (2011), "General Introduction to Facies Models", Geoscience, Reprint Series 1, Canada, 22 pp.

6. Avbovbo, A. (1978), J. American Association of Petroleum Geologist, 62. pp 295-300**.**

7. Artem Ratchkovski, David O. Ogbe and Akanni S. Lawal (1999), "Application of Geostatistics and Conventional Methods to Derive Hydraulic Flow Units for Improved Reservoir Description": A Case Study of Endicott Field, Alaska, SPE 54587.

8. Boggs, S. Jr. (2006), "Principles of Sedimentology and Stratigraphy", Fourth edition. 662 pp.

9. Bouma, A. H**. (**1962), "Sedimentology of Some Flysch Deposits": A Graphic Approach to Facies Interpretation. Elsevier. Amsterdam. 168 pp.

10. Burker, K.C.B. and Whiteman A.J. (1973), "Uplift, rifting and the breakup of Africa", Proc. Nato. Conf. on Continental Drift, Newcastle. Academic Press. In: Implications on Continental Drift to Earth Sciences, D.H. Tarling and S.K. Runcorn, (Eds), 1973.

11. Carman P.C (1937), "Fluid flow through granular beds", Transactions-Institution of Chemical Engineers, 15, 150–166.

12. Carman P.C (1956), "Flow of Gases through Porous Media", Academic Press, New York.

13. Clayton Deutsch, V. (2002), "Applied Geostatistics Series": Geostatistical Reservoir Modeling, Oxford University Press, Second Edition, pp 3-23.

14. Coates, G.R and Dumanoir J.L. (1981), "A new approach to improved log derived permeability", The Log Analyst, pp 17.

15. Darcy, H. (1856), "Les Fontaines Publiques de la Ville de Dijon", Dalmont, Paris.

16. Doust, H., Omatsola, E. J. (1990), J. American Association of Petroleum Geologist, pp.239-248.

17. Djebbar Tiab, and Erle C. Donaldson, (2015), "Petrophysics; Theory and Practice of Measuring Reservoir Rock and Fluid Transport Properties", 4th edition, Gulf Professional Publishing, Elsevier, Inc.

18. Ekweozor, M., Daukoru, E. J. (1994), American Association of Petroleum Geologist, pp.599- 614.
19. Evamy, B., Haremboure, J., Kamerling, P. et al. (1978), J. American Association of Petroleum Geologist, 62. pp 277-298.

20. Gunter, G. W., Finneran, J. M., Hartman, D. J. and Miller, J. D., (1997), "Early Determination of Reservoir Flow Units Using an Integrated Petrophysical Method", SPE 38679. SPE Annual Technical Conference and Exhibition, San Antonio, TX.

21. Hospers, J. (1965), J. American Association of Petroleum Geologist, 76. pp. 407-422.

22. Hulea IN, Nicholls CA (2011), "Carbonate rock characterization and modeling-capillary pressure and permeability in multimodal rocks-a look beyond sample specific heterogeneity", AAPG bulletin, April 10-13.

23. Hussain Ali Baker et al. (2013), "Permeability Prediction in Carbonate Reservoir Rock Using FZI", Petroleum Engineering Department, College of Engineering for University of Baghdad, published: Iraq Journal of Chemical and Petroleum Engineering Vol.14 No.3, pp. 49-54 ISSN: 1997-4884.
24. Iwuagwu, C. J. (1979), Master of Science Thesis: University of Alberta, Canada.

25. John Layman and Wayne Ahr (2004), "Porosity Characterization Utilizing Petrographic Image Analysis: Implications for Rapid Identification and Ranking of Reservoir Flow Units", Happy Spraberry Field, Garza County, Texas," prepared for presentation at AAPG International Conference & Exhibition, Cancun, Mexico, October 24-27, 2004.

26. Kaplan, A., Lusser, C., Norton, I. (1994), J. American Association of Petroleum Geologist, 60. pp. 230-237.

27. Keelan, D. (1982), J. Pet Tech.. pp. 2483-2491. Kulke, H. 1995. Regional Petroleum Geology of the World Part II: Africa, America, Australia and Antarctica. Berlin, Gebrüder Borntraege. pp. 143-172.

28. Kelsall J, Wakefield J. (2002), "Modeling spatial variation in disease risk", J Am Stat Assoc 97 (459): 692–701.

29. Kozeny J. (1927) "Ueber kapillare leitung des wassers im boden", Sitzungsberichte Akademie der Wissenschaften Wien, 136, 271– 306.

30. Lehner, P., De Ruiter, P. A. C. (1977), J. American Association of Petroleum Geologist, 61. pp. 961-981.

31. Leverett, M.C. (1941), "Capillary Behavior in Porous Solids", Transactions of the AIME 142,159 - 172.

32. Lowe, D. R. (1982), "Sediment gravity flows: Depositional models with special reference to the deposits of high-density turbidity currents": Journal of Sedimentary Petrology, 52. pp. 279-290.
33. Maghsood Abbaszadeh et al. (1996), "Permeability Prediction by Hydraulic Flow Units: Theory and Applications", National Oil Corporation; Hikari Fujii, SPE, Arabian Oil Co. Ltd.; and Fujio Fujimoto, Japan National Oil Corporation. Published SPE paper at the Formation Evaluation Conference in December 1996, SPE 30158, pp. 263-270.

34. Mayalla, M. E. J. (2006),"Turbidite channel reservoirs-Key elements in facies prediction", Marine and Petroleum Geology, 23, 8. pp. 821-841.

35. Middleton, G. V. (1993), "Sediment deposition from turbidity currents". Earth and Planetary Science, pp. 89-114.

36. Middleton, G. V., Hampton, M. A. (1973), "Sediment gravity flows. Mechanics of flow and deposition: Turbidites and Deep-Water Sedimentation", Pacific section SEPM, Los Angeles, California. G.V. Middleton and A.H. Bouma (Eds.). pp. 1-38.

37. Morris, R.L. and Biggs W.P. (1967), "Using log-derived values of water saturation and porosity": Transactions of the SPWLA Annual Logging Symposium, Paper X, 26p.

38. M.H. Rider (2002), "Well Geological Interpretation of Well Logs": Interprint Ltd, 2002.

39. Nwachukwu, S. (1972), J. Nigerian Geology Magazine, 109. pp. 411-419.

40. Omoboriowo A.O. (2012), "Depositional Environment and Petrophysical Characteristics of "LEPA" Reservoir, Amma Field", Eastern Niger Delta, Nigeria: International Journal of Pure and Applied Sciences and Technology, 10(2) (2012), pp. 38-61.

41. Pickering, K. T., Hiscott, R. N., and Hein, F.J. (1989). "Deep Marine Environments Clastic Sedimentation and Tectonics", Academic Division of Unwin Hyamnd, London. 416 p.

42. Posamentier, H. W., Kolla, V. (2003), "Seismic Geomorphology and Stratigraphy of Depositional Elements in Deep-Water Settings", Journal Sedimentary Research, 73, 3. pp. 367-388.
43. Reyment R.A. (1965), "Aspects of the Geology of Nigeria", University of Ibadan Press, 1965.
44. Reijers, T., Petters, S., Nwajide, C. (1997), "The Niger Delta Basin, African Basin. Sedimentary Basins of the World 3", R.C. Selley (Ed.). Elsevier Science**,** Amsterdam. pp. 151-172.
45. Rider, M. (1986), "The Geological Interpretation of Well Log", Blackie, Glasgow, pp. 151 -165.
46. Rose W. and Bruce W.A. (1944), "Evaluation of Capillary Characters in Petroleum Reservoir Rocks", Trans. AMIE, 186, 127-142.

47. Remy N., Boucher A. and Wu J. (2009), "Applied Geostatistics with SGeMS", Cambridge University Press, United Kingdom.

48. Remy N. (2004), "Geostatistical Earth Modeling Software": User's Manual.

49. Shanmugam, G. (2000), "50 years of the turbidite paradigm (1950s-1990s): deep-water processes and facies models - A critical perspective", Marine and Petroleum Geology, 17. pp 285- 342.
50. Sneider, R., King, H. (1978), J. American Association of Petroleum Geologist.

51. Stacher, P. (1995), "Present understanding of the Niger Delta hydrocarbon habitat", M.N. Oti, G. Postma (Ed.). pp. 257-267.

52. Shan Zhao et al. (2014), "Thickness, porosity, and permeability prediction: comparative studies and application of the geostatistical modeling in an Oil field", Environmental Systems Research 2014, 3:7 http://www.environmental systemresearch.com/content/3/1/7.

53. Stow, D.A.V., Johansson, M. (2000), "Deep-water massive sands: Nature, origin and hydrocarbon implications", Marine and Petroleum Geology. pp. 145-174.

54. Thomas, E. C., Stieber, S. J. (1975), "The distribution of shale in sandstones and its effect on porosity", Transactions of the SPWLA 16th Annual Logging, Symposium, June 4-7, 1975.

55. Tixier, M.P. (1949), "Evaluation of permeability from electric log resistivity gradient", Earth Science Journal, 2: 113-113.

56. Timur, A. (1968), "An investigation of permeability, porosity and residual saturation relationship for sandstone reservoirs", The Log Analyst, 9: 8-8.

57. Tinker S.W. (1996),"Building the 3-D jigsaw puzzle: Application of sequence stratigraphy to 3-D Reservoir characterization", Permain Basin, Amer. Assoc. Petrol. Geol. Bull., 80 pp. 460-482.
58. Tiab, D. (2015), Advance Petrophysics Lecture Material. Rock Typing, Reservoir Zoning and Flow Units. African University of Science and Technology, Abuja, FCT, Nigeria.

59. Tiab, D., Donaldson, E.C. (2004),"Theory and Practice of Measuring Reservoir Rock and Fluid Transport Properties", Second Edition. Gulf Professional Publishing, 200 Wheeler Road, Burlington, MA 01803, USA. Walker, R.G. 1984.

60. Tiab, D. (2000), Advances in Petrophysics, Vol. 1-Flow Units. Lecture Notes Manual, University of Oklahoma.

61. Tohid N.G. Borhani (2011), "Application of Hydraulic Flow Units and Intelligent Systems for Permeability Prediction in a Carbonate Reservoir": Research gate paper 262185449 published on Proceedings of the 3rd CUTSE International Conference Miri, Sarawak, Malaysia, 8-9 November, 2011.

62. Weber K.J (1971),"Sedimentological aspects of oil fields in the Niger Delta", Geol Mijnbouw 50:559–576.
63. Whiteman K.J. (1982),"Nigeria:Its Petroleum Geology, Resources and Potential", Graham and Trotman, 1982.
64. Yassine Mokrane and Smail Labed (2012), "Flow units approach for better reservoir modelling: application for the south part of the oil rim, hassi rmel field, Algeria", pp.12-20.

APPENDIX A: REGRESSIONS FOR FLOW UNITS IN WELL 1 AND WELL 2

Regressions:

Reg1 (type = MA; R = 0.916; R2 adj = 0.838; RMSE = 0.125691; nb = 240)

Equation: log10(RQI) = + 2.748763 * log10(PHI_Z) + 1.642137

Reg2 (type = MA; R = 0.953; R2 adj = 0.907; RMSE = 0.13622; nb = 185)

Equation: log10(RQI) = + 2.917751 * log10(PHI_Z) + 1.342623

Zonation: Top

APPENDIX B: DATA OF WELL 1 FOR FLOW UNIT CHARTS IN RESERVOIR X

Depth	Φ_T	Φe	K	RQI	Φz	nRQI	Φh	kh	Vsh
7555	0.352676	0.103925	2485.066	0.005018	0.115978	0.0001131	0.073555	0.002749	0.014605
7555.5	0.354846	0.113678	1985.011	0.008733	0.128258	0.0003629	0.063199	0.003929	0.013967
7556	0.385688	0.126352	1850.127	0.001111	0.144626	0.0009279	0.060643	0.001830	0.015094
7556.5	0.338197	0.128296	2076.178	0.002741	0.147178	0.0019036	0.065149	0.004919	0.019914
7557	0.352082	0.117582	2124.927	0.003186	0.133249	0.0031122	0.083854	0.002763	0.023948
7557.5	0.370451	0.263638	1791.014	0.003839	0.358027	0.004612	0.098846	0.002153	0.02662
7558	0.386332	0.273336	1641.912	0.003736	0.376151	0.060841	0.108466	0.002746	0.024225
7558.5	0.358028	0.279778	2097.096	0.004536	0.388460	0.178313	0.099854	0.002359	0.020247
7559	0.376152	0.296025	2141.807	0.044367	0.420504	0.197721	0.101626	0.002457	0.016662
7559.5	0.388461	0.289529	1873.977	0.004572	0.407516	0.114986	0.201652	0.198239	0.013381
7560	0.420504	0.28083	1731.835	0.004942	0.390491	0.129076	0.201662	0.106777	0.013387
7560.5	0.407517	0.265475	1931.821	0.004812	0.361424	0.0148522	0.201687	0.272414	0.009257
7561	0.390491	0.26088	2290.551	0.005046	0.352960	0.17229	0.201701	0.280238	0.007972
7561.5	0.361424	0.267168	2770.323	0.005343	0.364569	0.192936	0.230798	0.272756	0.10084
7562	0.35296	0.266582	2607.451	0.005573	0.363478	0.209873	0.201769	0.266645	0.008125
7562.5	0.364569	0.253138	2029.224	0.006368	0.338935	0.22615	0.317632	0.067226	0.119172
7563	0.363479	0.247626	1874.404	0.006468	0.329014	0.241694	0.1781968	0.067742	0.113478
7563.5	0.338935	0.264493	1518.246	0.006965	0.359606	0.256472	0.1802468	0.273419	0.156197
7564	0.329126	0.26682	970.3721	0.007814	0.363921	0.270831	0.1781968	0.273935	0.194243
7564.5	0.359607	0.258823	1265.167	0.007194	0.349214	0.283119	0.1802468	0.264839	0.120581
7565	0.363922	0.254552	1432.732	0.007814	0.341147	0.29327	0.1824237	0.044774	0.018292
7565.5	0.349206	0.26222	1195.006	0.078816	0.355417	0.301742	0.1845836	0.268516	0.01595
7566	0.341476	0.274233	1056.234	0.008347	0.377852	0.308561	0.1868942	0.072903	0.013598
7566.5	0.355418	0.188825	1453.923	0.008367	0.232779	0.313428	0.1891608	0.27729	0.012091
7567	0.377853	0.285031	1639.844	0.086028	0.398662	0.318243	0.1914874	0.070129	0.010451
7567.5	0.406123	0.167594	1706.985	0.086028	0.201336	0.324029	0.1939633	0.061032	0.006742
7568	0.398661	0.262606	1499.561	0.086028	0.356127	0.331345	0.1962942	0.290516	0.005856
7568.5	0.365363	0.249298	2017.58	0.088657	0.332086	0.340223	0.198411	0.150455	0.006299
7569	0.356127	0.222985	2542.355	0.009166	0.286976	0.349698	0.2003786	0.158769	0.00528

7569.5	0.332086	0.237137	3006.342	0.009366	0.310851	0.359964	0.2202294	0.150228	0.004607
7570	0.286977	0.244813	3527.48	0.009476	0.324175	0.371701	0.2041563	0.133876	0.004242
7570.5	0.310851	0.234044	3465.648	0.001000	0.305558	0.383865	0.2058371	0.131295	0.009233
7571	0.324176	0.226127	3234.532	0.001356	0.292201	0.395244	0.2072826	0.122525	0.007535
7571.5	0.305558	0.244448	2888.011	0.001945	0.323535	0.405272	0.2085519	0.117852	0.007665
7572	0.292201	0.252112	2959.973	0.001279	0.337098	0.415552	0.2099077	0.128821	0.011129
7572.5	0.323535	0.255863	2828.456	0.116241	0.343838.	0.425476	0.2112737	0.122696	0.011921
7573	0.337098	0.248875	2486.651	0.001993	0.264047	0.4434572	0.2126131	0.123849	0.010923
7573.5	0.343839	0.268396	1979.184	0.009793	0.267062	0.4443064	0.2140655	0.11185	0.00657
7574	0.331336	0.28357	1323.459	0.002453	0.271453	0.445169	0.2158335	0.101855	0.003214
7574.5	0.36686	0.294953	1442.287	0.001352	0.273994	0.445693	0.3028041	0.278645	0.001885
7575	0.39581	0.306909	1695.278	0.001356	0.279634	0.459159	0.3047023	0.272118	0.004679
7575.5	0.418346	0.180717	1961.564	0.147889	0.287467	0.4604822	0.306595	0.088772	0.007215
7576	0.442812	0.190336	2233.242	0.001524	0.292418	0.4653841	0.3085643	0.297923	0.007372
7576.5	0.441238	0.185832	2646.92	0.152408	0.29592	0.4766664	0.3103794	0.111275	0.005389
7577	0.429885	0.141332	2775.26	0.171907	0.297959	0.4870464	0.3123358	0.092447	0.006403
7577.5	0.41204	0.163061	2751.941	0.171907	0.30391	0.4974132	0.3144043	0.100553	0.007903
7578	0.414939	0.199482	2813.476	0.001797	0.307194	0.4977172	0.3163718	0.107414	0.008812
7578.5	0.406453	0.281958	2968.913	0.007716	0.306793	0.5080229	0.3182602	0.28996	0.011796
7579	0.386513	0.283082	2842.537	0.008852	0.293397	0.5483371	0.3201789	0.097687	0.014661
7579.5	0.353631	0.278337	2372.719	0.008956	0.275912	0.5486357	0.3219816	0.115742	0.021385
7580	0.304772	0.252726	2210.89	0.019392	0.271683	0.5488614	0.3236807	0.107936	0.029873
7580.5	0.307502	0.2604	2075.314	0.025933	0.261329	0.549009	0.3254564	0.073032	0.041372
7581	0.317249	0.270313	2064.186	0.021225	0.232001	0.5491221	0.327129	0.076194	0.054042
7581.5	0.32499	0.278672	1441.791	0.007871	0.195106	0.049198	0.3965058	0.288968	0.168003
7582	0.330362	0.263638	1076.164	0.021871	0.156769	0.049254	0.3986256	0.083097	0.183387
7582.5	0.350798	0.273336	860.5135	0.004593	0.145824	0.549245	0.4010345	0.255871	0.078289
7583	0.358181	0.279778	1181.046	0.001225	0.152828	0.049245	0.4036476	0.260323	0.076449
7583.5	0.36187	0.296025	1918.374	0.003978	0.145471	0.049245	0.4060464	0.061484	0.067902
7584	0.373738	0.289529	2599.124	0.023937	0.141149	0.049245	0.4082733	0.256194	0.053101
7584.5	0.390379	0.28083	2546.417	0.005996	0.13574	0.549245	0.4105901	0.257645	0.039751
7585	0.393139	0.265475	1906.118	0.002619	0.125489	0.049245	0.4131228	0.284708	0.027711
7585.5	0.373903	0.26088	2082.264	0.003196	0.116391	0.549245	0.4158075	0.101955	0.022031
7586	0.362348	0.267168	2118.819	0.027005	0.113013	0.049245	0.4183277	0.122092	0.028748
7586.5	0.351572	0.266582	1774.163	0.028256	0.111346	0.5492583	0.4207778	0.129478	0.032908
7587	0.350515	0.253138	2592.009	0.078256	0.109133	0.549259	0.4233305	0.122624	0.032534
7587.5	0.311208	0.247626	2894.682	0.086759	0.116462	0.549259	0.4259754	0.116044	0.031621
7588	0.281789	0.264493	2141.526	0.034551	0.127719	0.049259	0.4923261	0.113987	0.034673
7588.5	0.261676	0.26682	2363.852	0.033857	0.139907	0.049259	0.4940388	0.108354	0.03531
7589	0.290593	0.130074	2390.541	0.003331	0.167127	0.5492622	0.4957382	0.108673	0.032988
7589.5	0.339855	0.092528	2201.246	0.003457	0.194247	0.5493045	0.4974442	0.101535	0.03685
7590	0.375458	0.102409	1621.969	0.005413	0.208293	0.0493045	0.4990781	0.099301	0.0388

7590.5	0.367849	0.112237	1987.225	0.003543	0.202955	0.6693173	0.500753	0.106565	0.047608
7591	0.322607	0.133044	2315.412	0.005413	0.203978	0.5793994	0.5027775	0.123717	0.068187
7591.5	0.318359	0.141906	1669.53	0.007599	0.255499	0.5995499	0.5048116	0.135253	0.092579
7592	0.304502	0.150809	2168.612	0.037979	0.246883	0.6049636	0.5066498	0.135916	0.120906
7592.5	0.301955	0.148958	1949.601	0.042483	0.251217	0.0497857	0.5083148	0.128682	0.078806
7593	0.364304	0.139952	1713.588	0.050396	0.275600	0.0500239	0.5099121	0.133266	0.04832
7593.5	0.389328	0.128073	1498.146	0.049959	0.269122	0.0501417	0.5115128	0.09833	0.036679
7594	0.356194	0.125548	1707.208	0.042959	0.250452	0.0501709	0.5132136	0.549221	0.028916
7594.5	0.372119	0.134452	2066.162	0.008022	0.253659	0.0502256	0.5148461	0.049198	0.024167
7595	0.375617	0.147226	1791.555	0.05603	0.29494	0.0504134	0.5163459	0.049254	0.021644
7595.5	0.364267	0.158064	1531.453	0.05603	0.289573	0.0507199	0.5178228	0.549245	0.024021
7596	0.326456	0.122581	1372.403	0.05732	0.276989	0.0509241	0.5194434	0.049245	0.027917
7596.5	0.351016	0.127032	1282.043	0.019053	0.280535	0.05109	0.5211389	0.049245	0.023687
7597	0.371871	0.134645	1222.224	0.068574	0.281458	0.0512822	0.5228741	0.049245	0.021072
7597.5	0.332943	0.144129	1679.722	0.068574	0.285883	0.0514692	0.5246229	0.549245	0.021508
7598	0.363439	0.156733	1928.105	0.067171	0.29343	0.0516558	0.5264537	0.049245	0.022028
7598.5	0.350315	0.133051	2551.582	0.066335	0.298959	0.0518332	0.528433	0.549245	0.122228
7599	0.335276	0.120323	2754.812	0.066085	0.300307	0.0520946	0.5303484	0.097691	0.12242
7599.5	0.320278	0.116774	3379.448	0.007413	0.297642	0.0523487	0.5321565	0.298025	0.02305
7600	0.333076	0.123032	3787.204	0.007743	0.2991	0.0527894	0.5339134	0.090865	0.026061
7600.5	0.351522	0.104968	3344.444	0.08293	0.302141	0.0535044	0.5357872	0.286193	0.032729
7601	0.331617	0.102321	3161.691	0.075136	0.296428	0.0551147	0.5375661	0.098805	0.038016
7601.5	0.31687	0.095742	3627.958	0.019792	0.292193	0.0577387	0.5391735	0.105845	0.031346
7602	0.309794	0.095613	3916.346	0.084731	0.277989	0.0611334	0.6729718	0.101371	0.023293
7602.5	0.307123	0.103871	2539.118	0.087326	0.267248	0.0647394	0.6748623	0.098959	0.015666
7603	0.306185	0.112774	2127.848	0.927514	0.252829	0.0681908	0.6768518	0.106047	0.008783
7603.5	0.342524	0.109172	892.8526	0.985063	0.218153	0.0719443	0.6789021	0.103255	0.006111
7604	0.35877	0.111757	599.0244	0.091005	0.181456	0.0752781	0.6811647	0.114818	0.006886
7604.5	0.39352	0.121403	746.5735	0.009164	0.157001	0.6777258	0.6833725	0.115161	0.00971
7605	0.401326	0.118129	690.2725	0.164568	0.13227	0.6793928	0.6853179	0.105101	0.013946
7605.5	0.431413	0.125806	250.9008	0.009369	0.120726	0.0808637	0.6872853	0.119987	0.012858
7606	0.450945	0.143677	455.5229	0.002525	0.120971	0.6824302	0.6893287	0.126358	0.010983
7606.5	0.428045	0.134516	1044.916	0.001122	0.128952	0.6841089	0.6912177	0.089385	0.016506
7607	0.415363	0.137677	1144.692	0.007815	0.124401	0.6860049	0.6928914	0.290368	0.021927
7607.5	0.4319	0.138839	1622.979	0.006648	0.10671	0.6883316	0.6945511	0.102159	0.02738
7608	0.438491	0.141358	1726.388	0.008392	0.094411	0.790601	0.6962534	0.115481	0.034375
7608.5	0.370359	0.138898	1748.317	0.003299	0.094414	0.7929324	0.6977487	0.285171	0.04338
7609	0.342629	0.144478	1909.048	0.002467	0.092636	0.7954729	0.699168	0.287355	0.053062
7609.5	0.252938	0.152323	2143.014	0.002915	0.086514	07981758	0.7007354	0.28529	0.063485
7610	0.220579	0.160085	1768.071	0.001886	0.084311	0.7316912	0.7023065	0.272968	0.068214
7610.5	0.235081	0.137742	1253.908	0.197365	0.093076	0.730076	0.7035891	0.083161	0.070733
7611	0.228248	0.138315	794.6654	0.217612	0.097983	0.7252464	0.8156998	0.29738	0.073472

7611.5	0.164594	0.136781	751.9919	0.006447	0.093441	0.7174424	0.8182756	0.285916	0.084728
7612	0.19483	0.101827	1024.805	0.006548	0.101546	0.7493807	0.820576	0.106355	0.090397
7612.5	0.249191	0.074014	1305.457	0.260608	0.099892	0.7612242	0.8226327	0.112449	0.099816
7613	0.251944	0.105281	965.5264	0.278837	0.098481	0.7829248	0.8246301	0.117894	0.110331
7613.5	0.277821	0.101585	1089.911	0.180351	0.121243	0.7945355	0.8265368	0.117274	0.118871
7614	0.306177	0.093879	1288.715	0.001724	0.099973	0.8861295	0.8282585	0.097526	0.062865
7614.5	0.324587	0.124578	1039.613	0.001711	0.10278	0.8877171	0.8297895	0.288046	0.488764
7615	0.338973	0.108809	1610.831	0.001886	0.131955	0.819322	0.8311433	0.081788	0.035831
7615.5	0.353752	0.091888	2204.766	0.002292	0.174519	0.8720652	0.8326507	0.289217	0.034249
7616	0.33326	0.089173	3103.086	0.002397	0.25338	0.8828768	0.8343052	0.093945	0.030762
7616.5	0.297458	0.078744	2841.202	0.002787	0.245184	0.9424527	0.8361043	0.284014	0.031663
7617	0.255101	0.088046	2112.007	0.002912	0.226625	0.9560862	0.8379787	0.295496	0.036527
7617.5	0.251586	0.08763	1967.117	0.032668	0.249314	0.9575872	0.8399159	0.103231	0.031937
7618	0.278966	0.078155	1901.596	0.012779	0.084781	0.9591015	0.8421375	0.097481	0.330236
7618.5	0.302281	0.08157	2003.503	0.092838	0.088814	0.9605716	0.8442703	0.104827	0.029685
7619	0.273175	0.120318	1702.071	0.082989	0.136775	0.9720192	0.8461242	0.809133	0.332397
7619.5	0.281044	0.105495	892.8526	0.023542	0.117937	0.1975641	0.8479488	0.803973	0.03948
7620	0.294101	0.096365	599.0244	0.003192	0.106642	0.9853373	0.8497639	0.896473	0.343892
7620.5	0.274388	0.106401	746.5735	0.008398	0.119071	0.9874895	0.851524	0812905	0.042127
7621	0.318802	0.105957	690.2725	0.003546	0.118514	0.9896947	0.8533418	0.818524	0.037959
7621.5	0.356263	0.102513	250.9008	0.003794	0.114222	0.9818257	0.8550784	0.822597	0.035518
7622	0.401455	0.102735	455.5229	0.004596	0.114498	0.9841384	0.8567945	0.812741	0.235739
7622.5	0.386922	0.096443	1044.916	0.004279	0.106736	0.9867039	0.8584864	0.810434	0.039749
7623	0.347467	0.080738	1144.692	0.004493	0.08783	0.9949103	0.8601702	0.898376	0.042356
7623.5	0.336662	0.098676	1622.979	0.004538	0.109479	0.9912543	0.861987	0.901428	0.04695
7624	0.330005	0.127572	1726.388	0.004776	0.146227	0.9953025	0.8638654	0.984189	0.451736
7624.5	0.3329	0.144298	1748.317	0.014958	0.168631	0.9962335	0.8658043	0.980015	0.156697
7625	0.311611	0.145749	1909.048	0.005249	0.170617	0.9971053	0.9878989	0.95869	0.463415

APPENDIX C: DATA OF WELL 2 FOR FLOW UNIT CHARTS IN RESERVOIR X

Depth	Φ_T	Φe	K	RQI	Φz	nRQI	Φh	kh	Vsh
7555	0.362348	0.267168	2118.819	0.0027005	0.364569	0.0004925	0.017631	0.091793	0.028748
7555.5	0.351572	0.266582	1774.163	0.0027876	0.363394	0.0004983	0.008351	0.015963	0.032908
7556	0.350515	0.253138	2592.009	0.0026856	0.338933	0.0004359	0.014359	0.001553	0.032534
7556.5	0.311208	0.247626	2894.682	0.0028679	0.329126	0.0049659	0.001751	0.001344	0.031621
7557	0.281789	0.264493	2141.526	0.0304551	0.359606	0.0059959	0.013254	0.008996	0.034673
7557.5	0.261676	0.26682	2363.852	0.0313857	0.363921	0.0069259	0.016564	0.005687	0.03531
7558	0.290593	0.130074	2390.541	0.0033331	0.149523	0.0149262	0.014724	0.015742	0.032988
7558.5	0.339855	0.192528	2201.246	0.0343517	0.238433	0.0149345	0.015519	0.107906	0.03685
7559	0.375458	0.102409	1621.969	0.0354013	0.114093	0.0149045	0.016519	0.173032	0.0388

7559.5	0.367849	0.112237	1987.225	0.0354013	0.126426	0.0149173	0.106492	0.176194	0.047608
7560	0.322607	0.133044	2315.412	0.0354013	0.153461	0.1493994	0.109355	0.188968	0.068187
7560.5	0.318359	0.141906	1669.53	0.0375979	0.165373	0.1495499	0.108908	0.183097	0.092579
7561	0.304502	0.150809	2168.612	0.0378979	0.177591	0.1496836	0.292145	0.155871	0.120906
7561.5	0.301955	0.148958	1949.601	0.0042483	0.175030	0.01497857	0.350465	0.160323	0.078806
7562	0.364304	0.139952	1713.588	0.0045396	0.162725	0.10500239	0.360293	0.261484	0.04832
7562.5	0.389328	0.128073	1498.146	0.0049959	0.146885	0.10501417	0.378892	0.256194	0.036679
7563	0.356194	0.125548	1707.208	0.049259	0.143573	0.0501709	0.142698	0.257645	0.028916
7563.5	0.372119	0.134452	2066.162	0.0508022	0.155337	0.01502256	0.416551	0.284708	0.024167
7564	0.375617	0.147226	1791.555	0.0535603	0.172643	0.10504134	0.599641	0.301955	0.021644
7564.5	0.364267	0.158064	1531.453	0.0565603	0.187738	0.10507199	0.290353	0.322092	0.024021
7565	0.326456	0.122581	1372.403	0.0573302	0.139706	0.10509241	0.49911	0.329478	0.027917
7565.5	0.351016	0.127032	1282.043	0.0593053	0.145517	0.1105109	0.113052	0.522624	0.023687
7566	0.371871	0.134645	1222.224	0.0608574	0.155595	0.12512822	0.697892	0.616044	0.021072
7566.5	0.332943	0.144129	1679.722	0.0608574	0.168400	0.10514692	0.088215	0.088215	0.021508
7567	0.363439	0.156733	1928.105	0.0627171	0.185864	0.10516558	0.089845	0.089845	0.022028
7567.5	0.350315	0.133051	2551.582	0.0646335	0.198959	0.20518332	0.09178	0.09178	0.022228
7568	0.335276	0.120323	2754.812	0.0666085	0.136780	0.20520946	0.092523	0.092523	0.02242
7568.5	0.320278	0.116774	3379.448	0.7707413	0.197642	0.20523487	0.093235	0.093235	0.02305
7569	0.333076	0.123032	3787.204	0.707413	0.152991	0.0527894	0.095558	0.095558	0.026061
7569.5	0.351522	0.104968	3344.444	0.072903	0.117278	0.20535044	0.106474	0.106474	0.032729
7570	0.331617	0.102321	3161.691	0.751306	0.113983	0.20551147	0.129612	0.129612	0.038016
7570.5	0.31687	0.095742	3627.958	0.797923	0.105879	0.20577387	0.147032	0.147032	0.031346
7571	0.309794	0.095613	3916.346	0.847431	0.105721	0.20611334	0.124926	0.124926	0.023293
7571.5	0.307123	0.103871	2539.118	0.873326	0.167248	0.20647394	0.096449	0.096449	0.015666
7572	0.306185	0.112774	2127.848	0.927514	0.152829	0.20681908	0.067416	0.067416	0.008783
7572.5	0.342524	0.109172	892.8526	0.985063	0.118153	0.20719443	0.03922	0.03922	0.006111
7573	0.35877	0.111757	599.0244	0.091005	0.181456	0.20752781	0.027702	0.027702	0.006886
7573.5	0.39352	0.121403	746.5735	0.164318	0.157001	0.20777258	0.031076	0.031076	0.00971
7574	0.401326	0.118129	690.2725	0.14568	0.13227	0.20793928	0.043138	0.043138	0.013946
7574.5	0.431413	0.125806	250.9008	0.137169	0.120726	0.30808637	0.060559	0.060559	0.012858
7575	0.450945	0.143677	455.5229	0.025325	0.120971	0.30824302	0.05616	0.05616	0.010983
7575.5	0.428045	0.134516	1044.916	0.01111	0.128952	0.30841089	0.048454	0.048454	0.016506
7576	0.415363	0.137677	1144.692	0.007815	0.124401	0.30860049	0.070724	0.070724	0.021927
7576.5	0.4319	0.138839	1622.979	0.066548	0.161221	0.30883316	0.091405	0.091405	0.02738
7577	0.438491	0.141358	1726.388	0.031092	0.164629	0.3090601	0.111162	0.111162	0.034375
7577.5	0.370359	0.138898	1748.317	0.022959	0.094414	0.30929324	0.135119	0.135119	0.04338
7578	0.342629	0.144478	1909.048	0.0214367	0.092636	0.30954729	0.163942	0.163942	0.053062
7578.5	0.252938	0.152323	2143.014	0.191522	0.086514	0.30981758	0.192724	0.192724	0.063485
7579	0.220579	0.160085	1768.071	0.018866	0.084311	0.31006912	0.221506	0.221506	0.068214
7579.5	0.235081	0.137742	1253.908	0.197365	0.093076	0.31030076	0.233894	0.233894	0.070733
7580	0.228248	0.138315	794.6654	0.0217612	0.097983	0.31052464	0.240336	0.540336	0.073472

7580.5	0.164594	0.136781	751.9919	0.024747	0.093441	0.31074424	0.247221	0.547221	0.084728
7581	0.19483	0.101827	1024.805	0.032548	0.101546	0.31093807	0.274308	0.574308	0.090397
7581.5	0.249191	0.074014	1305.457	0.126608	0.099892	0.31112242	0.28727	0.528727	0.099816
7582	0.251944	0.105281	965.5264	0.278837	0.098481	0.4529248	0.307893	0.537893	0.110331
7582.5	0.277821	0.101585	1089.911	0.180351	0.121243	0.4645355	0.329701	0.529701	0.118871
7583	0.306177	0.093879	1288.715	0.172402	0.099973	0.4761295	0.346554	0.546554	0.062865
7583.5	0.324587	0.124578	1039.613	0.171111	0.10278	0.4877171	0.219852	0.519852	0.138764
7584	0.338973	0.108809	1610.831	0.188666	0.131955	0.4999322	0.149433	0.549433	0.035831
7584.5	0.353752	0.091888	2204.766	0.220907	0.174519	0.5510652	0.139926	0.539926	0.134249
7585	0.33326	0.089173	3103.086	0.231092	0.25338	0.5528768	0.221347	0.551347	0.030762
7585.5	0.297458	0.078744	2841.202	0.241747	0.245184	0.5560527	0.122927	0.522927	0.231663
7586	0.255101	0.088046	2112.007	0.249121	0.226625	0.5564862	0.626003	0.526003	0.336527
7586.5	0.251586	0.08763	1967.117	0.260608	0.249314	0.5758272	0.642203	0.542203	0.031937
7587	0.278966	0.078155	1901.596	0.274679	0.084781	0.5812915	0.726936	0.626936	0.030236
7587.5	0.302281	0.08157	2003.503	0.283058	0.088814	0.5556716	0.621122	0.621122	0.129685
7588	0.273175	0.120318	1702.071	0.293893	0.136775	0.6890192	0.619219	0.619219	0.132397
7588.5	0.281044	0.105495	892.8526	0.305142	0.117937	0.6983564	0.128493	0.628493	0.23948
7589	0.294101	0.096365	599.0244	0.319211	0.106642	0.6893373	0.651721	0.751721	0.243892
7589.5	0.274388	0.106401	746.5735	0.338984	0.119071	0.6891795	0.665518	0.765518	0.142127
7590	0.318802	0.105957	690.2725	0.354614	0.118514	0.7926947	0.660056	0.750056	0.037959
7590.5	0.356263	0.102513	250.9008	0.379419	0.114222	0.7818257	0.746846	0.746846	0.135518
7591	0.401455	0.102735	455.5229	0.40596	0.114498	0.8994384	0.71389	0.761389	0.035739
7591.5	0.386922	0.096443	1044.916	0.427879	0.106736	0.8847039	0.739624	0.739624	0.039749
7592	0.347467	0.080738	1144.692	0.440932	0.08783	0.8974903	0.752576	0.752576	0.242356
7592.5	0.336662	0.098676	1622.979	0.454383	0.109479	0.9771543	0.760769	0.760769	0.24695
7593	0.330005	0.127572	1726.388	0.471776	0.146227	0.9653025	0.874804	0.874804	0.251736
7593.5	0.330129	0.144298	1748.317	0.493528	0.016863	0.98652335	0.888905	0.888905	0.056697
7594	0.311611	0.145749	1909.048	0.512419	0.017617	0.99771053	0.943006	0.933006	0.263415
7594.5	0.330946	0.115911	2143.014	0.215984	0.131108	0.99890235	0.941318	0.932318	0.068442
7595	0.351571	0.09273	1768.071	0.219253	0.102207	0.99909181	0.95583	0.944483	0.067847

APPENDIX D: DATA OF WELL 3 FOR FLOW UNIT CHARTS FOR RESERVOIR X

Depth	Φ_T	Φe	K	RQI	Φz	nRQI	Φh	kh	Vsh
7505	0.35296	0.266582	2607.451	0.0051573	0.363478	0.0002983	0.002242	0.003591	0.008125
7505.5	0.364569	0.253138	2029.224	0.0063668	0.338935	0.0002265	0.002305	0.036414	0.013172
7506	0.363479	0.247626	1874.404	0.0063768	0.329126	0.0024194	0.0026061	0.005735	0.019478
7506.5	0.338935	0.264493	1518.246	0.0069685	0.359606	0.0256472	0.0032729	0.008297	0.026197
7507	0.329126	0.26682	970.3721	0.0071814	0.363921	0.0270831	0.0038016	0.006959	0.024243
7507.5	0.359607	0.258823	1265.167	0.0072814	0.349205	0.0283119	0.0031346	0.010992	0.020581
7508	0.363922	0.254552	1432.732	0.0071814	0.341475	0.0293327	0.023293	0.008637	0.018292

7508.5	0.349206	0.26222	1195.006	0.0879186	0.355417	0.0301742	0.015666	0.007659	0.01595
7509	0.341476	0.274233	1056.234	0.083477	0.377852	0.0308561	0.008783	0.068538	0.013598
7509.5	0.355418	0.288825	1453.923	0.008377	0.406123	0.1313428	0.006111	0.059157	0.012091
7510	0.377853	0.285031	1639.844	0.086028	0.398662	0.1318243	0.006886	0.053027	0.010451
7510.5	0.406123	0.267594	1706.985	0.009628	0.365362	0.1324029	0.00971	0.046242	0.006742
7511	0.398661	0.162606	1499.561	0.086028	0.194180	0.1331345	0.013946	0.03045	0.005856
7511.5	0.365363	0.249298	2017.58	0.008857	0.332086	0.1340223	0.012858	0.026585	0.006299
7512	0.356127	0.222985	2542.355	0.091366	0.286764	0.2349698	0.010983	0.028521	0.00528
7512.5	0.332086	0.237137	3006.342	0.091366	0.310851	0.2359964	0.016506	0.024047	0.004607
7513	0.286977	0.244813	3527.048	0.091366	0.324175	0.2371701	0.021927	0.021064	0.004242
7513.5	0.310851	0.134044	3465.648	0.001100	0.154793	0.2383865	0.02738	0.019438	0.009233
7514	0.324176	0.226127	3234.532	0.013056	0.287660	0.2395244	0.034375	0.040141	0.007535
7514.5	0.305558	0.244448	2888.011	0.011945	0.323535	0.2405272	0.04338	0.033881	0.007665
7515	0.292201	0.252112	2959.973	0.112794	0.337098	0.2415552	0.053062	0.153470	0.011129
7515.5	0.323535	0.155863	2828.456	0.116241	0.164351	0.2425476	0.063485	0.136780	0.011921
7516	0.337098	0.148875	2486.651	0.021979	0.164047	0.3434572	0.068214	0.132213	0.010923
7516.5	0.343839	0.268396	1979.184	0.119793	0.367062	0.3443064	0.070733	0.140292	0.00657
7517	0.331336	0.283571	1323.459	0.023453	0.371453	0.345169	0.126936	0.117278	0.003214
7517.5	0.36686	0.294953	1442.287	0.003512	0.373994	0.345693	0.121122	0.113983	0.001885
7518	0.39581	0.306909	1695.278	0.013512	0.339634	0.459159	0.119219	0.105879	0.004679
7518.5	0.418346	0.180717	1961.564	0.014789	0.187467	0.3460822	0.128493	0.419674	0.007215
7519	0.442812	0.190336	2233.242	0.052408	0.192418	0.4463841	0.151721	0.115910	0.007372
7519.5	0.441238	0.185832	2646.92	0.005408	0.19592	0.4466664	0.165518	0.127108	0.005389
7520	0.429885	0.141332	2775.26	0.007907	0.197959	0.4470464	0.160056	0.122551	0.006403
7520.5	0.41204	0.163061	2751.941	0.017107	0.130391	0.4474132	0.146846	0.125818	0.007903
7521	0.414939	0.199482	2813.476	0.181907	0.137194	0.4477172	0.121389	0.284361	0.008812
7512.5	0.406453	0.281958	2968.913	0.07716	0.306793	0.4480229	0.139624	0.133952	0.011796
7522	0.386513	0.253082	2842.537	0.001852	0.293397	0.4483371	0.152576	0.143910	0.014661
7522.5	0.353631	0.238337	2372.719	0.008852	0.345912	0.5486357	0.032502	0.167783	0.021385
7523	0.304772	0.252726	2210.89	0.009392	0.371683	0.5488614	0.103318	0.155422	0.029873
7523.5	0.307502	0.21604	2075.314	0.005933	0.361329	0.549009	0.024527	0.119868	0.041372
7524	0.317249	0.270313	2064.186	0.012225	0.332001	0.5491221	0.028978	0.157696	0.054042
7524.5	0.32499	0.178672	1441.791	0.021871	0.195106	0.549198	0.035465	0.195523	0.068003
7525	0.330362	0.263638	1076.164	0.021871	0.156769	0.5492354	0.039343	0.233351	0.083387
7525.5	0.350798	0.273336	860.5135	0.025393	0.145824	0.549245	0.051814	0.271179	0.078289
7523	0.358181	0.179778	1181.046	0.025399	0.152828	0.549265	0.063426	0.259043	0.076449
7523.5	0.36187	0.196025	1918.374	0.039378	0.145471	0.549245	0.089386	0.25457	0.067902
7524	0.373738	0.289529	2599.124	0.023978	0.141149	0.549245	0.119868	0.233088	0.053101
7524.5	0.390379	0.28083	2546.417	0.061996	0.003357	0.649245	0.157696	0.192835	0.039751
7525	0.393139	0.165475	1906.118	0.002696	0.125489	0.049245	0.195523	0.152582	0.027711
7525.5	0.373903	0.16088	2082.264	0.061996	0.116391	0.049245	0.233351	0.11233	0.022031
7526	0.362348	0.267168	2118.819	0.073005	0.113013	0.049245	0.271179	0.091793	0.028748

7526.5	0.351572	0.266582	1774.163	0.027856	0.111346	0.0492583	0.259043	0.115963	0.032908
7527	0.350515	0.253138	2592.009	0.038256	0.109133	0.249259	0.25457	0.130215	0.032534
7527.5	0.311208	0.247626	2894.682	0.086759	0.116462	0.049259	0.233088	0.128956	0.031621
7528	0.281789	0.264493	2141.526	0.004551	0.127719	0.349259	0.192835	0.125862	0.034673
7528.5	0.261676	0.26682	2363.852	0.013857	0.139907	0.049259	0.152582	0.136107	0.03531
7529	0.290593	0.130074	2390.541	0.033331	0.167127	0.3492622	0.143685	0.138213	0.032988
7529.5	0.339855	0.092528	2201.246	0.043517	0.194247	0.3493045	0.059157	0.130484	0.03685
7530	0.375458	0.102409	1621.969	0.054013	0.208293	0.0493045	0.053027	0.143257	0.00388
7530.5	0.367849	0.112237	1987.225	0.084013	0.202955	0.0493173	0.046242	0.14955	0.047608
7531	0.322607	0.133044	2315.412	0.054013	0.203978	0.0493994	0.103045	0.176774	0.068187
7531.5	0.318359	0.141906	1669.53	0.075979	0.255499	0.0495499	0.026585	0.233824	0.092579
7532	0.304502	0.150809	2168.612	0.030979	0.246883	0.0496836	0.028521	0.292145	0.120906
7532.5	0.301955	0.148958	1949.601	0.024083	0.251217	0.0497857	0.024047	0.350465	0.078806
7533	0.364304	0.139952	1713.588	0.050396	0.275600	0.0500239	0.132486	0.260293	0.04832
7533.5	0.389328	0.128073	1498.146	0.049299	0.269122	0.0501417	0.097042	0.178892	0.036679
7534	0.356194	0.125548	1707.208	0.049959	0.250452	0.0501709	0.1925379	0.142698	0.028916
7534.5	0.372119	0.134452	2066.162	0.058022	0.253659	0.0502256	0.1160769	0.116551	0.024167
7535	0.375617	0.147226	1791.555	0.015603	0.29494	0.0504134	0.1174804	0.199641	0.021644
7535.5	0.364267	0.158064	1531.453	0.006603	0.289573	0.0507199	0.1188905	0.009053	0.024021
7536	0.326456	0.122581	1372.403	0.057302	0.276989	0.0509241	0.2103006	0.009911	0.027917
7536.5	0.351016	0.127032	1282.043	0.059053	0.280535	0.05109	0.2121318	0.113052	0.023687
7537	0.371871	0.134645	1222.224	0.068574	0.281458	0.0512822	0.2324483	0.097892	0.021072
7537.5	0.332943	0.144129	1679.722	0.006857	0.285883	0.0514692	0.2322946	0.307893	0.021508
7538	0.363439	0.156733	1928.105	0.006277	0.29343	0.0516558	0.2120555	0.329701	0.022028
7538.5	0.350315	0.133051	2551.582	0.066335	0.298959	0.0518332	0.1257244	0.346554	0.022228
7539	0.335276	0.120323	2754.812	0.006085	0.300307	0.0520946	0.1062868	0.219852	0.02242
7539.5	0.320278	0.116774	3379.448	0.007743	0.297642	0.0523487	0.1161295	0.149433	0.02305
7540	0.333076	0.123032	3787.204	0.008413	0.2991	0.0527894	0.1177171	0.139926	0.026061
7540.5	0.351522	0.104968	3344.444	0.083293	0.302141	0.0535044	0.119322	0.132347	0.032729
7541	0.331617	0.102321	3161.691	0.051306	0.296428	0.0551147	0.1210652	0.522927	0.038016
75741.5	0.31687	0.095742	3627.958	0.097923	0.292193	0.6577387	0.1228768	0.526003	0.031346
7542	0.309794	0.095613	3916.346	0.084743	0.277989	0.0611334	0.124527	0.542203	0.023293
75742.5	0.307123	0.103871	2539.118	0.087326	0.267248	0.0647394	0.1260862	0.526936	0.015666
7543	0.306185	0.112774	2127.848	0.097514	0.252829	0.4681908	0.1275872	0.521122	0.008783
7543.5	0.342524	0.109172	892.8526	0.985063	0.218153	0.6719443	0.1291015	0.519219	0.006111
7544	0.35877	0.111757	599.0244	0.091005	0.181456	0.6752781	0.1305716	0.528493	0.006886
7544.5	0.39352	0.121403	746.5735	0.016438	0.157001	0.3777258	0.1320192	0.551721	0.00971
7545	0.401326	0.118129	690.2725	0.014568	0.13227	0.0793928	0.1335641	0.565518	0.013946
7545.5	0.431413	0.125806	250.9008	0.013769	0.120726	0.0808637	0.2308313	0.560056	0.012858
7546	0.450945	0.143677	455.5229	0.025325	0.120971	0.0824302	0.2325332	0.146846	0.010983
7546.5	0.428045	0.134516	1044.916	0.003211	0.128952	0.0841089	0.2343444	0.541389	0.016506
7547	0.415363	0.137677	1144.692	0.007815	0.124401	0.0860049	0.236151	0.139624	0.021927

7547.5	0.4319	0.138839	1622.979	0.266548	0.10671	0.0883316	0.2379896	0.152576	0.02738
7548	0.438491	0.141358	1726.388	0.231092	0.094411	0.090601	0.2393208	0.160769	0.034375
7548.5	0.370359	0.138898	1748.317	0.20959	0.094414	0.6929324	0.2403703	0.174804	0.04338
7549	0.342629	0.144478	1909.048	0.214367	0.092636	0.6954729	0.3106595	0.188905	0.053062
7549.5	0.252938	0.152323	2143.014	0.191522	0.086514	0.6981758	0.3085643	0.203006	0.063485
7550	0.220579	0.160085	1768.071	0.188666	0.084311	0.6006912	0.3103794	0.055196	0.068214
7550.5	0.235081	0.137742	1253.908	0.197365	0.093076	0.6030076	0.3123358	0.745122	0.070733
7551	0.228248	0.138315	794.6654	0.217612	0.097983	0.6052464	0.3144043	0.762868	0.073472
7551.5	0.164594	0.136781	751.9919	0.241747	0.093441	0.6074424	0.3163718	0.061864	0.084728
7552	0.19483	0.101827	1024.805	0.062548	0.101546	0.6093807	0.3182602	0.770689	0.090397
7552.5	0.249191	0.074014	1305.457	0.026608	0.099892	0.6112242	0.4060464	0.777556	0.099816
7553	0.251944	0.105281	965.5264	0.097837	0.098481	0.6129248	0.4082733	0.083891	0.110331
7553.5	0.277821	0.101585	1089.911	0.018351	0.121243	0.6145355	0.4105901	0.777859	0.118871
7554	0.306177	0.093879	1288.715	0.072432	0.099973	0.6161295	0.4131228	0.068706	0.062865
7554.5	0.324587	0.124578	1039.613	0.171111	0.10278	0.6177171	0.4158075	0.076061	0.038764
7555	0.338973	0.108809	1610.831	0.018666	0.131955	0.719322	0.4183277	0.077165	0.035831
7555.5	0.353752	0.091888	2204.766	0.012907	0.174519	0.7210652	0.4207778	0.085753	0.034249
7556	0.33326	0.089173	3103.086	0.023192	0.25338	0.7228768	0.4233305	0.092523	0.030762
7556.5	0.297458	0.078744	2841.202	0.024747	0.245184	0.724527	0.4259754	0.095719	0.031663
7557	0.255101	0.088046	2112.007	0.029121	0.226625	0.1260862	0.5527567	0.1061	0.036527
7557.5	0.251586	0.08763	1967.117	0.026608	0.249314	0.7275872	0.5544837	0.110633	0.031937
7558	0.278966	0.078155	1901.596	0.027679	0.084781	0.7291015	0.5563132	0.113227	0.030236
7558.5	0.302281	0.08157	2003.503	0.028358	0.088814	0.7305716	0.5579617	0.102423	0.029685
7559	0.273175	0.120318	1702.071	0.029893	0.136775	0.7320192	0.5594792	0.104213	0.032397
7559.5	0.281044	0.105495	892.8526	0.035142	0.117937	0.7335641	0.5611388	0.873248	0.03948
7560	0.294101	0.096365	599.0244	0.039211	0.106642	0.7353373	0.5630425	0.84489	0.043892
7560.5	0.274388	0.106401	746.5735	0.038984	0.119071	0.7374895	0.5651508	0.811054	0.042127
7561	0.318802	0.105957	690.2725	0.054614	0.118514	0.7396947	0.5670668	0.856041	0.037959
7561.5	0.356263	0.102513	250.9008	0.037949	0.114222	0.7418257	0.6667342	0.860337	0.035518
7562	0.401455	0.102735	455.5229	0.040596	0.114498	07441384	0.6687821	0.871704	0.035739
7562.5	0.386922	0.096443	1044.916	0.127879	0.106736	0.7467039	0.6709266	0.88332	0.039749
7563	0.347467	0.080738	1144.692	0.040932	0.08783	0.8491103	0.6729718	0.883567	0.042356
7563.5	0.336662	0.098676	1622.979	0.054383	0.109479	0.8512543	0.6748623	0.856751	0.04695
7564	0.330005	0.127572	1726.388	0.041776	0.146227	0.8533025	0.6768518	0.036962	0.051736
7564.5	0.3329	0.144298	1748.317	0.493528	0.168631	0.8552335	0.6789021	0.856986	0.056697
7565	0.311611	0.145749	1909.048	0.512419	0.170617	0.8571053	0.6811647	0.861107	0.063415
7565.5	0.330946	0.115911	2143.014	0.021984	0.131108	0.8590235	0.6833725	0.872321	0.068442
7566	0.351571	0.09273	1768.071	0.019253	0.102207	0.8609181	0.601256	0.810359	0.067847
7567.5	0.341546	0.082763	1253.908	0.024679	0.090231	0.8626807	0.7057982	0.139774	0.059428
7568	0.320231	0.083221	794.6654	0.033929	0.090776	0.8643552	0.7064827	0.171388	0.041228
7568.5	0.325396	0.098239	751.9919	0.001881	0.108942	0.8662109	0.7071875	0.881324	0.033585
7569	0.300948	0.106777	1024.805	0.002499	0.119541	0.8681627	0.7079523	0.917453	0.023455

7569.5	0.330862	0.072414	1305.457	0.002276	0.078067	0.8701541	0.7088981	0.921906	0.012326
7570	0.327515	0.080238	965.5264	0.029253	0.087238	0.8722981	0.7980764	0.925118	0.008025
7570.5	0.313208	0.072756	1089.911	0.027646	0.078465	0.9744169	0.7996407	0.916239	0.009846
7571	0.286598	0.066645	1288.715	0.002459	0.071404	0.9763261	0.8016167	0.135443	0.013089
7571.5	0.296052	0.067226	1039.613	0.024357	0.072071	0.9781968	0.8046651	0.929109	0.013565
772	0.285957	0.067742	1610.831	0.005289	0.072664	0.9802468	0.8075286	0.925376	0.011618
772.5	0.309794	0.073419	2204.766	0.068558	0.079237	0.9824237	0.8101161	0.92278	0.014379
7573	0.330252	0.073935	3103.086	0.078837	0.079838	0.9845836	0.8128189	0.924149	0.013675
7573.5	0.328532	0.064839	2841.202	0.028951	0.069334	0.9868942	0.8226327	0.95947	0.012622
7574	0.309743	0.044774	2112.007	0.030859	0.046873	0.9891608	0.8246301	0.955196	0.010183
7574.5	0.357929	0.068516	1967.117	0.034451	0.073556	0.9914874	0.8265368	0.945122	0.014522
7575	0.378089	0.072903	1901.596	0.003898	0.078636	0.9939633	0.8282585	0.962868	0.014271

APPENDIX E: DATA OF WELL 4 FOR FLOW UNIT CHARTS IN RESERVOIR X

Depth	Φ_T	Φe	K	RQI	Φz	nRQI	Φh	kh	Vsh
7550	0.317249	0.170313	2064.186	0.0022225	0.205273	0.0004922	0.010796	0.012091	0.054042
7550.5	0.32499	0.128672	1441.791	0.0011187	0.147736	0.0004998	0.00123	0.010451	0.068003
7551	0.330362	0.163638	1076.164	0.0025871	0.195654	0.0049234	0.003354	0.006742	0.083387
7551.5	0.350798	0.173336	860.5135	0.0525393	0.209681	0.0493173	0.002179	0.005856	0.078289
7552	0.358181	0.129778	1181.046	0.0426393	0.184811	0.0493994	0.002543	0.006299	0.076449
7552.5	0.36187	0.236025	1918.374	0.0023938	0.308943	0.0495499	0.002557	0.00528	0.067902
7553	0.373738	0.189529	2599.124	0.0033937	0.23385	0.0496836	0.002330	0.004607	0.053101
7553.5	0.390379	0.128083	2546.417	0.0026996	0.146898	0.0497857	0.001928	0.004242	0.039751
7554	0.393139	0.225475	1906.118	0.0661996	0.375489	0.0500239	0.152500	0.009233	0.027711
7554.5	0.373903	0.126088	2082.264	0.0761796	0.186391	0.0501417	0.00112	0.007535	0.022031
7555	0.362348	0.267168	2118.819	0.0027005	0.364569	0.0501709	0.000917	0.007665	0.028748
7555.5	0.351572	0.266582	1774.163	0.0067856	0.361346	0.1744169	0.001159	0.011129	0.032908
7556	0.350515	0.253138	2592.009	0.0278256	0.338933	0.1763261	0.003215	0.011921	0.032534
7556.5	0.311208	0.247626	2894.682	0.0286759	0.326912	0.1781968	0.001289	0.010923	0.031621
7557	0.281789	0.264493	2141.526	0.0314551	0.359606	0.1802468	0.001262	0.00657	0.034673
7557.5	0.261676	0.26682	2363.852	0.0338517	0.363733	0.1824237	0.136107	0.003214	0.03531
7558	0.250593	0.130074	2390.541	0.0153331	0.149523	0.1845836	0.138213	0.001885	0.032988
7558.5	0.339855	0.192528	2201.246	0.0113517	0.238433	0.2041563	0.130484	0.004679	0.03685
7559	0.375458	0.102409	1621.969	0.0154013	0.114093	0.2058371	0.143257	0.007215	0.0388
7559.5	0.367849	0.112237	1987.225	0.0035413	0.126426	0.2072826	0.14955	0.007372	0.047608
7560	0.322607	0.133044	2315.412	0.0055431	0.153461	0.2085519	0.176774	0.005389	0.068187
7560.5	0.318359	0.141906	1669.53	0.0875979	0.155499	0.2099077	0.233824	0.006403	0.092579
7561	0.304502	0.150809	2168.612	0.0975979	0.146883	0.2112737	0.292145	0.007903	0.120906
7561.5	0.301955	0.148958	1949.601	0.0142483	0.151217	0.2126131	0.350465	0.008812	0.078806
7562	0.364304	0.139952	1713.588	0.0150396	0.175600	0.2140655	0.260293	0.011796	0.04832

7562.5	0.389328	0.128073	1498.146	0.1492959	0.146922	0.2158335	0.178892	0.014661	0.036679
7563	0.356194	0.125548	1707.208	0.0692959	0.145452	0.217901	0.142698	0.021385	0.028916
7563.5	0.372119	0.234452	2066.162	0.0508022	0.353659	0.2201845	0.116551	0.029873	0.024167
7564	0.375617	0.247226	1791.555	0.0055603	0.392494	0.2225361	0.099641	0.041372	0.021644
7564.5	0.364267	0.158064	1531.453	0.0155603	0.189573	0.2246704	0.090353	0.054042	0.024021
7565	0.326456	0.122581	1372.403	0.0157302	0.176989	0.226363	0.09911	0.068003	0.027917
7565.5	0.351016	0.127032	1282.043	0.0025953	0.180535	0.227757	0.113052	0.083387	0.023687
7566	0.371871	0.234645	1222.224	0.0060854	0.381458	0.2292814	0.097892	0.078289	0.021072
7566.5	0.332943	0.244129	1679.722	0.1808574	0.385883	0.3308313	0.088215	0.076449	0.021508
7567	0.363439	0.156733	1928.105	0.1627171	0.192343	0.3325332	0.089845	0.067902	0.022028
7567.5	0.350315	0.243051	2551.582	0.1646335	0.398959	0.3343444	0.09178	0.053101	0.022228
7568	0.335276	0.120323	2754.812	0.0066085	0.187307	0.336151	0.092523	0.039751	0.02242
7568.5	0.320278	0.116774	3379.448	0.0070741	0.297642	0.3379896	0.093235	0.027711	0.02305
7569	0.333076	0.123032	3787.204	0.0107413	0.219913	0.3393208	0.095558	0.2349698	0.026061
7569.5	0.351522	0.104968	3344.444	0.0272903	0.302141	0.3403703	0.106474	0.2359964	0.032729
7570	0.331617	0.102321	3161.691	0.0075136	0.296428	0.341575	0.129612	0.2371701	0.038016
7570.5	0.31687	0.095742	3627.958	0.0797923	0.192193	0.3428766	0.147032	0.2383865	0.031346
7571	0.309794	0.295613	3916.346	0.0847431	0.277989	0.3440129	0.124926	0.2395244	0.023293
7571.5	0.307123	0.203871	2539.118	0.0873326	0.357248	0.3450656	0.096449	0.2405272	0.015666
7572	0.306185	0.212774	2127.848	0.0927514	0.332829	0.3461249	0.067416	0.2415552	0.008783
7572.5	0.342524	0.129172	892.8526	0.0985063	0.118153	0.347142	0.03922	0.2425476	0.006111
7573	0.35877	0.111757	599.0244	0.0091005	0.181456	0.3482723	0.027702	0.3434572	0.306886
7573.5	0.39352	0.121403	746.5735	0.0016438	0.157001	0.449651	0.031076	0.3443064	0.00971
7574	0.401326	0.118129	690.2725	0.0145268	0.133227	0.4509227	0.043138	0.345169	0.013946
7574.5	0.431413	0.125806	250.9008	0.0137169	0.120726	0.4521578	0.060559	0.345693	0.012858
7575	0.450945	0.143677	455.5229	0.0102525	0.120971	0.4532443	0.05616	0.459159	0.010983
7575.5	0.428045	0.134516	1044.916	0.0101331	0.128952	0.454212	0.048454	0.3460822	0.316506
7576	0.415363	0.137677	1144.692	0.0017815	0.124401	0.4551005	0.070724	0.4463841	0.021927
7576.5	0.34319	0.138839	1622.979	0.0026548	0.10671	0.4562107	0.091405	0.4466664	0.02738
7577	0.438491	0.141358	1726.388	0.0023192	0.094411	0.4577399	0.111162	0.4470464	0.334375
7577.5	0.370359	0.138898	1748.317	0.1020959	0.094414	0.4594287	0.135119	0.4474132	0.04338
7578	0.342629	0.144478	1909.048	0.0024367	0.092636	0.4611838	0.163942	0.4477172	0.053062
7578.5	0.252938	0.152323	2143.014	0.0191522	0.086514	0.4630822	0.192724	0.4480229	0.063485
7579	0.220579	0.160085	1768.071	0.0188666	0.084311	0.4650253	0.221506	0.4483371	0.068214
7579.5	0.235081	0.137742	1253.908	0.0197365	0.093076	0.4668415	0.233894	0.5486357	0.070733
7580	0.228248	0.138315	794.6654	0.0087612	0.097983	0.468623	0.240336	0.5488614	0.073472
7580.5	0.164594	0.136781	751.9919	0.0341747	0.093441	0.5705484	0.247221	0.549009	0.084728
7581	0.19483	0.101827	1024.805	0.002548	0.101546	0.5726302	0.274308	0.5491221	0.090397
7581.5	0.249191	0.274014	1305.457	0.026608	0.099892	0.5746994	0.28727	0.549198	0.099816
7582	0.251944	0.105281	965.5264	0.087837	0.098481	0.5765055	0.307893	0.5492354	0.110331
7582.5	0.277821	0.101585	1089.911	0.018351	0.121243	0.578309	0.329701	0.549245	0.118871
7583	0.306177	0.253879	1288.715	0.017242	0.099973	0.5799372	0.346554	0.549265	0.062865

7583.5	0.324587	0.124578	1039.613	0.017111	0.10278	0.5811873	0.219852	0.549245	0.038764
7584	0.338973	0.108809	1610.831	0.001866	0.131955	0.5821898	0.149433	0.549245	0.035831
7584.5	0.353752	0.291888	2204.766	0.002297	0.174519	0.5830094	0.139926	0.649245	0.034249
7585	0.33326	0.289173	3103.086	0.003192	0.25338	0.5837498	0.211347	0.049245	0.030762
7585.5	0.297458	0.178744	2841.202	0.004747	0.245184	0.5847016	0.222927	0.049245	0.031663
7586	0.255101	0.288046	2112.007	0.004121	0.226625	0.6856463	0.326003	0.049245	0.036527
7586.5	0.251586	0.108763	1967.117	0.006608	0.249314	0.6863135	0.342203	0.0492583	0.031937
7587	0.278966	0.278155	1901.596	0.002769	0.084781	0.6867794	0.326936	0.626936	0.030236
7587.5	0.302281	0.118157	2003.503	0.028358	0.088814	0.6872871	0.321122	0.621122	0.029685
7588	0.273175	0.120318	1702.071	0.029893	0.136775	0.6880409	03119219	0.218153	0.032397
7588.5	0.281044	0.105495	892.8526	0.030514	0.117937	0.6892166	0.328493	0.181456	0.03948
7589	0.294101	0.096365	599.0244	0.031921	0.106642	0.6907775	0.351721	0.157001	0.043892
7589.5	0.274388	0.106401	746.5735	0.038984	0.119071	0.6928677	0.3509227	0.13227	0.042127
7590	0.318802	0.105957	690.2725	0.034614	0.118514	0.7950811	0.4521578	0.120726	0.037959
7590.5	0.356263	0.102513	250.9008	0.003949	0.114222	0.797031	0.4532443	0.120971	0.035518
7591	0.401455	0.102735	455.5229	0.004596	0.114498	0.7987782	0.454212	0.128952	0.035739
7591.5	0.386922	0.096443	1044.916	0.004879	0.106736	0.7007988	0.4551005	0.124401	0.039749
7592	0.347467	0.080738	1144.692	0.040932	0.08783	0.7028041	0.4562107	0.10671	0.042356
7592.5	0.336662	0.098676	1622.979	0.054383	0.109479	0.7047023	0.4577399	0.094411	0.04695
7593	0.330005	0.127572	1726.388	0.071776	0.146227	0.706595	0.4594287	0.094414	0.251736
7593.5	0.3329	0.144298	1748.317	0.039358	0.168631	0.7085643	0.4611838	0.092636	0.056697
7594	0.311611	0.145749	1909.048	0.052419	0.170617	0.7103794	0.4630822	0.086514	0.063415
7594.5	0.330946	0.115911	2143.014	0.015984	0.131108	0.7123358	0.4650253	0.084311	0.068442
7595	0.351571	0.209273	1768.071	0.019253	0.102207	0.7144043	0.4668415	0.093076	0.067847
7595.5	0.341546	0.282763	1253.908	0.074679	0.090231	0.7163718	0.468623	0.097983	0.059428
7596	0.320231	0.083221	794.6654	0.003392	0.090776	0.7182602	0.5705484	0.093441	0.041228
7596.5	0.325396	0.298239	751.9919	0.018381	0.108942	0.7201789	0.5726302	0.101546	0.033585
7597	0.300948	0.106777	1024.805	0.024919	0.119541	0.7219816	0.5746994	0.099892	0.023455
7597.5	0.330862	0.072414	1305.457	0.012763	0.078067	0.7236807	0.5765055	0.098481	0.012326
7598	0.327515	0.080238	965.5264	0.019253	0.087238	0.7254564	0.578309	0.121243	0.008025
7598.5	0.313208	0.072756	1089.911	0.027646	0.078465	0.727129	0.5799372	0.099973	0.009846
7599	0.286598	0.266645	1288.715	0.023459	0.071404	0.7287891	0.5811873	0.10278	0.013089
7599.5	0.296052	0.264226	1039.613	0.024357	0.072071	0.7305289	0.5821898	0.131955	0.013565
7600	0.285957	0.261742	1610.831	0.025293	0.072664	0.7324623	0.5830094	0.35877	0.011618
7600.5	0.309794	0.123419	2204.766	0.026858	0.079237	0.7344482	0.5837498	0.39352	0.014379
7601	0.330252	0.173935	3103.086	0.027837	0.079838	0.8363024	0.5847016	0.401326	0.013675
7601.5	0.328532	0.264839	2841.202	0.002895	0.069334	0.8380325	0.6856463	0.431413	0.312622
7602	0.309743	0.244774	2112.007	0.003289	0.046873	0.8397521	0.6863135	0.450945	0.010183
7602.5	0.357929	0.268516	1967.117	0.034451	0.073556	0.8414268	0.6867794	0.428045	0.014522
7603	0.378089	0.272903	1901.596	0.038984	0.078636	0.8430579	0.062868	0.415363	0.014271
7603.5	0.395143	0.27729	2003.503	0.057288	0.083764	0.8546643	0.061864	0.4319	0.016498
7604	0.413129	0.270129	1702.071	0.037963	0.075418	0.8663595	0.070689	0.438491	0.018265

7604.5	0.376033	0.161032	2188.408	0.038867	0.064999	0.8781506	0.077556	0.370359	0.019924
7605	0.351571	0.230516	1702.729	0.004092	0.099525	0.8801293	0.083891	0.342629	0.018344
7605.5	0.324554	0.150455	1431.136	0.042499	0.177101	0.8922014	0.077859	0.252938	0.015993
7606	0.276017	0.158769	1057.751	0.017901	0.188735	0.8543317	0.068706	0.220579	0.271878
7606.5	0.301565	0.15028	954.9883	0.017242	0.176858	0.8563853	0.076061	0.235081	0.018164
7607	0.317711	0.133876	1101.164	0.016798	0.15457	0.8585778	0.077165	0.228248	0.020417
7607.5	0.29903	0.131295	1028.047	0.014359	0.151139	0.8607809	0.085753	0.164594	0.022228
7608	0.273159	0.122525	794.7643	0.015754	0.139634	0.8627306	0.092523	0.19483	0.023094
7608.5	0.262764	0.117852	725.0251	0.001469	0.133597	0.3645948	0.095719	0.249191	0.025957
7609	0.291155	0.128821	1074.655	0.005754	0.14787	0.8665638	0.441796	0.251944	0.027231
7609.5	0.315995	0.122696	1314.017	0.161131	0.139856	0.8686348	0.410633	0.277821	0.027817
7610	0.33121	0.123849	1273.144	0.004919	0.141355	0.8707493	0.421796	0.306177	0.024934
7610.5	0.312882	0.11185	1080.175	0.098342	0.125936	0.872731	0.443785	0.324587	0.025431
7611	0.341796	0.101855	834.7654	0.038563	0.113406	0.8746435	0.428314	0.710555	0.017153
7611.5	0.33785	0.078645	1175.489	0.038163	0.085358	0.876491	0.452353	0.757244	0.010127
7612	0.328314	0.072118	1225.384	0.182529	0.077723	0.9782872	0.448118	0.832486	0.312329
7612.5	0.352353	0.088772	1235.071	0.017631	0.09742	0.9801223	0.460193	0.897042	0.012829
7613	0.348118	0.09792	1570.135	0.180351	0.10855	0.9819925	0.442845	0.825399	0.013891
7613.5	0.360193	0.111275	1700.769	0.014359	0.125208	0.9838706	0.431773	0.835988	0.016757
7614	0.342845	0.092447	1676.028	0.014751	0.101864	0.9856985	0.665518	0.848853	0.019773
7614.5	0.331773	0.100553	1491.629	0.013254	0.111794	0.9875264	0.660056	0.858263	0.319839
7615	0.311218	0.107414	1653.354	0.016564	0.12034	0.9895061	0.646846	0.830892	0.013004
7615.5	0.325894	0.08996	1976.502	0.014724	0.098853	0.9916902	0.661389	0.820995	0.008253
7616	0.349813	0.097687	2035.414	0.015519	0.108263	0.9941745	0.739624	0.878786	0.013062
7616.5	0.392008	0.115742	1825.33	0.016519	0.130892	0.3965058	0.752576	0.082478	0.014082
7617	0.409804	0.107936	1474.707	0.006492	0.120995	0.9386256	0.760769	0.897656	0.216915
7617.5	0.402778	0.073032	1517.646	0.009355	0.078786	0.9410345	0.874804	0.890628	0.025258
7618	0.368147	0.076194	1781.229	0.008908	0.082478	0.9036476	0.888905	0.859177	0.035785
7618.5	0.326908	0.088968	2072.444	0.014218	0.097656	0.9060464	0.803006	0.864195	0.045817
7619	0.300861	0.083097	1689.833	0.019846	0.090628	0.9082733	0.821318	0.865512	0.049141
7619.5	0.298506	0.055871	1833.129	0.011665	0.059177	0.9105901	0.834483	0.859539	0.047836
7620	0.286654	0.060323	1952.528	0.012481	0.064195	0.9431228	0.832946	0.877453	0.052323
7620.5	0.299768	0.061484	1923.284	0.128617	0.065512	0.9515875	0.810555	0.843708	0.057456
7621	0.299292	0.056194	1694.732	0.013254	0.059539	0.9183277	0.857244	0.857097	0.042852
7621.5	0.338323	0.057645	1531.892	0.018416	0.061172	0.9207778	0.832486	0.889025	0.034472
7622	0.350114	0.084708	1392.5	0.001654	0.092548	0.9623335	0.897042	0.843708	0.232579
7622.5	0.332882	0.101955	2192.115	0.010656	0.11353	0.9759754	0.905399	0.857097	0.331478
7623	0.337842	0.122092	2706.649	0.017416	0.139072	0.9888192	0.935988	0.889025	0.230719
7623.5	0.303925	0.129478	3000.668	0.018796	0.148735	0.9814357	0.943708	0.951083	0.431119
7624	0.303321	0.122624	2281.387	0.002209	0.139763	0.9838299	0.957097	0.962296	0.234445
7624.5	0.341706	0.116044	2423.021	0.025721	0.131278	0.9966332	0.959025	0.95947	0.256222
7625	0.349926	0.113987	2238.378	0.002869	0.128652	0.9997953	0.951083	0.955196	0.272765

APPENDIX F: DATA OF WELL 5 FOR FLOW UNIT CHARTS IN RESERVOIR X

Depth	Φ_T	Φe	K	RQI	Φz	nRQI	Φh	kh	Vsh
7500	0.350315	0.133051	2551.582	0.0064335	0.153470	0.0007772	0.09178	0.021984	0.022228
7500.5	0.335276	0.120323	2754.812	0.0066085	0.136780	0.0007778	0.092523	0.019253	0.02242
7501	0.320278	0.116774	3379.448	0.0070413	0.132213	0.0007993	0.093235	0.024679	0.02305
7501.5	0.333076	0.123032	3787.204	0.0077413	0.140292	0.0008637	0.095558	0.033929	0.026061
7502	0.351522	0.104968	3344.444	0.0072903	0.117278	0.0008243	0.106474	0.001881	0.032729
7502.5	0.331617	0.102321	3161.691	0.0751306	0.113983	0.0841089	0.129612	0.002499	0.038016
7503	0.31687	0.095742	3627.958	0.0797923	0.105879	0.0008649	0.147032	0.002276	0.031346
7503.5	0.309794	0.295613	3916.346	0.0847431	0.419674	0.0008816	0.124926	0.129253	0.023293
7504	0.307123	0.103871	2539.118	0.0873326	0.115910	0.090601	0.096449	0.127646	0.015666
7504.5	0.306185	0.112774	2127.848	0.0927514	0.127108	0.0929324	0.067416	0.102459	0.008783
7505	0.342524	0.109172	892.8526	0.0985063	0.122551	0.0954729	0.002983	0.124357	0.006111
7505.5	0.35877	0.111757	599.0244	0.0091305	0.125818	0.1145355	0.002265	0.305289	0.006886
7506	0.39352	0.221403	746.5735	0.0164318	0.284361	0.1161295	0.024194	0.368558	0.00971
7506.5	0.401326	0.118129	690.2725	0.0024568	0.133952	0.1177171	0.0256472	0.378837	0.013946
7507	0.431413	0.125806	250.9008	0.0137169	0.143910	0.119322	0.0270831	0.428951	0.012858
7507.5	0.450945	0.143677	455.5229	0.0025325	0.167783	0.1210652	0.0283119	0.430859	0.010983
7508	0.428045	0.134516	1044.916	0.0031222	0.155422	0.1228768	0.0293327	0.434451	0.016506
7508.5	0.415363	0.137677	1144.692	0.0107815	0.159658	0.124527	0.0301742	0.070724	0.021927
7509	0.43193	0.138839	1622.979	0.0062658	0.161223	0.1260862	0.0308561	0.691405	0.02738
7509.5	0.438491	0.141358	1726.388	0.0102392	0.164629	0.1275872	0.1313428	0.611162	0.034375
7510	0.370359	0.138898	1748.317	0.0120959	0.161302	0.1291015	0.1318243	0.135119	0.04338
7510.5	0.342629	0.144478	1909.048	0.0214367	0.168877	0.1305716	0.1324029	0.163942	0.053062
7511	0.252938	0.152323	2143.014	0.0191522	0.179694	0.1320192	0.1331345	0.192724	0.063485
7511.5	0.220579	0.160085	1768.071	0.0018866	0.190596	0.1335641	0.1340223	0.221506	0.068214
7512	0.235081	0.137742	1253.908	0.0019735	0.159745	0.2308313	0.2349698	0.233894	0.070733
7512.5	0.228248	0.138315	794.6654	0.0021762	0.160516	0.2325332	0.2359964	0.240336	0.073472
7513	0.164594	0.136781	751.9919	0.0241747	0.158454	0.2343444	0.2371701	0.247221	0.084728
7513.5	0.19483	0.101827	1024.805	0.102548	0.113371	0.236151	0.2383865	0.274308	0.090397
7514	0.249191	0.274014	1305.457	0.0260608	0.099892	0.2379896	0.2395244	0.28727	0.099816
7514.5	0.251944	0.105281	965.5264	0.0078837	0.098481	0.2393208	0.2405272	0.307893	0.110331
7515	0.277821	0.101585	1089.911	0.180351	0.121243	0.2403703	0.2415552	0.329701	0.118871
7515.5	0.326177	0.293879	1288.715	0.1072402	0.099973	0.3106595	0.2425476	0.346554	0.062865
7516	0.324587	0.124578	1039.613	0.1173222	0.10278	0.3085643	0.3434572	0.219852	0.038764
7516.5	0.338973	0.108809	1610.831	0.0188666	0.131955	0.3103794	0.3443064	0.149433	0.035831
7517	0.353752	0.091888	2204.766	0.0220907	0.174519	0.3123358	0.345169	0.139926	0.034249
7517.5	0.33326	0.089173	3103.086	0.0231092	0.15338	0.3144043	0.345693	0.221347	0.030762
7518	0.297458	0.078744	2841.202	0.0241747	0.145184	0.3163718	0.459159	0.122927	0.031663

7519.5	0.255101	0.088046	2112.007	0.0249121	0.126625	0.3182602	0.3460822	0.126003	0.036527
7520	0.251586	0.08763	1967.117	0.0260608	0.149314	0.4060464	0.4463841	0.142203	0.031937
7520.5	0.378966	0.278155	1901.596	0.0274679	0.104781	0.4082733	0.4466664	0.126936	0.030236
7521	0.302281	0.08157	2003.503	0.0283058	0.108814	0.4105901	0.4470464	0.121122	0.029685
7521.5	0.273175	0.120318	1702.071	0.0293893	0.136775	0.4131228	0.4474132	0.119219	0.032397
7522	0.281044	0.105495	892.8526	0.0305142	0.117937	0.4158075	0.4477172	0.128493	0.03948
7522.5	0.294101	0.096365	599.0244	0.0319211	0.106642	0.4183277	0.4480229	0.151721	0.043892
7523	0.274388	0.106401	746.5735	0.0338984	0.119071	0.4207778	0.4483371	0.165518	0.042127
7523.5	0.318802	0.105957	690.2725	0.0354614	0.118514	0.4233305	0.5486357	0.160056	0.037959
7524	0.356263	0.102513	250.9008	0.0379419	0.114222	0.4259754	0.5488614	0.146846	0.035518
7524.5	0.401455	0.102735	455.5229	0.1040596	0.114498	0.5527567	0.549009	0.1389	0.035739
7525	0.386922	0.296443	1044.916	0.0427879	0.106736	0.5544837	0.5491221	0.139624	0.039749
7525.5	0.347467	0.280738	1144.692	0.0044932	0.08783	0.5563132	0.549198	0.152576	0.042356
7526	0.336662	0.298676	1622.979	0.0454383	0.109479	0.5579617	0.5492354	0.160769	0.04695
7526.5	0.330005	0.127572	1726.388	0.0471776	0.146227	0.5594792	0.549245	0.174804	0.051736
7527	0.332932	0.144298	1748.317	0.0493528	0.168631	0.5611388	0.549265	0.188905	0.056697
7527.5	0.311611	0.145749	1909.048	0.0512419	0.170617	0.5630425	0.549245	0.203006	0.063415
7528	0.309743	0.244774	2112.007	0.0302859	0.046873	0.5651508	0.549245	0.055196	0.010183
7528.5	0.357929	0.268516	1967.117	0.0314451	0.073556	0.5670668	0.649245	0.045122	0.014522
7529	0.378089	0.072903	1901.596	0.0338984	0.078636	0.6667342	0.049245	0.062868	0.014271
7529.5	0.395143	0.27729	2003.503	0.0357288	0.083764	0.6687821	0.049245	0.061864	0.016498
7530	0.413129	0.270129	1702.071	0.0370963	0.075418	0.6709266	0.049245	0.070689	0.018265
7530.5	0.376033	0.261032	2188.408	0.0388067	0.064999	0.6729718	0.049253	0.077556	0.019924
7531	0.351571	0.290516	1702.729	0.0409021	0.099525	0.6748623	0.249259	0.083891	0.018344
7531.5	0.324554	0.150455	1431.136	0.0421499	0.177101	0.6768518	0.049259	0.077859	0.015993
7532	0.276017	0.158769	1057.751	0.0179001	0.188735	0.6789021	0.349259	0.068706	0.017878
7532.5	0.301565	0.15028	954.9883	0.0172402	0.176858	0.6811647	0.049259	0.076061	0.018164
7533	0.317711	0.133876	1101.164	0.0167298	0.15457	0.6833725	0.3492622	0.077165	0.020417
7533.5	0.29903	0.131295	1028.047	0.0014959	0.151139	0.601256	0.3493045	0.085753	0.022228
7534	0.273159	0.122525	794.7643	0.0015754	0.139634	0.7057982	0.0493045	0.092523	0.023094
7534.5	0.262764	0.117852	725.0251	0.0149469	0.133597	0.7064827	0.0493173	0.095719	0.025957
7535	0.291155	0.128821	1074.655	0.0015754	0.14787	0.7071875	0.0493994	0.1061	0.027231
7535.5	0.315995	0.122696	1314.017	0.1161131	0.139856	0.7079523	0.0495499	0.110633	0.027817
7536	0.33121	0.123849	1273.144	0.0204919	0.141355	0.7088981	0.0496836	0.113227	0.024934
7536.5	0.312882	0.11185	1080.175	0.0298342	0.125936	0.7980764	0.0497857	0.102423	0.025431
7537	0.341796	0.101855	834.7654	0.0385163	0.113406	0.7996407	0.0500239	0.104213	0.017153
7537.5	0.33785	0.278645	1175.489	0.0385163	0.085358	0.8016167	0.0501417	0.073248	0.010127
7538	0.328314	0.272118	1225.384	0.0482529	0.077723	0.8046651	0.6501709	0.774489	0.012329
7538.5	0.352353	0.088772	1235.071	0.0176331	0.09742	0.8075286	0.6502256	0.711054	0.012829
7539	0.348118	0.219792	1570.135	0.0180351	0.10855	0.8101161	0.6504134	0.756041	0.013891
7539.5	0.360193	0.111275	1700.769	0.0143959	0.125208	0.8128189	0.6507199	0.760337	0.016757
7540	0.342845	0.292447	1676.028	0.0140751	0.101864	0.8226327	0.6509241	0.071704	0.019773

7540.5	0.331773	0.100553	1491.629	0.0132541	0.111794	0.8246301	0.1205109	0.708332	0.019839
7541	0.311218	0.107414	1653.354	0.0137564	0.12034	0.8265368	0.7512822	0.783567	0.184798
7541.5	0.325894	0.08996	1976.502	0.0021472	0.098853	0.8282585	0.7514692	0.756751	0.131962
7542	0.349813	0.297687	2035.414	0.015519	0.108263	0.8297895	0.0516558	0.736962	0.090425
7542.5	0.392008	0.115742	1825.33	0.022519	0.130892	0.8311433	0.0518332	0.856986	0.008829
7543	0.409804	0.107936	1474.707	0.006923	0.120995	0.8943179	0.8520946	0.861107	0.013784
7543.5	0.402778	0.073032	1517.646	0.090355	0.078786	0.8965109	0.8523487	0.872321	0.020029
7544	0.368147	0.076194	1781.229	0.089008	0.082478	0.8988065	0.8527894	0.838359	0.018816
7544.5	0.326908	0.288968	2072.444	0.104218	0.097656	0.9111487	0.8325044	0.839774	0.012996
7545	0.300861	0.283097	1689.833	0.109846	0.090628	0.9233349	0.8551147	0.871388	0.290233
7545.5	0.298506	0.055871	1833.129	0.001165	0.059177	0.9551707	0.8577387	0.871324	0.406754
7546	0.286654	0.260323	1952.528	0.012481	0.064195	0.9428297	0.9208637	0.887453	0.192683
7546.5	0.299768	0.061484	1923.284	0.128617	0.065512	0.9550427	0.9224302	0.909106	0.251486
7547	0.299292	0.256194	1694.732	0.132541	0.059539	0.9674834	0.9581908	0.915118	0.280633
7547.5	0.338323	0.157645	1531.892	0.011846	0.261172	0.9973241	0.9519443	0.916239	0.160456
7548	0.350114	0.284708	1392.5	0.001654	0.372548	0.9664821	0.9681908	0.925443	0.275137
7548.5	0.332882	0.101955	2192.115	0.001766	0.11353	0.9799904	0.9619443	0.939109	0.305199
7549	0.337842	0.122092	2706.649	0.017416	0.139072	0.9702064	0.9675781	0.935376	0.03665
7549.5	0.303925	0.129478	3000.668	0.018796	0.148735	0.9815101	0.9677258	0.931278	0.088937
7550	0.303321	0.122624	2281.387	0.002209	0.139763	0.9925379	0.9693928	0.944149	0.220036

APPENDIX G: DATA OF WELL 6 FOR FLOW UNIT CHARTS IN RESERVOIR X

Depth	Φ_T	Φe	K	RQI	Φz	nRQI	Φh	kh	Vsh
7525	0.341546	0.262763	1253.908	0.002749	0.356415	0.0001626	0.003294	0.002946	0.059428
7525.5	0.320231	0.123221	794.6654	0.003929	0.140538	0.0001652	0.002135	0.000555	0.041228
7526	0.325396	0.198239	751.9919	0.001830	0.247254	0.0001662	0.001062	0.007244	0.033585
7526.5	0.300948	0.106777	1024.805	0.004919	0.119541	0.0001687	0.001324	0.002486	0.023455
7527	0.330862	0.272414	1305.457	0.002763	0.374407	0.0001701	0.001960	0.097042	0.012326
7527.5	0.327515	0.280238	965.5264	0.002153	0.389348	0.0001798	0.001239	0.005399	0.008025
7528	0.313208	0.272756	1089.911	0.002746	0.375054	0.0001769	0.035988	0.006988	0.009846
7528.5	0.286598	0.266645	1288.715	0.002359	0.363596	0.0017632	0.043708	0.007308	0.013089
7529	0.296052	0.067226	1039.613	0.002457	0.072071	0.1781968	0.057097	0.017097	0.013565
7529.5	0.285957	0.067742	1610.831	0.002528	0.072664	0.1802468	0.059025	0.009025	0.011618
7530	0.309794	0.273419	2204.766	0.002558	0.376309	0.1824237	0.061083	0.050182	0.014379
7530.5	0.330252	0.273935	3103.086	0.003837	0.377287	0.1845836	0.063396	0.052096	0.013675
7531	0.328532	0.264839	2841.202	0.002951	0.360246	0.1868942	0.006947	0.105347	0.012622
7531.5	0.309743	0.044774	2112.007	0.030859	0.046873	0.1891608	0.105196	0.145196	0.010183
7532	0.357929	0.268516	1967.117	0.031451	0.367083	0.1914874	0.145122	0.01122	0.014522
7532.5	0.378089	0.072903	1901.596	0.038984	0.078636	0.1939633	0.101562	0.162868	0.014271
7533	0.395143	0.27729	2003.503	0.357288	0.383681	0.1962942	0.068264	0.061834	0.016498

7533.5	0.413129	0.070129	1702.071	0.037963	0.075418	0.198411	0.070689	0.178313	0.018265
7534	0.376033	0.061032	2188.408	0.388067	0.064999	0.2003786	0.077556	0.197721	0.019924
7534.5	0.351571	0.290516	1702.729	0.049021	0.409475	0.202294	0.083891	0.114986	0.018344
7535	0.324554	0.150455	1431.136	0.021499	0.177101	0.2041563	0.077859	0.129076	0.015993
7535.5	0.276017	0.158769	1057.751	0.017901	0.188734	0.2058371	0.068706	0.0148522	0.017878
7536	0.301565	0.150228	954.9883	0.017242	0.176786	0.2072826	0.076061	0.17229	0.018164
7536.5	0.317711	0.133876	1101.164	0.016798	0.154569	0.2085519	0.077165	0.192936	0.020417
7537	0.29903	0.131295	1028.047	0.014359	0.151138	0.2099077	0.085753	0.209873	0.022228
7537.5	0.273159	0.122525	794.7643	0.015754	0.139634	0.2112737	0.092523	0.22615	0.023094
7538	0.262764	0.117852	725.0251	0.149469	0.133597	0.2126131	0.095719	0.241694	0.025957
7538.5	0.291155	0.128821	1074.655	0.015754	0.147869	0.2140655	0.10615	0.256472	0.027231
7539	0.315995	0.122696	1314.017	0.016131	0.139856	0.2158335	0.110633	0.270831	0.027817
7539.5	0.33121	0.123849	1273.144	0.020499	0.141355	0.3028041	0.1127	0.283119	0.024934
7540	0.312882	0.11185	1080.175	0.029834	0.125936	0.3047023	0.102423	0.29327	0.025431
7540.5	0.341796	0.101855	834.7654	0.038563	0.113406	0.306595	0.104213	0.301742	0.017153
7541	0.33785	0.278645	1175.489	0.038763	0.386279	0.3085643	0.073248	0.308561	0.010127
7541.5	0.328314	0.272118	1225.384	0.048259	0.373849	0.3103794	0.04489	0.313428	0.012329
7542	0.352353	0.088772	1235.071	0.017633	0.097420	0.3123358	0.052324	0.318243	0.012829
7542.5	0.348118	0.297923	1570.135	0.018351	0.424345	0.3144043	0.056041	0.324029	0.013891
7543	0.360193	0.111275	1700.769	0.014359	0.125208	0.3163718	0.060337	0.331345	0.016757
7543.5	0.342845	0.092447	1676.028	0.014751	0.101864	0.3182602	0.071704	0.340223	0.019773
7544	0.331773	0.100553	1491.629	0.013541	0.111794	0.3201789	0.08332	0.349698	0.019839
7544.5	0.311218	0.107414	1653.354	0.030564	0.12034	0.3219816	0.083567	0.359964	0.013004
7545	0.325894	0.28996	1976.502	0.001472	0.098853	0.3236807	0.056751	0.371701	0.008253
7545.5	0.349813	0.097687	2035.414	0.005519	0.108263	0.3254564	0.036962	0.383865	0.013062
7546	0.392008	0.115742	1825.33	0.001519	0.130892	0.327129	0.056986	0.395244	0.014082
7546.5	0.409804	0.107936	1474.707	0.006493	0.120995	0.3965058	0.061107	0.405272	0.216915
7547	0.402778	0.073032	1517.646	0.090355	0.078786	0.3986256	0.072321	0.415552	0.025258
7547.5	0.368147	0.076194	1781.229	0.089008	0.082478	0.4010345	0.10359	0.425476	0.35785
7548	0.326908	0.288968	2072.444	0.001428	0.097656	0.4036476	0.139774	0.4434572	0.045817
7548.5	0.300861	0.083097	1689.833	0.009846	0.090628	0.4060464	0.171388	0.4443064	0.049141
7549	0.298506	0.255871	1833.129	0.001665	0.059177	0.4082733	0.181324	0.445169	0.047836
7549.5	0.286654	0.260323	1952.528	0.021248	0.064195	0.4105901	0.177453	0.445693	0.052323
7550	0.299768	0.061484	1923.284	0.028617	0.065512	0.4131228	0.1906	0.459159	0.057456
7550.5	0.299292	0.256194	1694.732	0.032541	0.059539	0.4158075	0.205118	0.4604822	0.042852
7551	0.338323	0.257645	1531.892	0.018416	0.061172	0.4183277	0.162309	0.4653841	0.034472
7551.5	0.350114	0.284708	1392.5	0.021654	0.092548	0.4207778	0.135443	0.4766664	0.032579
7552	0.332882	0.101955	2192.115	0.007656	0.11353	0.4233305	0.129109	0.4870464	0.031478
7552.5	0.337842	0.122092	2706.649	0.017416	0.139072	0.4259754	0.125376	0.4974132	0.030719
7553	0.303925	0.129478	3000.668	0.018796	0.148735	0.4923261	0.12278	0.4977172	0.031119
7553.5	0.303321	0.122624	2281.387	0.022209	0.139763	0.4940388	0.124149	0.5080229	0.034445
7554	0.341706	0.116044	2423.021	0.025721	0.131278	0.4957382	0.135353	0.5483371	0.036222

7554.5	0.349926	0.113987	2238.378	0.028369	0.128652	0.4974442	0.141208	0.5486357	0.02765
7555	0.370764	0.108354	2462.911	0.002823	0.121521	0.4990781	0.112112	0.5488614	0.022384
7555.5	0.385366	0.108673	2348.591	0.025643	0.121923	0.500753	0.093102	0.549009	0.01737
7556	0.373614	0.101535	2676.682	0.024777	0.113009	0.5027775	0.074092	0.5491221	0.012165
7556.5	0.364653	0.099301	2332.224	0.023199	0.110249	0.5048116	0.053329	0.049198	0.010876
7557	0.382817	0.106565	2300.815	0.067665	0.119275	0.5066498	0.048011	0.049254	0.008829
7557.5	0.392721	0.123717	2073.547	0.068668	0.141184	0.5083148	0.039416	0.549245	0.013784
7558	0.348744	0.135253	2020.725	0.034045	0.156408	0.5099121	0.059908	0.049245	0.020029
7558.5	0.354445	0.135916	1717.503	0.008965	0.157295	0.5115128	0.084289	0.049245	0.018816
7559	0.366946	0.128682	1570.532	0.097334	0.147687	0.5132136	0.07967	0.049245	0.012996
7559.5	0.367816	0.133266	1583.411	0.009964	0.153756	0.5148461	0.056719	0.549245	0.011485
7560	0.339677	0.09833	1889.103	0.083725	0.109053	0.5163459	0.050534	0.049245	0.009529
7560.5	0.336278	0.069787	1611.035	0.088874	0.075022	0.5178228	0.042379	0.549245	0.010555
7561	0.344565	0.065865	1405.863	0.078898	0.070509	0.5194434	0.046675	0.049245	0.011405
7561.5	0.374039	0.072345	1233.603	0.073185	0.077987	0.5211389	0.050203	0.5492583	0.010471
7562	0.379895	0.083396	1087.922	0.092166	0.090983	0.5228741	0.046327	0.549259	0.008563
7562.5	0.376864	0.113286	1569.936	0.077266	0.127759	0.5246229	0.038286	0.549259	0.00815
7563	0.370526	0.117111	1511.843	0.039208	0.132645	0.5264537	0.03652	0.049259	0.008483
7563.5	0.328428	0.121469	2043.86	0.005468	0.138263	0.528433	0.037944	0.049259	0.010968
7564	0.352798	0.113063	2029.239	0.062628	0.127475	0.5303484	0.048395	0.5492622	0.015764
7564.5	0.355888	0.296252	2070.621	0.003849	0.106504	0.5321565	0.067803	0.5493045	0.020697
7565	0.327049	0.103596	1841.255	0.005072	0.115568	0.5339134	0.086807	0.0493045	0.021409
7565.5	0.305683	0.097691	1904.532	0.006371	0.108268	0.5357872	0.089478	0.6693173	0.021873
7566	0.297508	0.298025	2567.899	0.048271	0.108678	0.5375661	0.091204	0.5793994	0.020377
7566.5	0.30877	0.090865	2190.446	0.065755	0.099946	0.5391735	0.085603	0.5995499	0.022035
7567	0.30641	0.286193	2103.156	0.053594	0.094323	0.6729718	0.091809	0.6049636	0.026555
7567.5	0.332144	0.098805	2010.679	0.059248	0.109638	0.6748623	0.108235	0.0497857	0.024773
7568	0.366891	0.105845	1752.865	0.072273	0.118375	0.6768518	0.101841	0.0500239	0.021922
7568.5	0.379564	0.101371	2143.355	0.071613	0.112806	0.6789021	0.091389	0.0501417	0.019379
7569	0.364211	0.098959	2259.385	0.056342	0.109828	0.6811647	0.081821	0.0501709	0.017635
7569.5	0.338097	0.106047	2220.965	0.008899	0.118627	0.6833725	0.07512	0.0502256	0.017276
7570	0.371024	0.103255	1819.592	0.007927	0.115144	0.6853179	0.073729	0.0504134	0.016286
7570.5	0.39038	0.114818	2135.466	0.006539	0.129712	0.6872853	0.069858	0.0507199	0.018546
7571	0.357418	0.115161	2376.315	0.005469	0.130149	0.6893287	0.078637	0.0509241	0.016381
7571.5	0.36036	0.105101	1625.642	0.007546	0.117445	0.6912177	0.070232	0.05109	0.008702
7572	0.391834	0.119987	1333.838	0.008332	0.136346	0.6928914	0.038877	0.0512822	0.005349
7572.5	0.403151	0.126358	1553.58	0.007328	0.144633	0.6945511	0.02435	0.0514692	0.005708
7573	0.395478	0.089385	1885.431	0.067968	0.098159	0.6962534	0.025933	0.0516558	0.009986
7573.5	0.351152	0.290368	1949.759	0.065817	0.099346	0.6977487	0.044297	0.0518332	0.015133
7574	0.317306	0.102159	2404.459	0.079694	0.113783	0.699168	0.065305	0.0520946	0.016902
7574.5	0.353303	0.115481	2614.874	0.004466	0.130558	0.7007354	0.072273	0.0523487	0.015883
7575	0.362587	0.285171	2959.257	0.056372	0.093101	0.7023065	0.068273	0.0527894	0.013753

7575.5	0.384653	0.287355	2734.763	0.049976	0.095716	0.7035891	0.059784	0.0535044	0.013507
7576	0.395641	0.28529	2365.91	0.065664	0.093243	0.8156998	0.058791	0.0551147	0.011111
7576.5	0.400393	0.272968	1976.622	0.065879	0.078711	0.8182756	0.048988	0.0577387	0.012261
7577	0.396248	0.083161	1533.641	0.055752	0.090704	0.820576	0.053723	0.0611334	0.016612
7577.5	0.341659	0.29738	1405.229	0.083364	0.107886	0.8226327	0.77326	0.0647394	0.021165
7578	0.328143	0.285916	1840.961	0.093412	0.093991	0.8246301	0.713829	0.0681908	0.025926
7578.5	0.30765	0.106355	1859.151	0.011754	0.119013	0.8265368	0.628134	0.0719443	0.024992
7579	0.285432	0.112449	2165.03	0.015688	0.126695	0.8282585	0.542441	0.0752781	0.025309
7579.5	0.250478	0.117894	2120.051	0.017944	0.133651	0.8297895	0.456746	0.6777258	0.02351
7580	0.209997	0.117274	1957.326	0.186411	0.132854	0.8311433	0.371053	0.6793928	0.023003
7580.5	0.195812	0.097526	1770.657	0.192342	0.108065	0.8326507	0.095385	0.0808637	0.025118
7581	0.206674	0.288046	1684.1	0.195173	0.096547	0.8343052	0.103087	0.6824302	0.033536
7581.5	0.222214	0.081788	2294.642	0.018112	0.089073	0.8361043	0.132323	0.6841089	0.043686
7582	0.287183	0.289217	2397.828	0.036887	0.097956	0.8379787	0.164886	0.6860049	0.055524
7582.5	0.229933	0.093945	2594.217	0.035998	0.103686	0.8399159	0.199718	0.6883316	0.082192
7583	0.21386	0.284014	2320.979	0.049325	0.09172	0.8421375	0.268367	0.790601	0.133763
7583.5	0.183997	0.295496	2051.275	0.033984	0.105579	0.8442703	0.374308	0.7929324	0.201435
7584	0.129288	0.103231	2189.445	0.026487	0.115114	0.8461242	0.480247	0.7954729	0.120233
7584.5	0.097826	0.097481	2314.572	0.016822	0.10801	0.8479488	0.586188	07981758	0.106754
7585	0.085159	0.104827	2212.056	0.098342	0.117103	0.8497639	0.692129	0.7316912	0.232683
7585.5	0.074762	0.109133	1805.739	0.027343	0.122502	0.851524	0.75516	0.730076	0.331486
7586	0.070321	0.103973	1854.997	0.027675	0.116038	0.8533418	0.793082	0.7252464	0.310633
7586.5	0.070427	0.096473	1937.414	0.026548	0.106773	0.8550784	0.800595	0.7174424	0.326056
7587	0.062984	0.102905	1929.399	0.023192	0.114709	0.8567945	0.818556	0.7493807	0.305137
7587.5	0.051625	0.118524	1885.306	0.020959	0.134461	0.8584864	0.827352	0.7612242	0.325199
7588	0.055002	0.122597	1959.11	0.024367	0.139726	0.8601702	0.824768	0.7829248	0.33665
7588.5	0.079625	0.12741	2053.451	0.191522	0.146013	0.861987	0.832193	0.7945355	0.388937
7589	0.109419	0.110434	2032.795	0.018866	0.124144	0.8638654	0.835444	0.8861295	0.320036
7589.5	0.152803	0.118376	1843.894	0.019765	0.13427	0.8658043	0.830595	0.8877171	0.294784
7590	0.199702	0.11428	1769.683	0.021762	0.129025	0.9878989	0.848556	0.819322	0.232624
7590.5	0.238206	0.104189	2402.78	0.024747	0.116307	0.9994273	0.873502	0.8720652	0.210622
7591	0.249369	0.098015	2572.253	0.002548	0.108666	0.9994278	0.902068	0.8828768	0.184798
7591.5	0.27503	0.095869	2472.75	0.026608	0.106034	0.9994301	0.902193	0.9424527	0.131962
7592	0.307784	0.092735	1028.67	0.027883	0.102213	0.9994513	0.905444	0.9560862	0.090425
7592.5	0.315074	0.099092	877.308	0.180351	0.109991	0.9994752	0.910326	0.9575872	0.05645
7593	0.321097	0.09043	753.7707	0.172402	0.09942	0.9995045	0.913829	0.9591015	0.031863
7593.5	0.348434	0.102009	660.8842	0.171111	0.113597	0.9995747	0.948134	0.9605716	0.025361
7594	0.339991	0.110703	835.101	0.188666	0.124483	0.9997029	0.952441	0.9520192	0.02228
7594.5	0.347821	0.089318	1026.185	0.022907	0.098078	0.999821	0.953716	0.9975641	0.023702
7595	0.355118	0.093882	1039.392	0.023192	0.103609	1.0000000	0.957946	0.9853373	0.021933